# DEVELOPMENT AND PROPERTY ASSESSMENT OF HIGH PERFORMANCE HYBRID FIBER REINFORCED CONCRETE

*A dissertation Submitted in Fulfillment of the Requirement for the Award of the Degree of*

MASTER OF ENGINEERING

in Structural Engineering

Submitted By

HITESH GUPTA

801624014

Under Supervision of

**Dr. Prem Pal Bansal**

Associate Professor and Head

Civil Engineering Department

**Mr. Raju Sharma**

Lecturer

Civil Engineering Department


CIVIL ENGINEERING DEPARTMENT

THAPAR INSTITUTE OF ENGINEERING & TECHNOLOGY

(A DEEMED TO BE UNIVERSITY), PATIALA, PUNJAB

JULY, 2018

## DECLARATION

I, Hitesh Gupta hereby declare that the work presented in this dissertation entitled "Development and property assessment of High Performance Hybrid Fiber Reinforced Concrete" in fulfillment of the requirement for the award of degree of Master of Engineering (Structural Engineering) submitted at the Civil Engineering Department, Thapar Institute of Engineering & Technology (Deemed to be University), Patiala is an authentic record of my work carried out under supervision of Dr. Prem Pal Bansal (Associate Professor and Head, CED, Thapar Institute of Engineering & Technology, Patiala ) and Mr. Raju Sharma (Lecturer, CED, Thapar Institute of Engineering & Technology, Patiala ) from January to July, 2018. The matter presented in this has not been submitted either in part or full to any other university or institute for the award of any other degree.

Hitesh

Date: 25|07|2018

(Hitesh Gupta)

(801624014)

25/7/18

Dr. Prem Pal Bansal
Associate Professor and Head
Civil Engineering Department
Thapar Institute of Engineering & Technology
(A Deemed To Be University), Patiala, Punjab

Mr. Raju Sharma
25|07|2018
Lecturer
Civil Engineering Department
Thapar Institute of Engineering & Technology
(A Deemed To Be University), Patiala, Punjab

Date:

# ACKNOWLEDGEMENT

Time has provided me the cherished opportunity to express my heartfelt gratitude to my guides Dr. Prem Pal Bansal, Associate Professor and Head, CED, and Mr. Raju Sharma, Lecturer, CED, Thapar Institute of Engineering & Technology, Patiala, who permitted me to carry out research work under their able guidance. I shall ever remain indebted to them for their meticulous guidance, constructive criticism, clear thinking, keen interest, constant encouragement, and forbearance right from the beginning of this research to its completion.

The cheerful support of my friends and colleagues is sincerely appreciated. Special words of appreciation go to Sh. Sunit Kumar, Sh. Ram Simran, Sh. Virender Singh and other laboratory colleagues who helped me in my experimental work. I am also thankful to all the staff members of the Civil Engineering Department for their full cooperation and help.

Above all, I thank my parents, whose love and affectionate blessing have been a constant source of inspiration in making this manuscript a reality. I render my gratitude to the almighty who bestowed self-confidence, ability, and strength in me to complete this work.

(Hitesh Gupta)

(801624014)

# ABSTRACT

High Performance Concrete (HPC) is the lifeline of the modern construction industry. The excellent mechanical and durability characteristics of HPC attained the attention of researchers to use this material for the construction of high rise structures, water retaining structures and long span bridges. However, the brittle failure behavior of HPC was the limitation of this material for the construction of important structures. Further, the usage of fibers in mono/hybrid state in HPC impart the ductility, bridge the cracks, and retain the strength for a longer period because of excellent fiber matrix interface. Still, the study on the development of HPC with hybrid fiber (short and long steel fibers) is conducted very less. Therefore, in the present experimental study, the HP-HFRC (High Performance Hybrid Fiber Reinforced Concrete) is prepared by using the Modified Andreasen and Andersen particle packing model.

The Modified A & A mix design model is based on the attainment of optimum particle packing density. The workability and compressive strength were the main criteria to finalize the design mix of HPHFRC. The effect of usage of Natural sand and the expensive Indian standard sand are also evaluated. It has been found that the Modified A & A model is reliable to design the mix for HPHFRC with excellent mechanical, durability and microstructure properties. In addition to that, a marginal difference in the mechanical and durability properties of Natural sand contained HPHFRC (NS) and Standard sand contained HPHFRC (SS) is found. A little higher presence of calcium hydroxide compound found in XRD analysis could be one of the reasons for the slightly lower strength of HPHFRC (NS) than HPHFRC (SS).

In the present study, the designed mix prepared by Modified A & A model fulfills the criteria's of High Performance Concrete. The strength properties of prepared HPHFRC can be improved further, with the application of heat or steam curing and achieve the strength criteria of Ultra High Performance Concrete (UHPC).



Keywords: *HPHFRC, mix design model, hybrid fibers*

# TABLE OF CONTENTS

# LIST OF TABLES

# LIST OF FIGURES

# LIST OF EQUATIONS

# ABBREVIATIONS

# CHAPTER 1

# INTRODUCTION

## 1.1 GENERAL

Concrete is the most widely used material in the world. Humans have been using concrete in their pioneering architectural feats since 3000 BC. The Egyptians used the early forms of concrete to build pyramids. They mixed straw and mud to form bricks and used lime and gypsum to make mortars. The Greeks used the same material but as this material could easily dissolve in water, they added volcanic ash from the Pozzuoli town (that's how the name pozzolana came). Using this material they had made marvelous structures like the Colosseum, the largest amphitheater ever built or the Pantheon in Rome, the world's largest nonreinforced concrete dome that is still standing even after more than 2000 years of its construction. With the falling of the Roman Empire, concrete use became rare until the technology was redeveloped around the 1950s with the invention of Portland cement, which is the main constituent used in modern day concrete. Today, Concrete is omnipresent in our built environment - be it in roads, buildings, bridges, or railways.

At the beginning of the twentieth century, industrialization and urbanization expanded in the world at a very fast pace. During this period, skyscrapers for residential space or commercial offices were built in major American cities. Construction of these high rise structures required concrete having higher compressive strength. During 1950s concrete having a compressive strength of 35 MPa was called as High Strength Concrete (HSC). In 1960s concrete possessing compressive strength 41 to 55 MPa and later in 1970s 65 MPa was called as HSC. Along with high strength, the durability of concrete also became an important parameter for the mix design of concrete which lead to the origin of a new generation concrete termed as "High Performance Concrete (HPC)."

High Performance Concrete is a concrete which satisfies specific requirements in performance and uniformity that can't be conventionally fulfilled with the usage of traditional materials and production practices. Generally, concrete possessing compressive strength above 80 MPa and high durability performance is termed as HPC. Generally, a HPC also possesses high strength but strength is not at all times the foremost requirement. In today's time concrete possessing compressive strength above 120 MPa, along with excellent durability properties is called as Ultra High Performance Concrete (UHPC).

In the present time, there is a global growth in concrete consumption is mainly due to the rapid industrialization of developing countries most of them are in Asia, Africa, and Latin America whereas, in the developed world, the demand is driven more by the need to repair, replace and retrofit existing structures. So, the need of the hour is to develop a construction material which should be strong enough to bear the mammoth load of high rise structures and should also be durable to retain the structure safe throughout its lifespan.

Ultra-High Performance Concrete (UHPC), also known as reactive powder concrete (RPC), a high-strength, durable material has the potential to meet the above-mentioned needs. RPC is the general term used for a new class of concrete developed by French Corporation BOUYGUES in 1993. The elimination of coarse aggregate is the key aspect of this concrete. It is formulated by combining Portland cement, SCM (silica fume, ground granulated blast furnace slag, rice husk ash, etc), fine silica sand, water, HRWRA, and steel, plastic or organic fibers. Using it as an alternative to traditional concrete presents a golden opportunity for future engineers to design new concrete structures which would last longer, more sustainable, require lesser space, and lower maintenance.

But commercially available UHPC costs about 20 times more than the normal concrete in the USA. This high cost of production had been a major reason for not widespread usage of UHPC all over the world especially in developing countries like India. Generally, the mix proportions are fixed without any detailed investigation which resulted in non utilization of a large portion of expensive binder portion content. So, mix proportioning of UHPC with the well defined design mix models results in optimum utilization of binders and a reduction in the cost of production of UHPC *(Yu R. et al. 2014).*

Addressing this concern, this study is focussed on to see the possibility of development of HPHFRC with Natural sand rather than very expensive silica sand using Modified Andreasen and Andersen particle packing model. As studied from the previous literature, hybrid fibers reinforced concrete systems results in better fresh and hardened properties than the one having only a single type of fibers. Therefore hybrid steel fibers are used throughout this course.

## 1.2 ULTRA-HIGH PERFORMANCE CONCRETE (UHPC)

UHPC is a new class of cementitious materials that are characterized by a compressive strength greater than 120 MPa and high durability *(Mueller and Haist 2009).* The French Association of Civil Engineering (AFGC) Interim Recommendations for UHPFRC defines Ultra High Performance Concrete to possess the following properties: Compressive strength is greater than

150 MPa, a high binder content with special aggregates, and internal fiber reinforcement to ensure nonbrittle behaviour.

UHPFRC (Ultra high-performance fiber reinforced concrete) can be described as a composite containing a large volume of steel fibers (considering workability 1.5 to 3% of the volume of concrete), high silica fume dosage (generally 25 % of the cement), a low water-binder ratio (usually less than 0.2), and lack of coarse aggregate *(Wille et al. 2011)*. It has outstanding material characteristics such as self-compaction, very high mechanical and durability properties which results in excellent environmental resistance *(Graybeal 2007)*. Typical strengths are 150 to 200 MPa (21755.7 to 29007.5 psi) in compression, 7 to 15 MPa in uniaxial tension *(Rossi et al 2005; Richard and Cheyrezy1995; Benson and Karihaloo 2005)* and 20 to 48 MPa in flexural. Furthermore, UHPFRC exhibit strain hardening under tension *(Benson and Karihaloo 2005; Habel et al. 2008)* and high energy absorption capacity *(Habel and Gauvreau 2008; Bindiganavile et al. 2002)*. In addition, UHPFRC show improved structural behavior when compared to conventional concrete. The main hindrance to the practical application of UHPC was its brittle failure mode. With fibers addition in the UHPC, this brittle mode has been transformed to more ductile failure mode and thus the term Ultra High Performance Fiber Reinforced Concrete (UHPFRC) originated. As the cost of a unit volume of steel fibers to be incorporated in UHPC is generally very higher than that of the same volume of a concrete matrix, so efficient utilization of fibers becomes a necessity to make cost effective UHPFRC. From the recent research in UHPFRC, it has been found that usage of multi characteristic fibers (hybridization) in the concrete mix results in effective and economical usage of fibers. In this way, a new term Ultra High Performance Hybrid Fiber Reinforced Concrete (UHPHFRC) came into existence.

To further enhance mechanical and durability performances of HPC, techniques like heat curing and the application of pressure are often used in the construction industry but these procedures restrict the HPC only as a factory product and not as a cast in situ material. This study is therefore aimed at the formation of Hybrid Fiber Reinforced HPC without the necessity for heat curing. Short fibers were used for bridging the micro-cracks while the long fibers to prevent the development of macro-cracks.

## 1.3. KEY PARAMETERS AND INGREDIENTS OF UHPFRC

### 1.3.1. GENERAL

UHPFRC is composed of cement, aggregates, water, additives, fibers, and admixtures. The difference between UHPFRC and conventional concrete mix design lies in particular in the size

of the aggregates, amount of binder, and the presence of fibers. The usage of quite a large dosage of super-plasticizers so as to obtain an acceptable workability is also a feature of the UHPFRC. UHPFRC has much denser matrix than a conventional concrete. Optimizing the packing density of granular constituents (i.e. cement, SCM, and aggregates) results in a dense matrix *(Toutlemonde and Resplendino 2011)* and thus improves both mechanical and durability properties.

### 1.3.2. MATRIX

The matrix phase in concrete is stated to consist of free water, cement, supplementary cementitious materials and the filler fraction of the aggregates. The matrix, therefore, consists of both chemically reactive and inert materials. Some function as both packing density enhancing and chemically reactive materials.

#### *1.3.2.1. Particle packing*

Particle packing is a fundamental requirement for making UHPFRC. The high cost of raw materials is the main obstacle in the widespread usage of UHPFRC in the construction industry. A more densely packed concrete requires less binder content which ultimately reduces the cost. Thus with optimum particle packing of constituents materials of UHPFRC, the above-mentioned obstacle could be crossed over. Compatibility and acceptable flow in the fresh state of concrete is a big challenge concerning packing and the concrete, which could be solved with the introduction of large amounts of fine particles having the same size as that cement or below *(Vogt et al. 2010).*

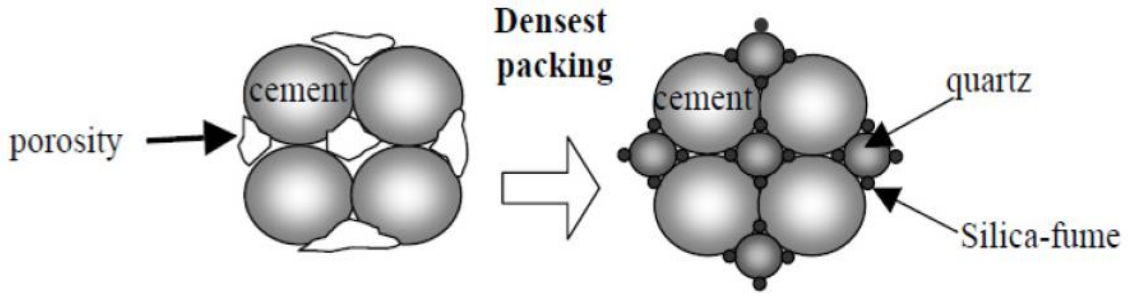


Figure 1. 1: Packing mix design *(Okuma 2006).*

#### *1.3.2.2. Water-binder ratio*

The term binder is defined as the chemically reactive materials in the matrix, which includes cement and supplementary cementitious materials. In a mix to ensure optimal properties, water to binder (w/b) ratio is a crucial parameter. In the production of UHPC, a very low w/b ratio is

usually adopted. Water binder ratio as low as 0.08 was adopted *(Richard, P. et al. 1994)* but with this dense packing cannot be guaranteed. Generally, w/b-ratio below 0.25 ensures a rational balance between the flow properties and the strength of the hardened concrete. In the case of UHPFRC typically it lies between 0.16 and 0.2. But with water binder ratio of 0.25, *Wille et al (2011)* got compressive strength greater than 150 MPa. From this, it can be understood that water binder ratio is not the only parameter that governs the strength of UHPC. The type of ingredients, their properties, particle size distributions, the curing method adopted, the mixing method (vertical or horizontal) and the placing techniques etc. also affect the strength of UHPFRC.

*1.3.2.3. Cement*

A cement is a binder used for construction that sets, solidifies, adheres to other materials, and binds them together. Cement is rarely used on its own, but instead to bind sand (fine aggregate) and gravel (coarse aggregate) together. As per *IS 456: 2000 (Clause 8.2.4.2)* cement content in concrete should not exceed 450 kg/$m^3$. But in making UHPFRC cement content generally lies between 600 to 1000kg/$m^3$, which is far more than normally required in conventional concrete. The fineness of cement should lie between 3000 to 4500 $cm^2$/kg.Since, UHPFRC has a very low water/ binder ratio, Portland cement with a low $C_3A$ (Tricalcium Aluminate) can be preferred because of its low water demand.

*1.3.2.4. Silica Fume*

Silica Fume (SF) is a by-product in the production of silicon metal and ferrosilicon alloys during the smelting process. One of the most beneficial uses for SF is as a mineral admixture in concrete. Because of its physical and chemical properties, it is a very reactive pozzolan. Silica fume particles are far smaller than the cement particles (approx. 1/100). This smaller size makes it a very effective filler and subsequently enhances the packing density *(Mueller and Haist 2009)*. Silica fume contents of 20 to 30 % of the binder were proposed to get dense packing in UHPFRC *(Xing et al. 2006).*

Silica fume generally has the following main characteristics:

- An amorphous structure.
- The average size of spherical particles around 0.1 μm.
- $SiO_2$ content 85-98 %.

Silica fume can be regarded as a water replacement in terms of water demand and workability especially for High Strength Concrete (HSC). A certain portion of water is essential to fill the

void space even in a pure cement paste binder to make flow possible. The inclusion of water-reducing admixtures disperses the cement flocks and reduces the void space volume and ultimately, the water demand.

With the addition of silica fume, further water reduction is possible since it can take the place of the water in the void space and, along with that, increase the workability when superplasticizers are used. There is a possibility of the existence of "ball-bearing effect" of the spherically shaped silica fume particles that enhance the mobility of the irregular cement particles *(Jacobsen et al. 2009).*

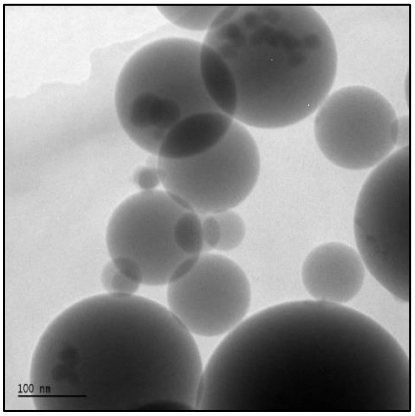


Figure 1. 2: Silica fume particles viewed in a transmission electron microscope *(Source: Wikipedia).*

SF is an essential part of UHPFRC, primarily due to the followings:

- The optimum packing density of all the ingredients is a key factor for the production of UHPC *(Mueller and Haist 2009).*
- During the hydration of cement, Calcium Hydroxide (CH) is produced and with that silica fume reacts and produces more of the Calcium Silicate Hydrate (CSH) gel, which has much higher strength compared to CH. Thus the pore system earlier filled with CH would now fill with stronger CSH gel, particularly in the critical, Interfacial Transition Zone (ITZ), which results in a remarkable increase in strength.

*1.3.2.5. Ground Granulated Blast-furnace Slag*

GGBS is obtained from molten iron slag (a byproduct from the steel and iron industry) by quenching process from a blast furnace. The slag is composed of silicates, aluminosilicates, and calcium-aluminosilicates (in other words silica, lime, and alumina) with small amounts of iron oxides, alkali, and magnesia. The molten iron slag is quenched in water or steam. This produces a glassy, granular product that is dried and ground to the fineness of cement or even

more. This fine powder is known as GGBS, which can be used in concrete as a partial replacement of cement or as an addition to cement.

The reaction of this fine powder with water results in the formation of cementitious hydration products. GGBS usage in concrete structures enhances its durability, by giving higher resistance to chloride penetration, to attacks by sulphate and reducing the risk of damage during alkali-silica reactions *(Malagavelli and Rao 2010).* Concrete made with GGBS cement results in greater ultimate strength than OPC made concrete due to finer particles of GGBS than cement particles (micro filler effect) and also due to more formation of CSH gel than OPC cement. Also, GGBS cement on hydration produces less free lime which is responsible for increasing the porosity of the concrete. The slower rate of setting of concrete produced with GGBS cement than OPC results in the lower heat of hydration. This reduced the initial cracks in concrete but would result in a delay in construction work due to a slow setting.

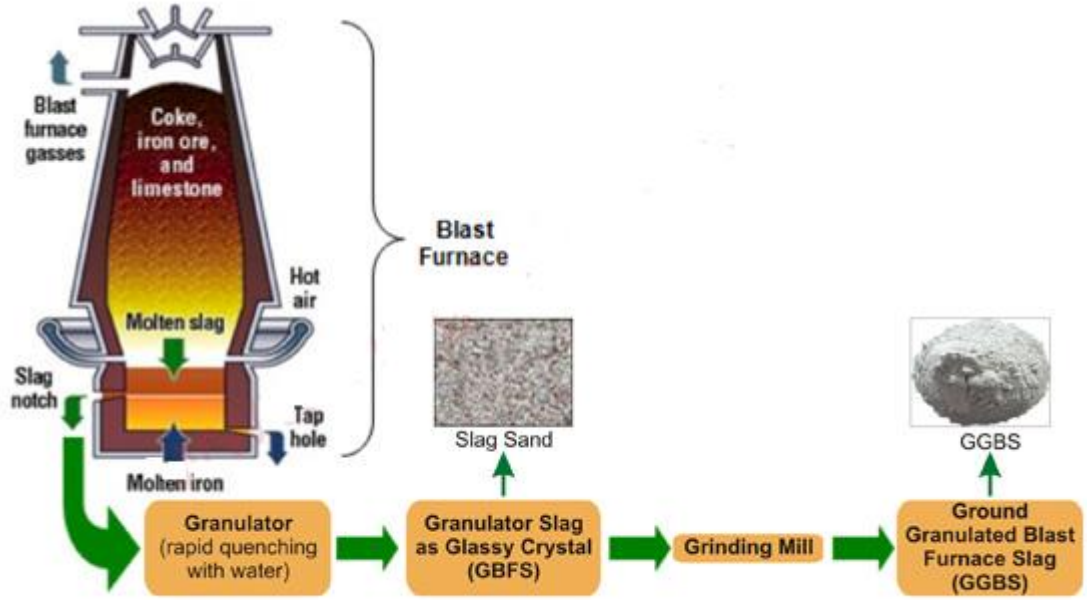


Figure 1. 3: Schematic diagram of the production of GGBS *(Suresh and Nagaraju 2015).*

### 1.3.3. AGGREGATES

The aggregates used in UHPFRC should have a total grain size distribution and which arrange a high packing density *(Mueller and Haist 2009)*. The largest fractions of the aggregate have been discarded by most of the researchers since long in making of UHPFRC. The reason being the Interfacial Transition Zone (ITZ) between coarse aggregate and the cement matrix is usually the weak spot of normal strength concrete. With the elimination of coarse aggregates,

such weaknesses are minimized. The mean particle size in UHPFRC is usually below 1 mm, yet in the production of UHPFRC, aggregates up to 16 mm have also been successfully used *(Habel 2004).* If the maximum aggregate size is around 0.5 mm, the term reactive powder concrete (RPC) can be used *(Mueller and Haist 2009).* It is necessary to have the high mechanical strength of the aggregate so as to prevent it from becoming the weak part of the concrete *(Toutlemonde and Resplendino 2011)*. Very high strength aggregates like calcined bauxite or granite can be used.

Generally, expensive silica sands are used in the production of UHPFRC. However, natural sand can be normally used as a replacement for silica sand, while still preserving good mechanical performance and ductile behaviour. Natural sand use does not necessarily influence UHPFRC strength significantly *(Yang et al. 2009).*

### 1.3.4. SUPERPLASTICIZER

Due to the low water/binder ratio, the use of superplasticizers is essential to have a sufficient workable concrete. A large dosage of superplasticizer as up to 5 percent of the mass of cement is required *(Mueller and Haist 2009)*. Without the development of superplasticizer additives, the development of UHPC could not have happened. Only Polycarboxylate Ethers (PCE), the third generation of plasticizers allow saving an ample amount of water to make a workable concrete *(Deeb et al. 2012).*

A good compatibility of superplasticizer and the binder paste results in less requirement of superplasticizer. Addition of superplasticizer in gradual steps rather than single addition results in its better efficiency *(Tue et al. 2008).* Superplasticizer content commonly used in the range between 1.4 and 2.4 % of the weight of cement *(Wille et al. 2011).*

### 1.3.5. FIBERS

UHPCs are highly brittle, and the term “performance" in its name depends on the addition of fibers. The reason for high brittle nature of UHPC is its very high strength and homogeneity. The role of fibers in UHPC is to increase the ductility of the material in tension and to eradicate explosive failure in compression. The fibers increase both tensile and flexural strength of the concrete, whereas their contribution is modest to the compressive strength. Steel fiber of 13 mm length and 0.2 mm diameter is the most common size used in UHPFRC *(Heinz et al. 2004).*

The role of the fibers in concrete is explained in light of the cracking process *(Rossi 2001).* Fibers effect is different on material and structural properties of UHPFRC.

When workability is not of significance long fibers can work on both micro and macro cracks, instead, at both the material and the structural level. This implies to for example dry roller-compacted FRCs *(Rossi 2001).* It is known from previous studies, that there is an upper limit for the dosage of long fibers that can be used in concrete without affecting workability excessively. Nevertheless, depending on the type of concrete and its application, the fiber content can vary remarkably. When the workability is of importance, a larger quantity of short fibers and a smaller quantity of long fibers could be used. This is the case of pumped, poured, or sprayed concretes *(Rossi 2001).*

When considering "short" or "long" fibers, and the amounts needed of each type, the *effect of scale* has to be considered. The geometry of the structure and the stress type will have an effect on the crack opening. A particular size of fibers that is effective on the crack opening for a small-sized structure may not be effective for the larger one. The mechanical characteristics of the matrix and also the largest diameter of the aggregate particles are of importance. In a highly compact matrix having a good bondage with the fibers, even fibers regarded as short can function on a structural level *(Rossi 2001).*

In a concrete mix, the amount of fibers added is calculated as a percentage (%) of the total volume of the composite (fibers and concrete) termed as Volume fraction ($V_f$). The fibers aspect ratio (l/d) or slenderness is calculated by dividing fiber length by its diameter. Fiber factor is another way for the characterization and comparison of the properties of different FRCs *(Hughes and Fattuhi 1976).*

Fiber factor = Volume fraction * Aspect ratio = $V_f \cdot l/d$

The wide use of steel fiber in UHPFRC is due to the many favorable properties of it: High strength, high ductility, high modulus of elasticity, and brilliant durability even in the alkaline environment of the concrete. Bond failure between the fiber and its surrounding matrix, is a usual failure, due to their limited aspect ratio *(Mueller and Haist 2009).*

### 1.4. ADVANTAGES OF UHPC

- Excellent fresh concrete properties as having high workability and requires no external vibration.
- Less material is required to achieve the same structural requirements as that of normal reinforced concrete which significantly decreases the weight of the structure. UHPFRC structure weights about 1/3 (or 1/2) of the normal reinforced concrete weight structure.

- Excellent mechanical properties (very high compressive, tensile and flexural strengths).
- UHPC is highly adaptable from clay-like to self-compacting.
- Outstanding durability properties because of negligible capillary pores and low porosity, which results in exceptional resistance against chloride penetration and corrosion.
- Very low permeable to water and aggressive solutions.
- Magnificent resistance to freeze and thaw cycles.
- UHPC makes a good bond with steel reinforcement than traditional concrete.
- High energy absorption capacity, thus ideal for structures subjected to severe loads (e.g., impact, blast, earthquake, etc.).
- Use of stirrups is avoided because of high shear capacity.
- Slender sections of UHPFRC lead to lesser inertia loads as compared to normal reinforced concrete so better seismic performance.


Figure 1. 4: Sectional dimensions of an L-shaped wall, build by conventional concrete and UHPFRC *(Lei et al. 2012).*

## 1.5. AIM OF THE THESIS

The aim of this thesis is to develop a mix design of HPHFRC using Modified Andreasen and Andersen particle packing model. The high cost of raw materials is the main hindrance to the widespread use of UHPHFRC. So, the effect of replacement of expensive Indian Standard sand

with comparative cheaper graded Natural sand on the fresh and hardened properties of HPHFRC is also studied.

The usual practice of elevated temperature curing or application of pressure restricts UHPHFRC only as a factory controlled product. Therfore, to also make it a cast in situ material, curing of all the specimens in the present study have been done at ambient temperature. To give a concise literature review of Fiber Reinforced HPC and UHPC is also aimed at in this report.

## 1.6. ORGANISATION OF THE THESIS

- Chapter 2

A concise literature study about the various design mix models for HSC has been discussed. Along with that, the effect of SCMs, single fiber and Hybrid fiber system on the fresh and hardened properties of HPC and UHPC have also been reported in this chapter.

- Chapter 3

In this chapter, various types of materials used and their physical and chemical properties are discussed. The fresh and hardened tests performed on the proposed mix design of HPHFRC and their testing procedures as per codal provisions are also discussed.

- Chapter 4

In this chapter, the adopted design mix methodology and the experimental work done for the mix design of HPHFRC are discussed.

- Chapter 5

In this chapter, discussions are made on the results obtained from the various tests performed on the proposed mix design of HPHFRC.

- Chapter 6

Significant conclusions are summarized in this Chapter.

# CHAPTER 2

# LITERATURE REVIEW

## 2.1. INTRODUCTION

In this chapter, a concise literature study on the various mix design models for HSC has been discussed. The effect of SCMs, single fiber system and hybrid fiber system on fresh and hardened properties of HPC and UHPC have also been presented. The high cost of raw materials, high carbon dioxide emission and energy consumption for the production of UHPFRC are the causes that hinder its wider application. Hence, in recent decades, efforts have been done to attenuate both its economic and environmental impact. Usage of industrial byproducts like GGBS, silica fume etc., as pozzolanic materials , filler materials like limestone, quartz powder to replace a fraction of cement, design methodologies used for optimum particle packing of constituents materials, and hybridization of fibers to optimize its use are some of work that have been done to achieve the above discussed objectives. The common characteristics used to define UHPFRC are given in Figure 3.1.

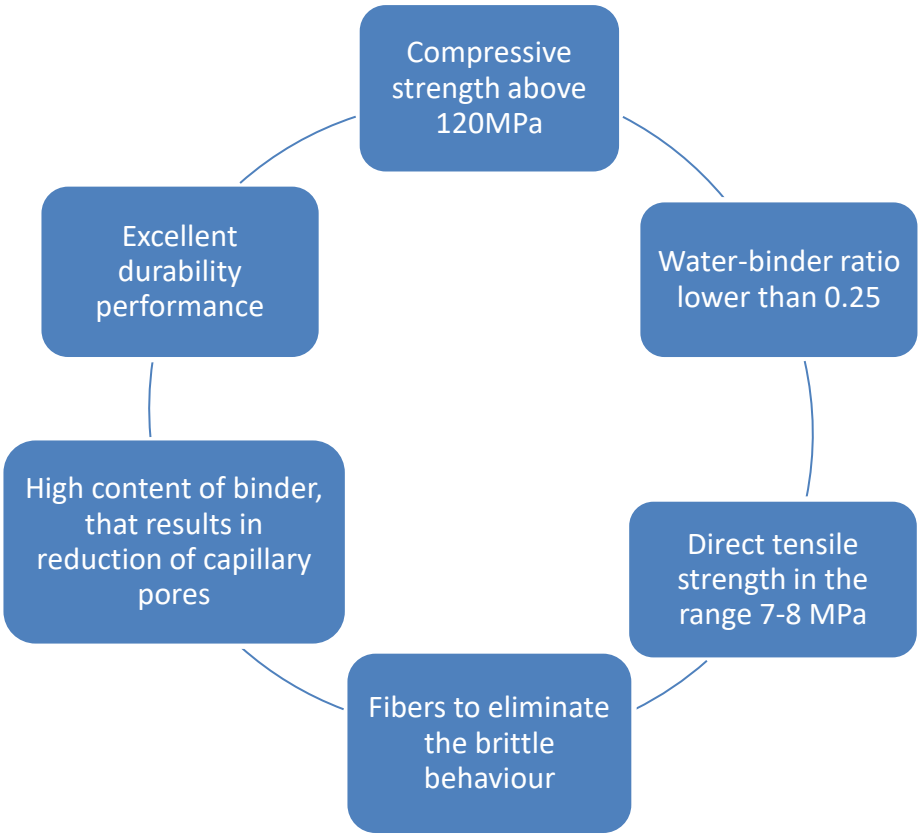


Figure 2. 1: Common characteristics of UHPFRC.

## 2.2. CONCRETE MIX DESIGN METHODS

The scientifically mix designed concrete is more acceptable because of its replicability rather than mix design with trials and errors. There have been numerous design methods that may be used for mix design of high strength concretes (HSCs) *(Khaloo et al. 2017).* The simplest method for the design of HSC having compressive strength up to 41 N/mm$^2$ is ACI 211.1. The main drawbacks of mix design concrete using this method were the negligence of the usage of high range water reducing admixtures and mineral admixtures, which are must for the production of UHSC.

Although, some of the drawbacks are overcome by the ACI 363R and ACI 211.4R yet there are some drawbacks of the usage of these methods for mix designing of UHSC:

- As per ACI documents, there should be initial slump value in the range between 25 and 50 mm, before the addition of water reducing agent so to adequate water is available for hydration of cement and the productiveness of water reducing agent. But this approach is not preferred for the production of UHSC because of its effect on pore system and eventually on mechanical and durability properties.
- Neglecting the silica fume important in the production of UHSC, ACI 211.4R is based on the replacement of fraction of cement with fly ash and along with that no guideline regarding its maximum limit in the concrete.
- Then came the Aitcin method, which was proposed for the mix design of HPC having a compressive strength in the range between 40 and 160 N/mm$^2$. This mix design approach is dependent on both empirical data and mathematical calculations based on Absolute volume method. The design mix procedure is shown in Figure 2.2.

Although Aitcin method has been successful in producing UHSC, it results in exhaustive testing and adjustments due to its drawbacks as given below:

- Based on the saturation point concept, this method can be used to approximately calculate the initial mixing water. But it takes a lot of time to determine the saturation point of the water reducing agent from the Marsh cone test.
- The initial dosage of water is represented as a function of the high range water reducing admixture saturation point at a water- binder ratio of 0.35. But for UHSC the water-binder ratio lies between 0.17 and 0.26 which could result in the wrong estimation of the water demand as there is an increase in saturation point with a decrease in water-binder ratio.

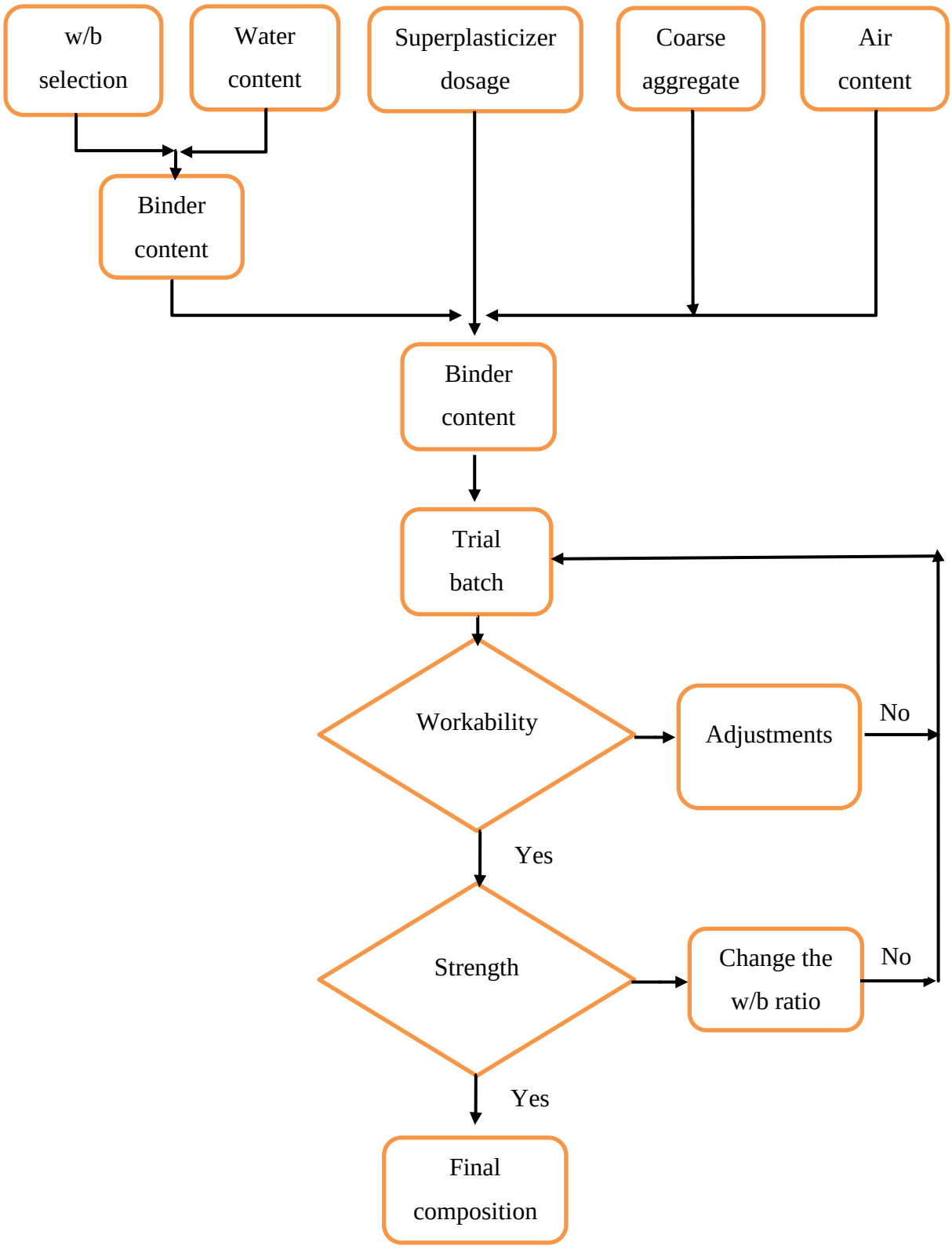


Figure 2. 2: Aitcin method mix design procedure *(Khaloo et al. 2017)*

*Khaloo et al. (2017)* proposed a new mix design methodology as shown in Figure 2.3. In the proposed methodology has been summarized in three major phases as:

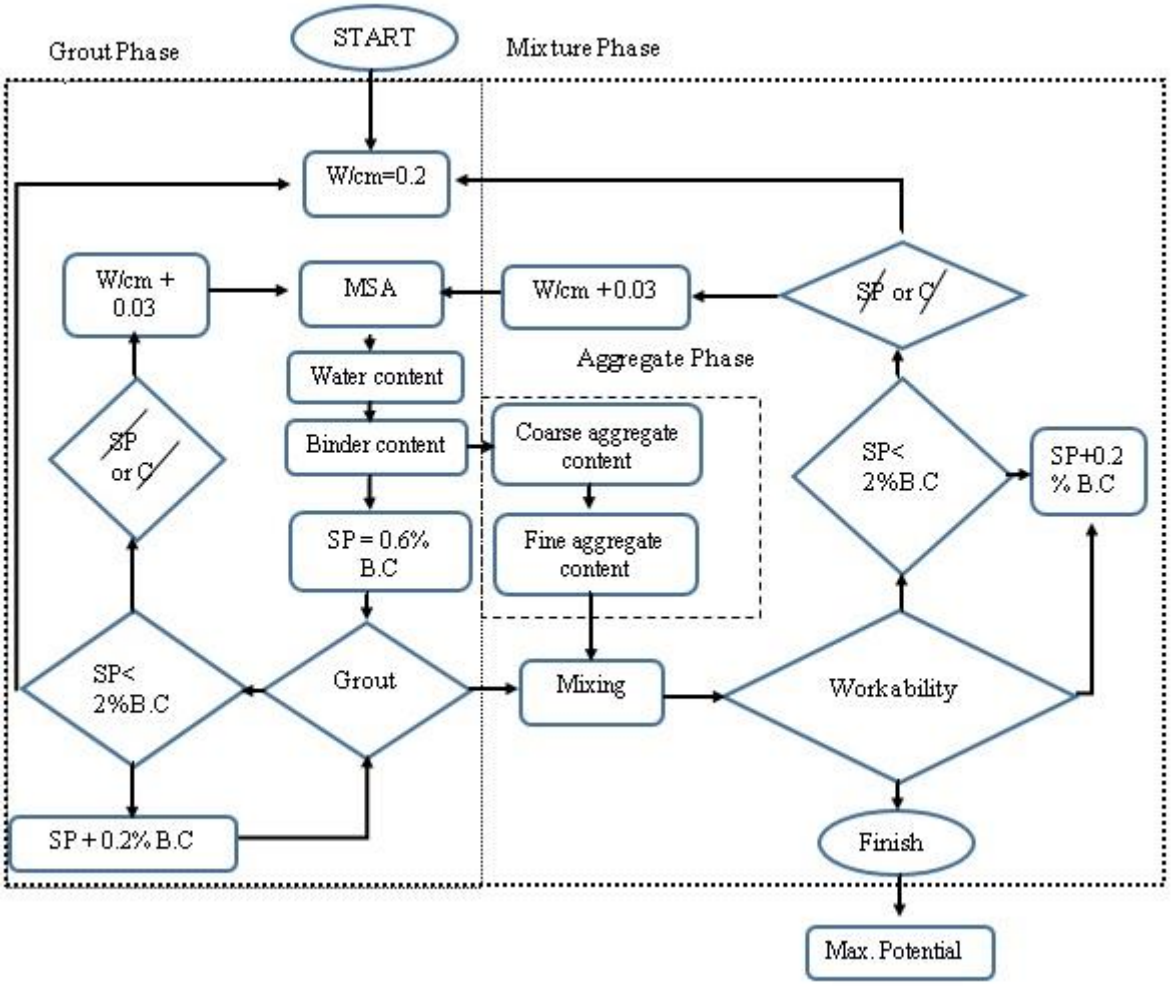


Figure 2. 3: Mix design procedure proposed by *Khaloo et al. 2017.*

- Grout phase: The initial ratios for grout mix are fixed depending upon the maximum size of aggregate (MSA), water content, SCMs quantities, and HRWRA quantity. Trial mixes and adjustments are required to get the best mix proportions.
- Aggregate phase: Firstly the coarse aggregate content is obtained as a function of MSA as already suggested by ACI 211.4R. The Absolute Volume Method (AVM) is used to obtain the fine aggregate proportion. But the fineness modulus of the fine aggregate should be in range 2.5 to 3.2.
- Mixture phase: The grout and the aggregates are mixed and workability of the mix is assessed.

Minimization of voids or the optimization of the particle packing of the granular ingredients is a different approach for the mix design of concrete. *Larrard and Sadran (1994) and (2002)* suggested the LPD Model, the CPSS Model for the design of concrete. Since, these methods

are based on the discrete components (cement, aggregates etc.) packing fraction and their combinations, so it is very difficult to incorporate very fine particles in these design models.

Another mix design method is an integral particle size distribution of continuously graded components. *Fuller and Thompson (1907)* stated in their work that the concrete properties could be enhanced by a geometric continuous grading of the aggregates. Form the work of Andreasen and Andersen (A & A) *(Funk and Dinger 2013)* and *Fuller and Thompson (1907)*, it was concluded that theoretically it is possible to attain minimum porosity by the optimal particle size distribution (PSD) of all the ingredients in the concreter mix, as shown in the Eq. ( 2.1).

$$P(D) = \left(\frac{D}{D_{max}}\right)^{q} \tag{2.1}$$

Where D is the particle size (μm)

P(D) is a fraction of the total particles smaller than the size D

$D_{max}$ is the maximum solid particle size (μm)

q is the distribution modulus and it determines the fraction between the fine and coarse particles in the mix.

Nevertheless, in Eq. (2.1), the minimal particle size is not considered, but in actual, there is a lower size limit, with which a more efficient particle packing model could be developed. That's why *Funk and Dinger (2013)* suggested a new model based on the A & A equation.

In this study the mix design of UHPC is based on, this so called modified Andreasen and Andersen (modified A & A), which is given in Eq. (2.2).

$$P\left(D_i^{i+1}\right) = \frac{\left(D_i^{i+1}\right)^{q} - D_{min}^{q}}{D_{max}^{q} - D_{min}^{q}} \tag{2.2}$$

Where $D_{min}$ is the minimum particle size (μm)

D is calculated by the geometric mean of the above and below sieve size of the respective proportion procured by particle size analysis.

$$D_i^{i+1} = \sqrt{D_i D_{i+1}} \qquad \text{for } i=1, 2, \ldots,n-1 \tag{2.3}$$

Where i is the discrete particle sizes considered.

## 2.3. WORKABILITY

Workability is an important and essential requirement for the production of UHPFRC. The reason being the usage of fibers has imparted ductility in the brittle UHPC but uniform distribution of fibers is must to make a reliable and consistent concrete. Workability of concrete decreases with the inclusion of steel fibers because of two reasons: firstly, the mechanical interaction between the concrete paste and the fibers, and secondly, due to the interlocking of fibers. Practical application of UHPFRC is mostly in prestressed bridge girders or heavily reinforced joints of bridge decks or slender architectural shapes which require a self-flowing concrete. Since, the production of HPC or UHPC requires the usage of SCMs therefore, their effect on the flowability of the mix is also very significant.

### 2.3.1. EFFECT OF SCMS

SCMs like silica fume, fly ash, and GGBS, etc. apart from enhancing the mechanical properties also affect the fresh properties of concrete. Particle size and shape of SCMs are two important parameters that primarily affects the workability of concrete.

**Mazloom et al. (2004)** had studied the effect of silica fume on the workability of HSC. Cement had been replaced by silica fume with 0, 6, 10, 15 percentages. From the test results, it has been observed that workability of mix decreases with increase in percentage replacement of cement with silica fume. The reason being the comparative very small size particles of silica fume than cement particles which are having very high specific surface area causes scarcity of free available water for workability. The requirement of superplasticizer for achieving a constant slump of 100 mm increases with the increase in percentage cement replacement with silica fume.

**Kou et al. (2011)** had examined the role of silica fume, GGBS, fly ash and metakaolin on the properties of natural and recycled aggregate concrete. Due to the very high surface areas of silica fume and metakaolin particles as compared to cement particles, the workability of mix decreases with the partial replacement of cement with these SCMs. However, workability of mix increases with the partial replacement of cement with fly ash and GGBS. The increase in workability due to the inclusion of fly ash and GGBS can be attributed to the spherical shape of fly ash particles and due to the glassy texture of GGBS particles surface.

### 2.3.2. EFFECT OF THE SINGLE FIBER SYSTEM

In this fiber system, only one type of fiber is used in the concrete. The percentage of fibers incorporated in concrete, shape and aspect ratio of fiber affects the workability of the mix.

**Yang et al. (2009)** had tried many possibilities for reducing the cost of UHPFRC mix by replacing generally used expensive silica sand with two locally available natural sand and recycled glass cullet (RGC). The effect of curing at 20$^{o}$ C and 90$^{o}$ C on mechanical and ductility properties of UHPFRC were also studied. GGBS and silica fume were used as supplementary cementitious materials. Steel fibers of length 13 mm and 0.2 mm diameter were used. The silica sand used had a limited grading distribution (nearly 90% particles) in the range between 150 and 300 micrometers. The two types of locally available sand were sieved and particles above 5 mm were rejected. The RGC were used as medium sized aggregates as per BS EN 13139 (2002). The flow ability of mixes before and the addition of steel fibers were determined using flow table as per BS EN 4551 Part1. The flow diameter observed for concrete mix having silica sand was 244 mm which decreases with the usage of ordinary sand and RGC as given in Table 2.1.

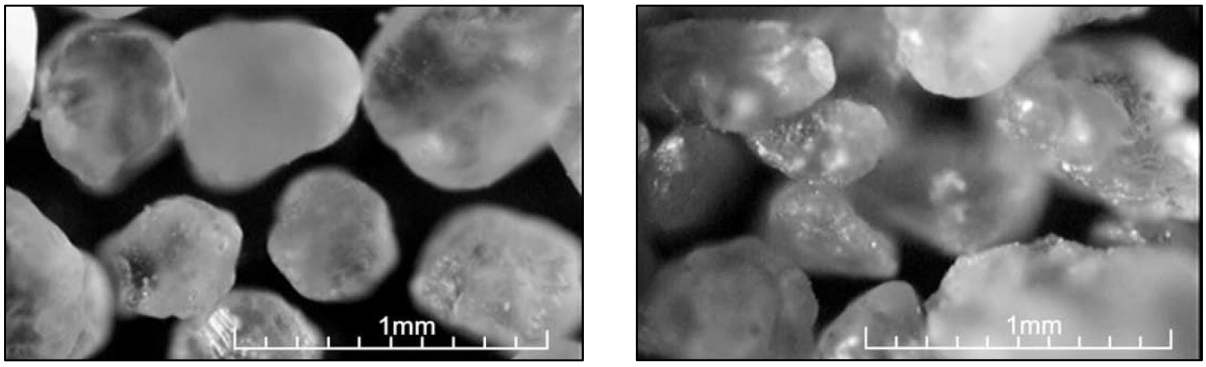


(A) (B)

Figure 2. 4: Micrograph of (A) Silica sand particles (B) Fine Ordinary Sand type I *(Yang S.L. et al. 2009).*

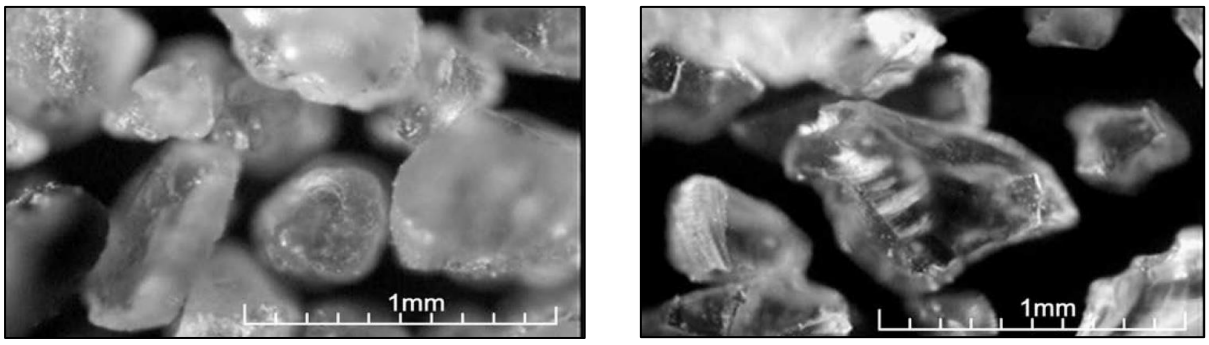


(A) (B)

Figure 2. 5: Micrograph of (A) Fine Ordinary Sand type II (B) Recycled glass cullet *(Yang S.L. et al. 2009).*

It can be attributed to the most spherical shape of silica sand particles than the ordinary sand and RGC particles as shown in Figure 2.4 and Figure 2.5. With the addition of 2% fibers by volume of concrete, flow diameters of all the mixes decrease nearby 10 mm.

Table 2. 1: Flow table test values of mixes with and without fibers *(Yang S.L. et al. 2009).*

| Type of sand | | Silica sand | Ordinary sand-I | Ordinary sand-II | Recycled glass cullet |
|---|---|---|---|---|---|
| Spread (mm) | W/o fibers | 244 | 197 | 239 | 185 |
| | With fibers | 232 | 182 | 228 | 175 |

**Yu et al. (2014)** had developed a design mix of concrete using the Modified A&A particle packing model with the replacement of partial cement with fillers (limestone and quartz powder). Short straight steel (SSF) fibers of length 13 mm and diameter 0.2 mm were used in this study. It had been found that there was a linear decrease in the relative slump flow ability of UHPFRC with the increase in steel fiber content. Another observation was the improvement in the flowability of UHPFRC with the inclusion of fillers as a partial replacement of cement.

**Abbas et al. (2015)** have investigated the effect of steel fiber length and content on the nechanical and durability properties of UHPC. The fibers length used were 8 mm, 12 mm, 16 mm and contents 1%, 3% and 6% of the volume of concrete. As obvious, the flowabilty of mix reduced slightly with the increase in fiber length and content.

2.3.3. EFFECT OF THE HYBRID FIBER SYSTEM

Hybrid fiber system could be formed with the mixed usage of different shape, size or materials fibers in the concrete. Different types of fibers have different characteristics, therefore, hybrid fibers system has resulted in effective and economical usage of fibers in concrete.

**Yu et al. (2015)** presented a method to develop UHPFRC by the effective utilization of fibers and binders in the design mix using the hybridization design of fibers and the Modified Andreasen and Andersen (Modified A&A) particle packing model. To make an economical and sustainable concrete a fraction of cement was replaced by the limestone powder which was added as a filler material. Nano silica (slurry) incorporated as a pozzolanic material Normal sand of particle size 0 to 2 mm and micro sand of particle size 0 to 1 mm were used. Binder content of 620 kg/m$^3$ was used in this study which is remarkably lower than used in the normal mix design of UHPC. The types of steel fibers used are given in Table 2.2.

Table 2. 2: Physical properties of steel fibers *(Yu R. et al. 2015).*

| Type of Steel fibers | Short straight fiber (SSF) | Long straight fiber (LSF) | Hooked fiber (HF) |
|---|---|---|---|
| Length (mm) | 6 | 13 | 35 |
| Diameter (mm) | 0.16 | 0.2 | 0.55 |

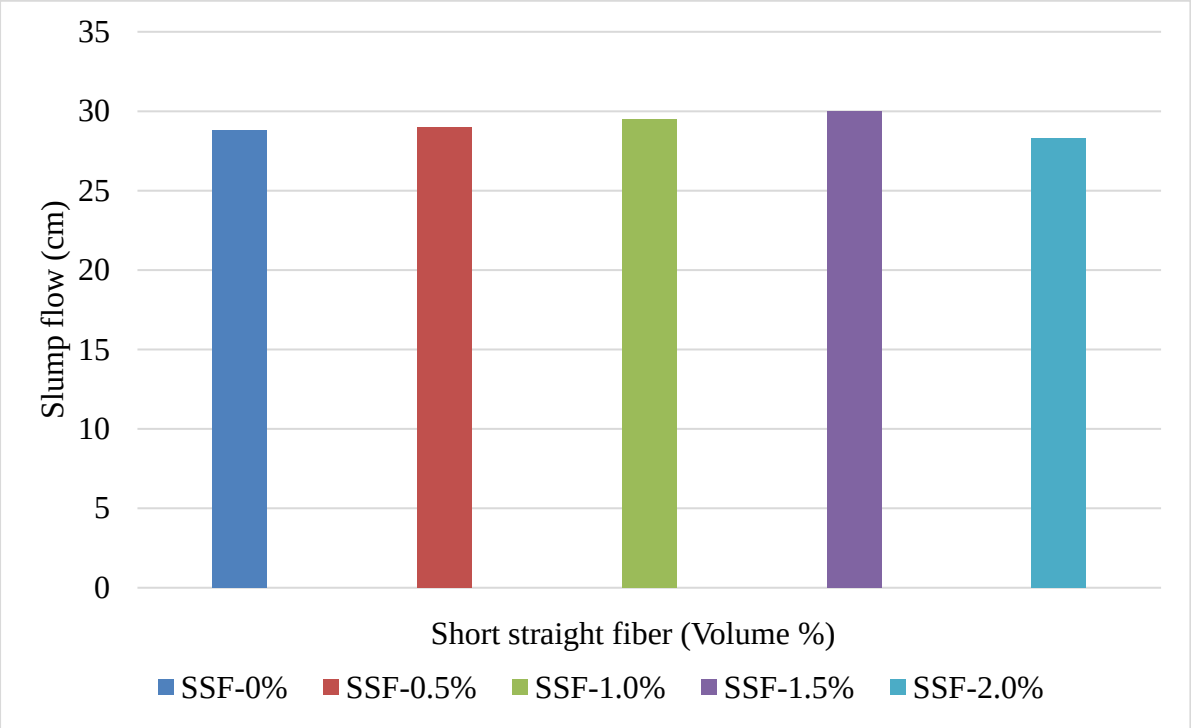


Figure 2. 6: Slump flow value at different percentages of short and long straight steel fibers with a fixed total 2 % volume of fibers *(Yu R. et al. 2015).*

The effects of the different proportions and hybridizations of the steel fibers on the flow ability of the design mix were studied. From the results, it had been clear that all the design mixes can be called as Self compacting mortar as all of them had slump flows greater than 25 cm as shown in Figure 2.6. It has been observed that slump flow first increases with the increase of short straight fibers amount and then suddenly decreases when there were only short straight fibers. The slump flow values of all the mixes with long hooked fibers was nearby 85 cm, which is far more than with straight fibers because different cone size was used for macro hooked fibers. UHPHFRC having long hooked and short straight fibers had the highest slump flow value (88.5 cm). In this study, it has been concluded that hybrid fiber system results in greater workability compared to concrete having a single fiber system.

It has been shown from the previous studies that mineral admixtures like silica and metakaolin decrease the workability of concrete whereas fly ash and GGBS on other hand increases it. The inclusion of fibers decreases the flow ability of UHPFRC especially the steel fibers with higher aspect ratio. From the literature, it is clear that the concrete mix incorporating fibers with higher aspect ratios are less workable even at a lower dosage than the mix having fibers with lower aspect ratio.

## 2.4. MECHANICAL PROPERTIES

UHPFRC is characterized by its excellent mechanical properties like compressive strength above 120 MPa, flexural strength in the range 20 to 50 MPa and uniaxial tensile strength in the range 5 to 10 MPa. Effects of SCMs, single fiber and hybrid fiber system on the mechanical properties of concrete are briefly discussed in this section. Mineral admixture like silica fume and metakaolin improves the mechanical performance of concrete due to its both filler and pozzolanic reactions effect *(Goldman and Bentur 1994).* Filler effect because of very fine particles of these mineral admixtures as compared to cement particles. The pozzolanic effect due to the reaction of siliceous and aluminous components present in these mineral admixtures with calcium hydroxide (byproduct during cement hydration) in presence of water results in additional CSH gel. Mineral admixtures like fly ash and GGBS which are generally of the same size of cement affect the mechanical performance of concrete by pozzolanic reactions only.

### 2.4.1. COMPRESSIVE STRENGTH

In general, concrete performs well in compression but the usage of supplementary cementitious materials, HRWRA, the elimination of coarse aggregates, and the reduction in water cement ratio leads to the formation of concrete having a compressive strength greater than 120MPa. The common ingredients used in the production of UHPFRC are the cement, silica fume, silica sand, quartz powder, steel fibers, superplasticizer, and water. But the cost of some of the ingredients are very high so tremendous research work had been done in the past few decades to find out their replacements. Since the high cost of steel fibers is also an issue so the hybridization of different types of fibers is also looked as a solution to reduce the high material cost of UHPFRC.

*(A) Effect of SCMs*

**Tasdemir (2003)** studied the effect of partial replacement of sand with various mineral admixtures on water sorptivity of concrete. The increasing order of compressive strength was concrete with fly ash, sandstone filler, limestone powder and silica fume. The highest

compressive strength with silica fume could be attributed to its very fine particles (filler effect) and pozzolanic effect. On the other hand, due to a very high particle size of fly ash as compared to silica fume so, the filler effect of fly ash would be very less and also the pozzolanic effect is also low compared to silica fume. Even, the compressive strength of mixes with fly ash and sandstone filler were less than the controlled specimen which could be attributed to the larger particle size of these mineral admixtures as compared to silica fume and limestone filler.

**Ho et al. (2003)** studied the various mixes with different proportions of cement, silica fume, fly ash, GGBS at both standard water curing at 27$^{o}$C and steam curing at 55$^{o}$C for 8 hours (SC8). There had been a 40 % increase in one day compressive strength with steam curing and results are even more remarkable with the incorporation of silica fume. With the incorporation of 20 and 30 % of fly ash as OPC replacement, compressive strength decreases. GGBS, silica fume and silica fume mixed with fly ash specimens at varying proportions of OPC at (SC8) curing condition resulted in a similar range of strength as that of OPC specimens.

**Mazloom et al. (2004)** had studied the effect of silica fume on the compressive strength of HSC. Cement had been replaced by silica fume with 0, 6, 10, 15 percentages. There had been a 21 % increase in compressive strength on 15 % replacement of cement with silica fume at 28 days. Another observation was the same compressive strength of controlled sample and sample having a different amount of silica fume at 400 days. So, silica fume addition in concrete helps in enhancing short term strength only.

**Kou et al. (2011)** had examined the role of silica fume, GGBS, fly ash and metakaolin on the mechanical properties of natural and recycled aggregate concrete. It has been observed that the compressive strength of concrete increases at 10 % and 15 % replacement of cement by silica fume and metakaolin respectively for both natural and recycled aggregate at 28 days. However, at 90 days there is a marginal increase in compressive strength on replacement of cement with these two mineral admixtures.

The compressive strength of concrete decreases at 35 % and 55 % replacement of cement by fly ash and GGBS respectively for both natural and recycled aggregate at 28 days. Even at 90 days, the compressive strength of concrete with fly ash and GGBS were less than controlled, silica fume and metakaolin specimens. But, the strength gain from 4 to 90 days in case of fly ash and GGBs specimens was more than for silica fume and metakaolin specimens. So, it can be concluded that mineral admixtures like silica fume and metakaolin enhance both 28 days

and 90 days strength whereas mineral admixtures like fly ash and GGBS only show their effects after a long period of time.

*(B) Effect of the single fiber system*

**Reda et al. (1999)** had used different types and combinations of fine and coarse aggregates in making UPHC. In this study, 3-6 mm long and 7.6 μm diameter micro carbon fibers were used to improve the mechanical properties of concrete. After casting of 50 mm cubical specimens pressure in the range of 0 to 80 MPa was applied to the fresh concrete. Hot water (HW) curing at 50$^{o}$ C of the samples were done so as to minimize the shrinkage and thermal cracks. Some of the specimens were oven dried (OV) at 200$^{o}$ C two days before testing. The compressive strength of one of the specimens reached 240 MPa, which were oven dried and 80MPa pressure was applied to it. Mixtures containing calcined bauxite aggregates had a very dense microstructure and showed outstanding mechanical strength even with no pressure application. This was attributed to the improved bond between aggregate and the binder paste at an elevated temperature as shown in Figure 2.7. After analyzing compressive strength results of different UHPC mixtures, ones containing micro carbon fibers had shown better compressive strength than with mixtures with no fibers.

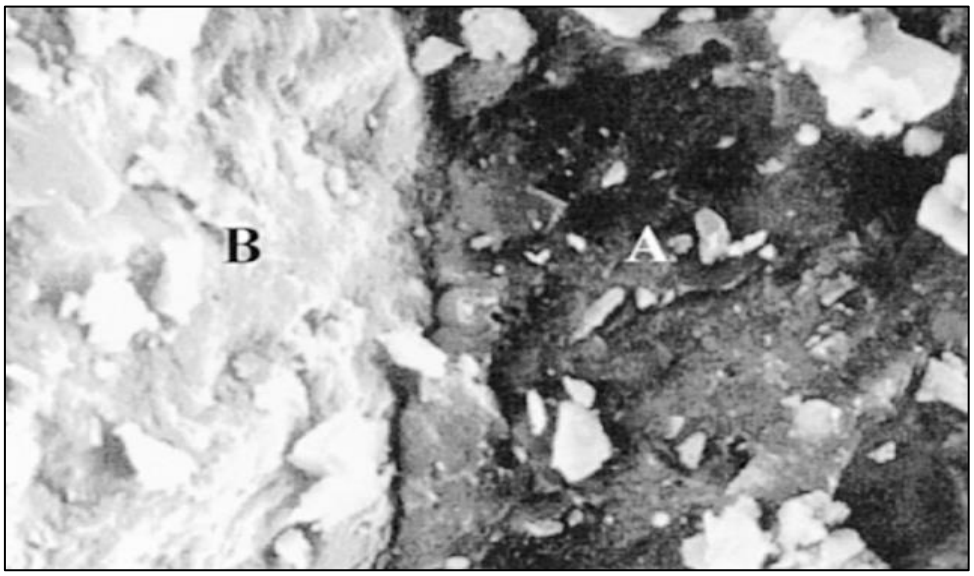


Figure 2.7: SEM Micrograph showing the transition zone in UHPC mixture: (A) aggregate, (B) cement paste. X1210 *(Reda M.M. et al. 1999).*

**Yang et al. (2009)** had tried many possibilities for reducing the cost of UHPFRC mix by replacing generally used expensive silica sand with two locally available natural sand and

recycled glass cullet (RGC). The effect of curing at 20$^{o}$ C and 90$^{o}$ C on mechanical and ductility properties of UHPFRC were also studied.

There is very little variation observed in the compressive strength with the replacement of silica sand with FOS-I (fine ordinary sand type I) and FOS-II (fine ordinary sand type II). The compressive strength of the specimens having SS, FOS-I and FOS-II cured at 20$^{o}$ C were nearby 120 MPa whereas specimens cured at 90$^{o}$ C were in the range 168 to 179 MPa at 28 days. On the other hand, RGC specimens had compressive strength varied from 105 to 155 MPa at 20$^{o}$ C and 90$^{o}$ C curing at 28 days.

The lower strength of UHPFRC having RGC can be attributed to the fact that RGC sand was produced by crushing of large glass particles which could have generated initial micro cracks in the sand particles. The very flat and smooth surface of RGC particles could be the reason for the weak bond between RGC particles and the binder paste.

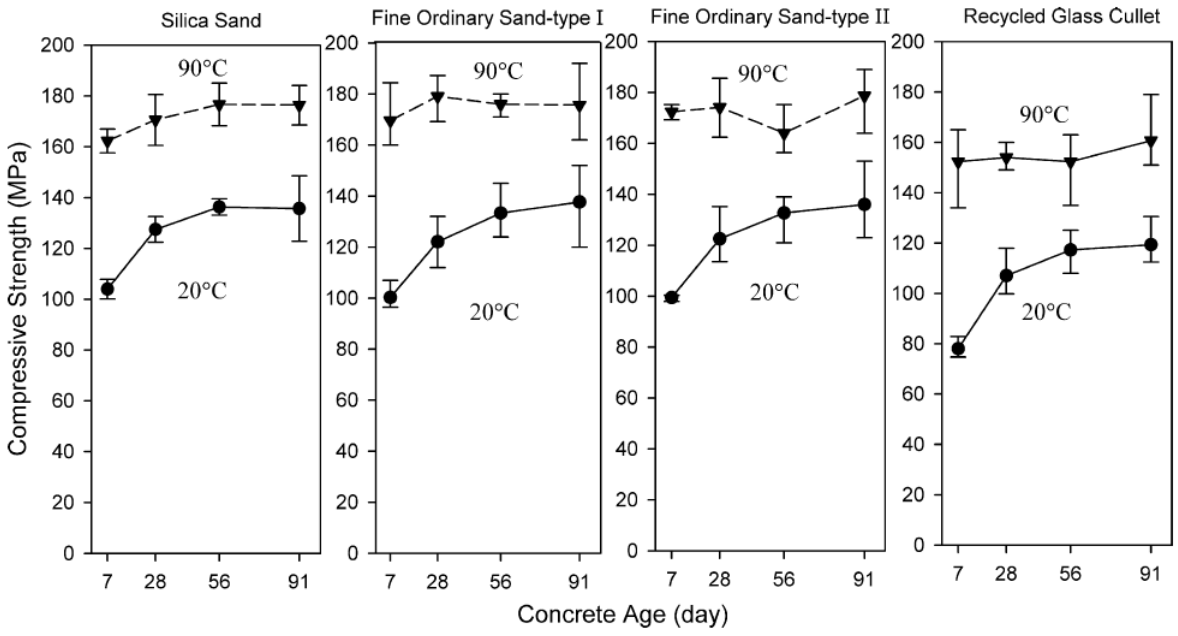


Figure 2. 8: Effect on compressive strength with the substitution of silica sand with FOS (I and II) and RGC *(Yang S.L. et al. 2009).*

**Prem et al. (2012)** have investigated mixes of UHPC reinforced with steel fibers having different aspect ratios (40, 81) and the percentage of fibers (2.0, 2.5). The curing cycle followed includes water curing for the first 3 days after demolding of specimens followed by hot air curing at 200$^{o}$ C for 2 days and again water cured until the age of 28 days. The compression test was performed on 100 mm cubic specimens. It has been observed that the mixes having same fiber volume whatever their aspect ratios result in more than 25 % increment in

compressive strength than that of the control mix having 0 % of fibers. From the results, it was noticed that the compressive strength does not affect much by changing reinforcement index of fibers.

**Abbas et al. (2015)** have examined the effect of steel fiber length and content on the nechanical and durability properties of UHPC. The fibers length used were 8 mm, 12 mm, 16 mm and contents 1%, 3% and 6% of the volume of concrete. It is observed that there had been a marginal increase in compressive strength with the inclusion of steel fibers but the fiber length had no appreciable influence on the compressive strength of the UHPC specimen. Another important observation was that the sudden explosive behaviour of UHPC without fibers changes to ductile behaviour with the addition of steel fibers.

*(C) Effect of the hybrid fiber system*

**Yu et al. (2015)** presented a method to develop UHPFRC by the effective utilization of fibers and binders in the design mix using the hybridization design of fibers and the Modified Andreasen and Andersen (Modified A&A) particle packing model. As previously discussed, binder content of 620 kg/m$^3$ was used in this study which is remarkably lower than used in the normal mix design of UHPC. The compressive strength results demonstrated that with the addition of steel fibers remarkably increases the compressive strength. Further, UHPC with hybrid long straight fibers (1.5% volume of concrete) and short straight fibers (0.5% volume of concrete) showed the maximum compressive strength as illustrates in Figure 2.9.

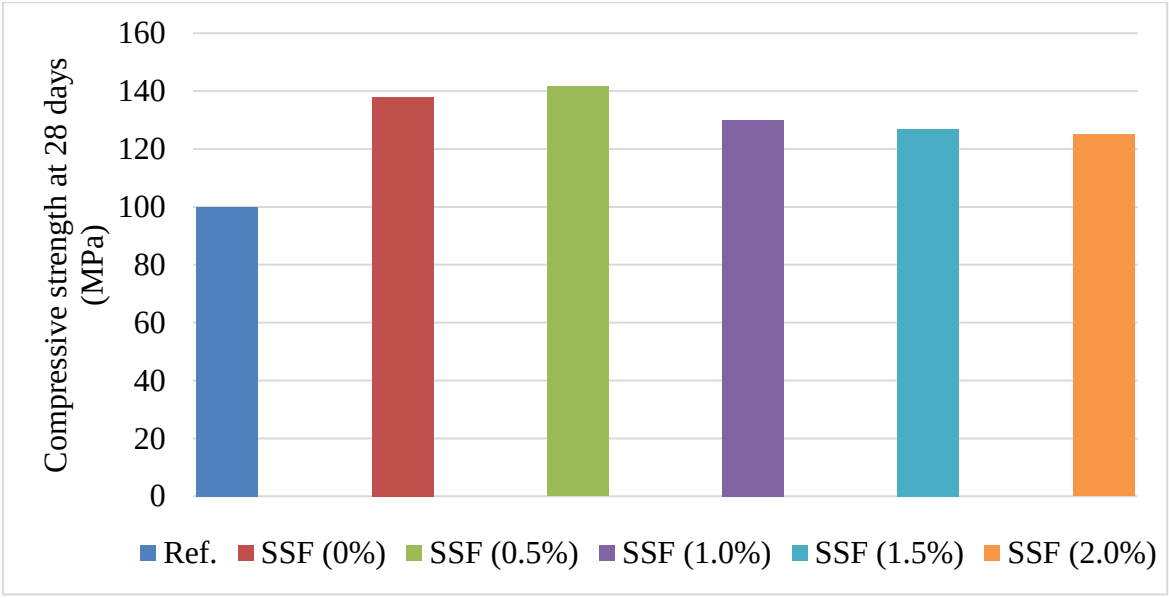


Figure 2.9: Compressive strength of the mixes with only straight steel fibers (Ref.: UHPFRC without fibers) *(Yu R. et al. 2015).*

Also, UHPC with long hooked fibers hybrid with short straight fibers results in more compressive strength than hybridization with long straight fibers as shown in Figure 2.10. This can be attributed to a larger number of SSF than LSF for the same volumetric amount which results in the more homogeneous concrete mix. Form the test results, it has been shown that even with a comparatively less binder and fiber content, UHPFRC could be made using the Modified A & A model and hybrid fibers.

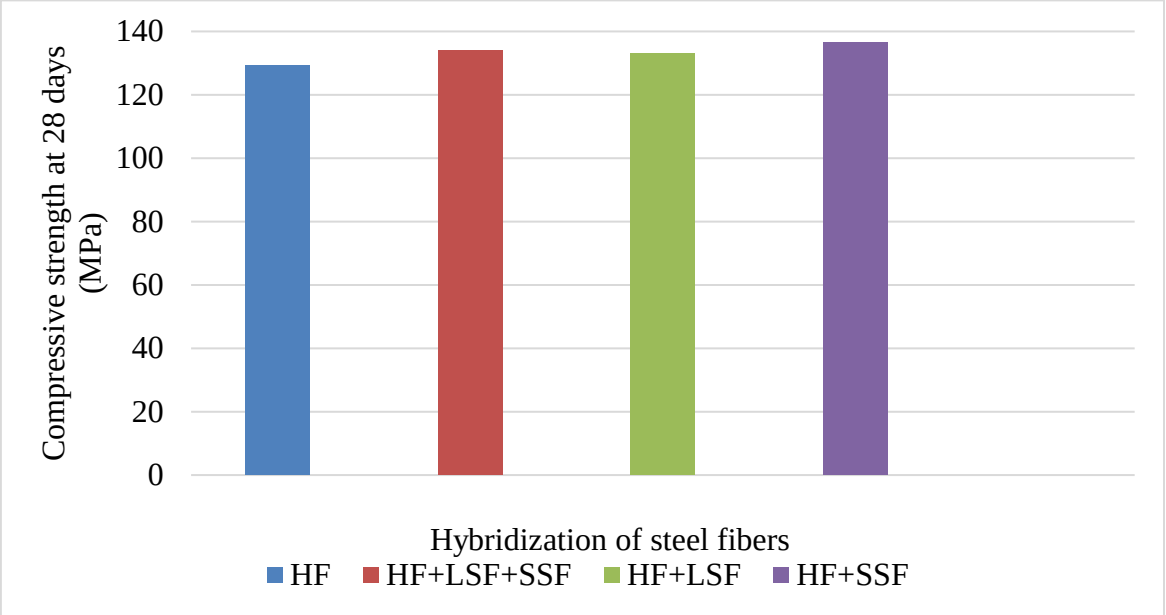


Figure 2. 10: Compressive strength of the mixes with straight and hooked steel fibers *(Yu R. et al. 2015).*

**Alkaysi et al. (2016)** had produced UHPFRC with three different types of cement and varying the silica fume quantity from 0 to 25% of the cement weight. The main objective of this study was to determine the effect of various material parameters on the durability properties of non-registered mixtures of UHPFRC.

Table 2. 3: Mix proportions of various mixes of UHPFRC *(Alkaysi M. et al. 2016).*

| Name | C | SF | Sp | Fiber (%) | F100 | F12 | Comp. Strength (MPa) |
|---|---|---|---|---|---|---|---|
| | White | | | | | | |
| W-25 | 1 | 0.25 | 0.25 | 1.5 | 0.26 | 1.06 | 195 |
| W-15 | 1 | 0.25 | 0.15 | 1.5 | 0.29 | 1.14 | 188.8 |

| | | | | | | | |
|---|---|---|---|---|---|---|---|
| W-00 | 1 | 0.25 | 0 | 1.5 | 0.31 | 1.26 | 173.6 |
| | Portland type V | | | | | | |
| V-25 | 1 | 0.25 | 0.25 | 1.5 | 0.26 | 1.05 | 174.3 |
| V-15 | 1 | 0.25 | 0.15 | 1.5 | 0.28 | 1.14 | 187.4 |
| V-00 | 1 | 0.25 | 0 | 1.5 | 0.31 | 1.26 | 177.8 |
| | Type I/GGBS | | | | | | |
| IG-25 | 1 | 0.25 | 0.25 | 1.5 | 0.26 | 1.06 | 172.9 |
| IG-15 | 1 | 0.25 | 0.15 | 1.5 | 0.28 | 1.14 | 181.2 |
| IG-00 | 1 | 0.25 | 0 | 1.5 | 0.31 | 1.26 | 190.9 |

The mix proportions of different UHPCs are given in Table 2.3. Portland Type I white cement, Portland Type V, and 50–50 blend of Portland Type I and GGBS are three types of cement used. Two grades of silica sand used are F100 (10% of the particles are greater than 300 μm and 90% are smaller than 1000 μm) and F12 (10% of the particles are greater than 50 μm and 90% are smaller than 300 μm). The compressive strength of all the mixes is more than 170 MPa as given in Table 2.3.

It can be concluded from the previous studies that mineral admixtures like silica fume, metakaolin remarkably increases the short term compressive strength of concrete whereas fly ash and GGBS decreases it. The cement content in UHPFRC could be reduced with the usage of fillers without much effect on the compressive strength. There is an increase in the compressive strength of UHPC on the addition of fibers. Short crimped or hooked fibers are more effective in compression than long straight fibers. But at higher contents of steel fibers, compressive strength was not affected much *(Reda et al. 1999; Schmidt et al. 2003).* The reason being an excessive concentration of steel fibers results in the bundling of fibers which leads to the development of weak spots and ultimately compressive strength could be reduced.

### 2.4.2. SPLIT TENSILE STRENGTH

Since the brittle failure of UHPC had been a major limitation in the practical application of UHPC but with the introduction of fiber reinforced UHPC this behaviour has transformed from

brittle to ductile behaviour. Short fibers enhance the tensile strength of UHPFRC and the macro fibers are more effective in enhancing the ductility and hence the requirement of reinforcements could be eliminated. As a result of which UHPFRC could be better alternate material for difficult structural shapes.

*(A) Effect of SCMs*

**Kou et al. (2011)** had examined the role of silica fume, GGBS, fly ash and metakaolin on the split tensile strength of natural and recycled aggregate concrete. It has been observed that split tensile strength of concrete increases at 10 % and 15 % replacement of cement by silica fume and metakaolin respectively for both natural and recycled aggregate at 28 days. However, at 90 days there is a marginal increase in split tensile strength on replacement of cement with these two mineral admixtures. The reason for improved tensile strength could be due to the formation of the dense matrix because of both filler and pozzolanic effect of these mineral admixtures at interfacial transition zone.

*(B) Effect of the single fiber system*

**Prem et al. (2012)** have investigated mixes of UHPC reinforced with steel fibers having different aspect ratios and percentage of fibers. The curing regime has already been discussed previously in this literature review. The inclusion of steel fibers in UHPC had resulted in excellent tensile behaviour test. The split tensile strength at 2.5% fiber volume increased by more than 200% than that of the control mix. Long fibers showed a greater tensile strength than short fibers.

**Khater and Ahmed (2016)** had developed UHPC using natural crushed basalt (grading in the range between 1.18 to 10 mm) and desert fine sand.

Table 2. 4: Physical properties of steel fibers used in this study *(Khater, H., and Ahmed, S. 2016).*

| Type of Steel fibers | Hooked fiber (HF1) | Hooked fiber (HF2) |
|---|---|---|
| Length (mm) | 50 | 30 |
| Diameter (mm) | 1 | 1 |
| Aspect ratio | 50 | 30 |

Types of steel fibers used are given in Table 2.4. With the addition of 1 % steel fibers, the increase in split tensile strength was 34 %. At 3 % steel fibers (aspect ratio 50) split tensile strength increases by 66 % compared to 0 % fibers mix. Another observation was the brittle failure of UHPC without fibers and large ductile failure of UHPC with fibers.

*(C) Effect of the hybrid fiber system*

**Mohammadi et al. (2008)** had studied the effect of hybrid corrugated steel fibers of 20 (fiber length 25 mm) and 40 (fiber length 50 mm) aspect ratios on the split tensile strength of concrete. The total fiber content varied were 1, 1.5 and 2 % with different fractions of short and long fibers. It had been found that with increasing fiber content, there is an increase in split tensile strength of concrete. The maximum increase in strength was of 59 % with respect to controlled specimen (0 % fiber content) at 2 % fiber content (35 % long and 65 % short fibers).

From the previous studies it can be concluded that with the incorporation of steel fibers, the tensile strength of UHPC increases drastically. More advantageous is the transformation of failure mode from brittle to ductile. Fibers with its concrete holding capacity do not allow splitting of the specimen into two halves even after attainment of peak load which is due to post cracking behaviour of fiber reinforced concrete

### 2.4.3. FLEXURAL STRENGTH

High flexural strength is one of the characteristics of UHPFRC. The reason for high flexural strength is the dense matrix and uniform distribution of steel fibers. Tremendous research had been done in the past few decades to see the effect of replacement of partial cement with filler materials on the flexural strength of UHPFRC.

The Orientation of fibers is the key for the flexural strength of UHPFRC. Vertically casted specimens resulted in five times lesser flexural strength than horizontally casted because of parallel and perpendicular orientation of fibers to the crack surface for vertically and horizontally casted specimens respectively *(Steil et al. 2004).*

*(A) Effect of SCMs*

**Köksal et al. (2008)** examined the effect of incorporation of silica fume and steel fibers on the flexural strength of HSC. With the increase in the silica fume content, flexural strength of the concrete increases. The maximum increase was 64.9 % with respect to controlled specimen (0 % silica fume) at 15 % silica fume content.

**Yardımcı et al. (2009)** studied the effect of different curing regime on the flexural strength of concrete incorporating various mineral admixtures. It had been found that the flexural strength of concrete decreases with both with steam and autoclave curing. The reduction during steam curing is more than autoclave curing. This could be attributed to the reduction in bond strength between concrete paste and fibers. With the inclusion of GGBS and/ or fly ash, there had been an enhancement in flexural strength at all curing regime.

*(B) Effect of the single fiber system*

**Yang et al. (2009)** had tried many possibilities for reducing the cost of UHPFRC mix by replacing generally used expensive silica sand with two locally available natural sand and recycled glass cullet (RGC). The effect of curing at 20$^{o}$ C and 90$^{o}$ C on mechanical and ductility properties of UHPFRC were also studied.

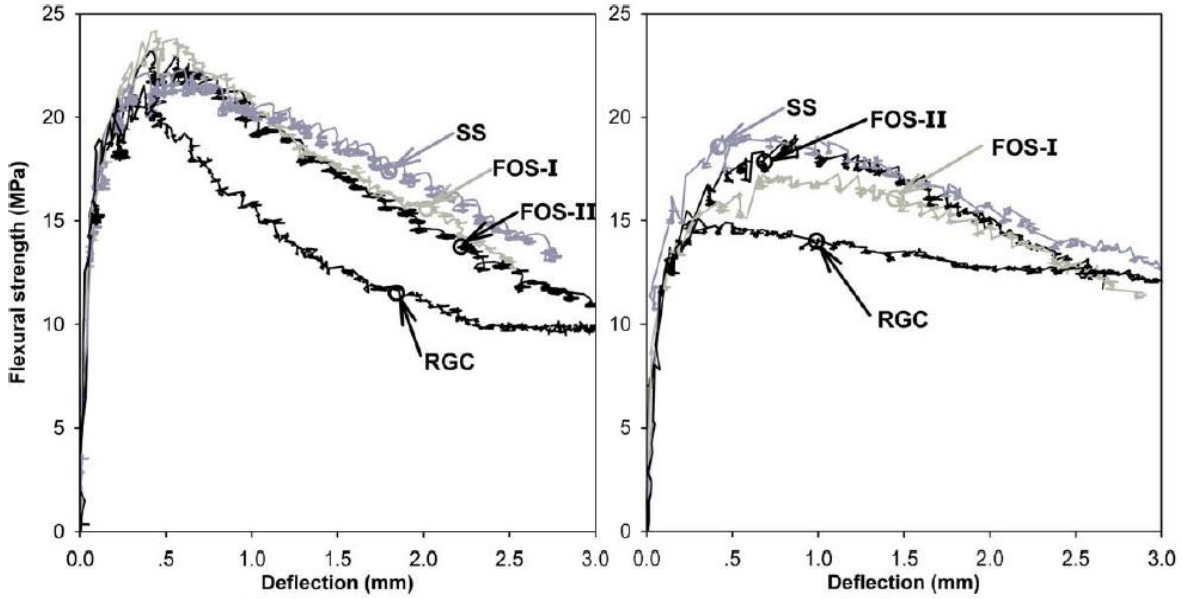


(A) (B)

Figure 2. 11: Flexural strength (MPa) versus deflection (mm) curve of specimens (50*50*200 mm) cured at (A) 90$^{o}$ C (B) 20$^{o}$ C *(Yang S.L. et al. 2009)*

It has been observed that 90$^{o}$ C cured specimens to have higher flexural strength but also the steeper decreasing rate of flexural stress after reaching ultimate value than that of 20$^{o}$ C cured specimens as shown in Figure 2.11. There is not much difference observed in the flexural strength of silica sand UHPFRC specimens and both types of ordinary sand UHPFRC specimens but glass cullet UHPFRC specimens showed 10% lesser flexural strength. The reason being more porous RGC UHPFRC specimens than SS and ordinary sand as indicated

by the density measurements of the hardened concrete specimens. Flexural strength of the specimens cured at 90$^{o}$ C did not vary much with age and only 4 MPa increase of strength is observed for all the types of sand UHPFRC flexure specimens from 7 to 56 days of curing as shown in Figure 2.12.

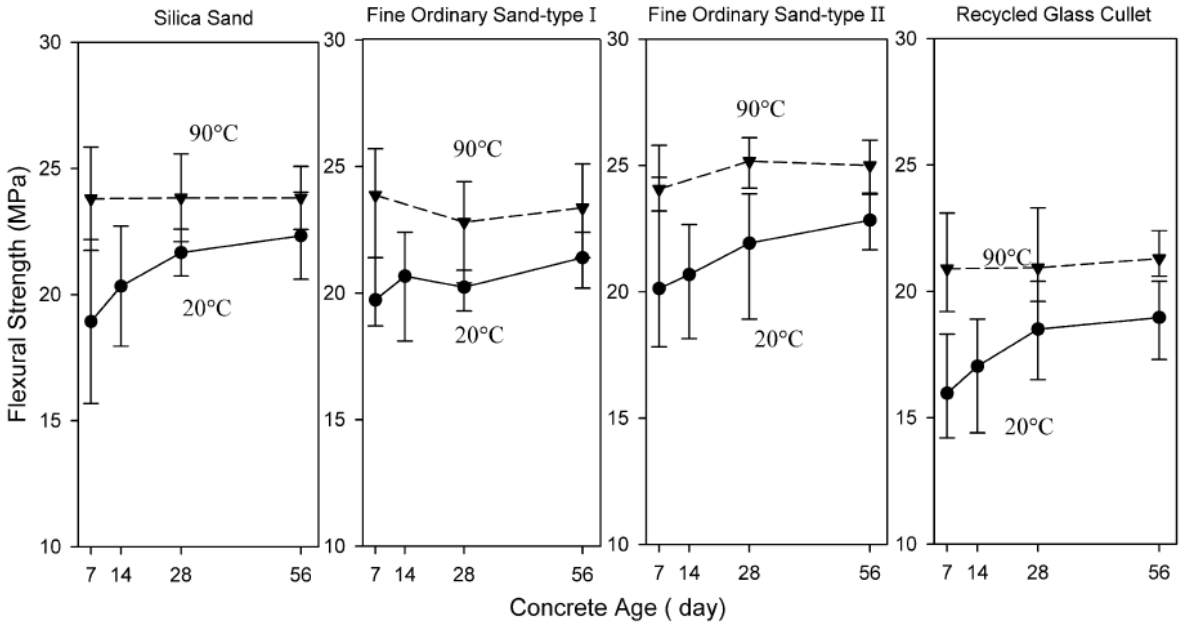


Figure 2. 12: Effect on flexural strength with the substitution of silica sand with FOS (I and II) and RGC *(Yang S.L. et al. 2009).*

**Prem et al. (2012)** have investigated mixes of UHPC reinforced with steel fibers having different aspect ratios and percentage of fibers. The curing regime has already been discussed previously in this literature review. A simply supported beam is tested under third point loading to determine the flexural strength of UHPC. A linear relationship is observed between the flexural strength of the mixes and the reinforcement index. The flexural strength at 2.5% fiber volume increased by 275% than that of the control mix. So, the purpose of inclusion of steel fibers in UHPC to enhance the tensile strength has been fulfilled effectively.

**Yu et al. (2014)** had developed a mix design of concrete based on the Modified A&A particle packing model with the replacement of partial cement with fillers (limestone and quartz powder). Short straight steel (SSF) fibers of length 13 mm and diameter 0.2 mm were used in this study. Three different types of UHPFRC mixtures were designed with varying cement content as discussed previously. The flexural strength improvement ratio was small at lower fiber percentages but it at a higher percentage of steel fibers (2.5 % volume of concrete) flexural strength improvement ratio was as high as 129.34 %. It had been found that UHPFRC having

flexural strength around 27 MPa could be produced with only 650 kg/m$^3$ of binder content as compared to the reference mixture having a flexural strength of 33.5 MPa with 919 kg/m$^3$ of binder content. There is nearly a 20% reduction in flexural strength on reducing the binder content by 29 %. With the reduction in binder content there is a reduction in the cost of production of UHPFRC and strength, so a balance could be made between the economy and the required strength.

*(C) Effect of the hybrid fiber system*

**Yu et al. (2015)** presented a method to develop UHPFRC by the effective utilization of fibers and binders in the design mix using the hybridization design of fibers and the Modified Andreasen and Andersen (Modified A&A) particle packing model.


Figure 2. 13: Flexural strength of the mixes with straight and hooked steel fibers (Reference: UHPFRC without fibers) *(Yu R. et al. 2015).*

As previously discussed, binder content of 620 kg/m$^3$ was used in this study which is remarkably lower than used in the normal mix design of UHPC. The test results demonstrated that with the addition of steel fibers significantly increases the flexural strength. The increase in strength depends on the various hybridization of fibers. Further, UHPC with hybrid long straight fibers (1.5% volume of concrete) and short straight fibers (0.5% volume of concrete) showed the maximum flexural strength as illustrates in Figure 2.13. On the other hand, UHPFRC with only short straight fibers had a flexure strength of 21.5 MPa at 28 days. This can be attributed to the fact that short fibers are better oriented when hybrid with long fibers, than on their own.

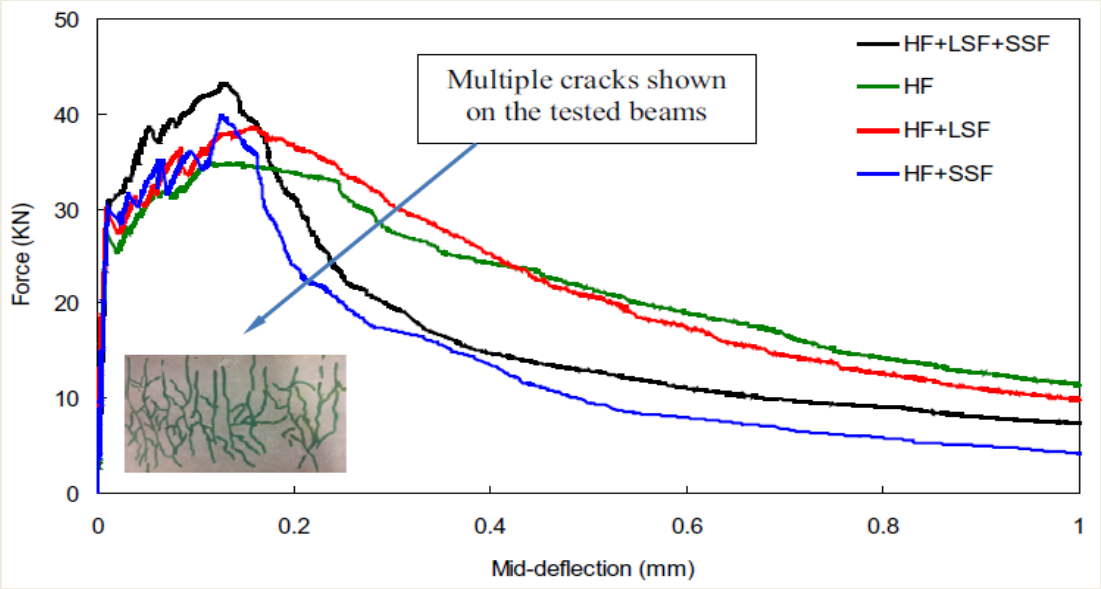


Figure 2. 14: Flexure test results of UHPFRC beams with various combinations of hooked fibers with other types of fibers *(Yu R. et al. 2015).*

From the load and mid span deflection curve as shown in Figure 2.14, it is observed that first crack loads for all the hybrid fibers concrete mixes are almost same and greater than mix with only hooked fibers. The peak load during the flexure tests is maximum for the ternary fibers reinforced concrete mix. It has been observed that endurance force of UHPC reinforced with only short straight fibers or hybrid with long fibers steeply declines after reaching peak load than with only long hooked fibers or hybrid with long straight fibers. Though short straigth fibers work effectively in limiting the growth of microcracks but are less effective after reaching peak load, which is due to a shorter length and lower binding force with the concrete mix than the long or hooked fibers.

From the previous literature, it has been observed that the addition of mineral admixtures resulted in an increase in flexural strength. Also, UHPFRC having short fibers hybrid with long fibers performed better in flexural than only short fiber system. The endurance force of UHPC having short fibers only decreases steeply rather than a gradual decrease of UHPC having long fibers. Though short straigth fibers work effectively in limiting the growth of microcracks but are less effective after reaching peak load, which is due to a shorter length and lower binding force with the concrete mix than the long or hooked fibers. There is not much difference observed in the flexural strength of silica sand UHPFRC specimens and ordinary sand UHPFRC specimens.

## 2.5. DURABILITY PROPERTIES

UHPFRC is characterized by its excellent durability properties. The reason for high durability properties of UHPC is due to the remarkable decrease in the number and size of pores *(Heinz and Ludwig 2004; Herold and Muller 2004).* Porosity in UHPC is reduced mainly by reducing the water binder ratio and due to heat curing. The filler effect and pozzolanic effect of mineral admixtures improve the microstructure of concrete. Application of pressure is also a major tool in the reduction of porosity of UHPC because it significantly reduces the entrapped air and the extra water in the mix *(Richard and Cheyrezy 1995; Bonneau et al.1997).* The role of fibers on durability properties of concrete is minimal.

### 2.5.1. SORPTIVITY

Due to dense pore structure, UHPFRC exhibit very low water absorption capacity which varies from 10 to 60 times lesser than that of High Performance Concrete and Normal Strength Concrete, respectively *(Schmidt et al. 2005).*

*(A) Effect of SCMs*

**Tasdemir (2003)** studied the effect of partial replacement of sand with various mineral admixtures on water sorptivity of concrete. The water sorptivity coefficients were higher for mixes with fly ash and sandstone filler as compared to the controlled specimen. The reason being the coarse particles of these mineral admixtures as a result of which the pores are not filled completely and consequently increases more water adsorption. Microfiller materials like silica fume and limestone powder fill the capillary pores and results in low sorptivity.

**Ho et al. (2003)** studied the various mixes with different proportions of cement, silica fume, fly ash, GGBS at both standard water curing at 27$^{o}$C and steam curing at 55$^{o}$C for 8 hours (SC8). The (SC8) curing condition resulted in the formation of very porous OPC, fly ash and GGBS mixes as water absorption values were twice that obtained at normal water curing (27$^{o}$C) at 3 days. Although GGBS mix at high strength levels shows a lower rate of water absorption but silica fume specimens showed the lowest water absorption. It had been concluded that the incorporation of silica fume in concrete could be seen as a better product for the precast industry due to its higher early age strength and durability performance.

*(B) Effect of the single fiber system*

**Prem et al. (2012)** have investigated mixes of UHPC reinforced with steel fibers having different aspect ratios and percentage of fibers. The curing regime has already been discussed previously in this literature review. This test was performed on 100 mm diameter and 50 mm

height cylinders. From the results, it was concluded that more sorptivity is induced in th UHPC with the presence of fibers. It could be attributed to the increase in the porosity at the fiber and cement matrix.

**Abbas et al. (2015)** have investigated the effect of steel fiber length and content on the nechanical and durability properties of UHPC. As previously discussed the length of the fiber used were 8 mm, 12 mm, 16 mm and contents 1%, 3% and 6% of the volume of concrete. The sorptivity values obtained during the water sorptivity test were lower than that of HPC and normal concrete. It has been observed that sorptivity coefficients were not affected much by fiber length. At a higher dosage of fibers, sorptivity coefficients decreased appreciably. It can be attributed to the reduction of less connected pores with the inclusion of higher percentages of fibers amount resulting in denser microstructure and hence improved durability performance.

**Ramezanianpour et al. (2013)** studied the effect of inclusion of polypropylene fiber on the water sorptivity of concrete. The water sorptivity coefficients for all polypropylene fiber reinforced concrete specimens were found be less than the controlled specimen (0 % fibers). With the addition of fibers firstly, sorptivity coefficient decreases and then after 9 kg/m$^3$ of fiber content it started to increase. The increase in water sorptivity could be attributed to a significant increase in air content with the after a certain limit of the addition of fibers.

*(C) Effect of the hybrid fiber system*

As per the author knowledge, a study on the effect of hybrid fiber system on water sorptivity of HPC or UHPC has not been done it now.

From the previous literature, it can be concluded that with the addition of fibers could increase or decrease the water sorptivity depending upon whether the addition of fibers causes an increase in the air content or breaks the continuity of pores respectively.

2.5.2. RAPID CHLORIDE PERMEABILITY

Chloride ion permeability basically depends upon the exposure solution and period of exposing, water binder ratio and the curing conditions *(Thomas et al. 2012; Scheydt et al. 2012).*

*(A) Effect of SCMs*

**Kou et al. (2011)** had examined the role of silica fume, GGBS, fly ash and metakaolin on the chloride ion permeability of natural and recycled aggregate concrete. It has been observed that resistance to chloride ion permeability of concrete increases with the inclusion of these mineral admixtures. The replacement of cement with these mineral admixtures are 10 %, 15 %, 35 %,

55 % by silica fume, metakaolin, fly ash and GGBS respectively. The increasing order of resistance to chloride penetration is silica fume, metakaolin, fly ash, and GGBS specimens. The excellent performance of GGBS to resistance against chloride ion penetration could be attributed to the latent hydraulicity reaction of this mineral admixture, which densifies the microstructure of concrete *(Yeau and Kim 2005).* Hence, it can be concluded that silica fume and metakaolin can enhance both the mechanical and durability properties whereas fly ash and GGBS can remarkably improve the durability properties of the concrete.

**Uysal et al. (2012)** studied the effect of partial replacement of cement with various mineral admixtures on chloride ion permeability. There had been an increase in the resistance against chloride ion penetration with an increase in the replacement percentage of cement with all the mineral admixtures. GGBS specimens showed the best result against chloride ion resistance. After that fly ash specimens performed better. Both being the pozzolanic admixture performed better than fillers (marble, basalt and limestone powder).

**Alkaysi et al. (2016)** had produced UHPFRC with three different types of cement and varying the silica fume quantity from 0 to 25% of the cement weight. The main objective of this study was to determine the effect of various material parameters on the durability properties of non-registered mixtures of UHPFRC.

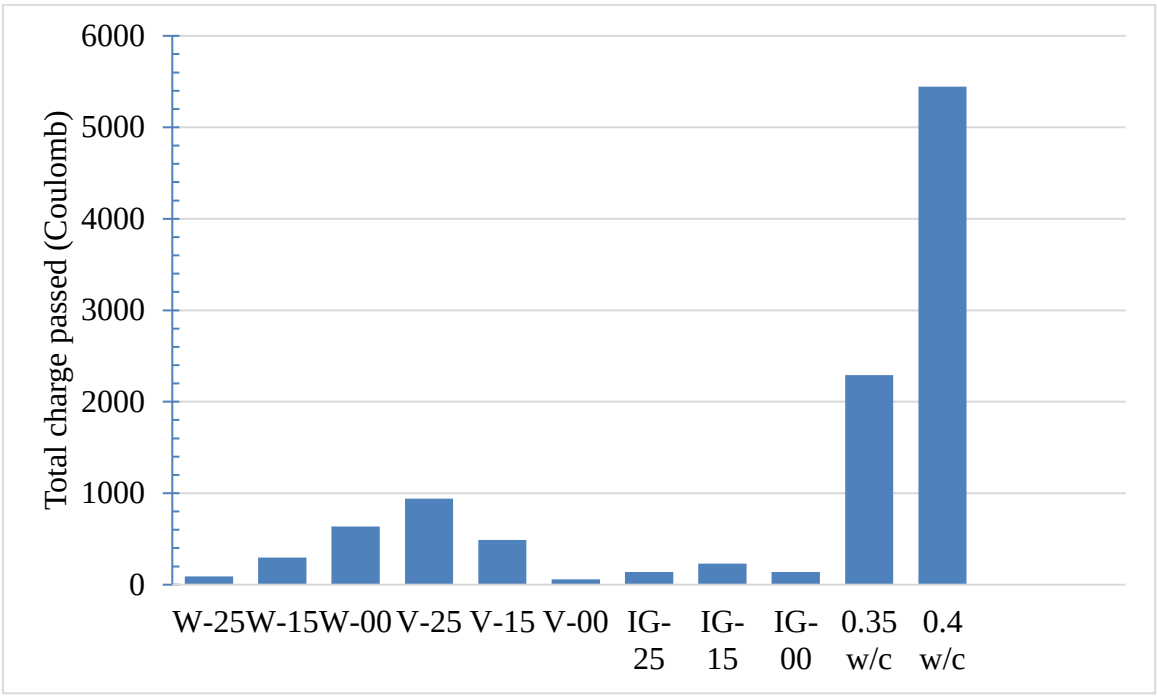


Figure 2. 15: Total charge passed in Coulombs for UHPC and RC mix *(Alkaysi M. et al. 2016).*

UHPC mixes with all the three types of cement and different silica fume percentages exhibit excellent resistance to chloride penetration as shown in Figure 2.15. Maximum resistance to chloride ion penetration is shown by Portland Type I/GGBS Cement blend after which white cement and then by Portland type V cement specimens of UHPFRC. Concretes incorporating 0% silica powder performed the best in chloride resistance than all other percentages.

*(B) Effect of the single fiber system*

**Prem et al. (2012)** have investigated mixes of UHPC reinforced with steel fibers having different aspect ratios and percentage of fibers. The curing regime has already been discussed previously in this literature review. According to *ASTM, C. 1202-12 (2012).* 50mm thick slice of 100mm diameter cylinder was used for this test. From the experimental results, it has been observed that UHPC with fibers is more resistant to chloride ion permeability than without fibers. This may be attributed to the filling of pores by the micro fibers.

*(C) Effect of the hybrid fiber system*

**Blunt et al. (2015)** studied the effect of polyvinyl alcohol (PVA) and two hooked steel fibers with different aspect ratios on the corrosion behaviour after cyclic flexural loading. The incorporation of hybrid fibers had resulted in a reduction in corrosion rate. This could be attributed to the hybrid fibers system which causes the replacement of large cracks by small micro cracks. Whereas, the control specimen (without fibers) after cyclic flexural loading results in the formation of large cracks which causes an increase in the corrosion rate.

From the previous literature, it was observed that the addition of mineral admixtures resulted in enhanced durability performance. Along with that, the problem of short circuiting with the usage of steel fibers could be eliminated with the usage of short steel fibers and random disconnected distribution of fibers *(Graybeal 2006; Ahlborn et al. 2008).* Thermal treatment results in better chloride ion permeability than water cured samples.

# CHAPTER 3

# MATERIALS AND EXPERIMENTAL TESTS

## 3.1. GENERAL

In this chapter, various types of materials used and their physical and chemical properties are discussed. The fresh and hardened tests performed on the proposed mix design of HPHFRC and their testing procedures as per codal provisions are also discussed.

## 3.2. MATERIALS

To determine the material properties of the ingredients used in the production of UHPFRC, relevant codes of practice were followed. The various ingredients used were 53 Grade Ordinary Portland Cement (OPC 53), silica fume, GGBS, Natural sand, Indian standard sand, potable water, High performance super plasticizer, two types of steel fibers. Testing of materials used is very important to check whether the materials used are in accordance with their relevant codes of practice. Also, some of the materials properties like specific gravity are required for mix design of any concrete.

### 3.2.1. ORDINARY PORTLAND CEMENT

OPC 53 Grade from ACC Cement plant in Bilaspur, Himachal Pradesh was used throughout the course of this study.


Figure 3. 1: 53 Grade OPC cement used in the present study.

There were no lumps observed which indicate the freshness of cement. The physical properties of the cement obtained are compared with the physical requirements for 53 grade OPC as per

*IS 12269, 2013 (Table 3)* are given in Table 3.1. A plastic sheet was warped around cement bags to prevent cement from dampness.

Table 3. 1: Properties of OPC 53 Grade.

| Characteristics | Values Obtained Experimentally | Value Specified by *IS 12269: 2013* | Test method Referred to code |
|---|---|---|---|
| Specific Gravity | 3.12 | - | *IS 4031 Part 11* |
| Standard Consistency (%) | 30 | - | *IS 4031 Part 4* |
| Setting Time (minutes) | | | *IS 4031 Part 5* |
| Initial | 120 | 30 (Minimum) | |
| Final | 320 | 600 (Maximum) | |
| Compressive Strength ($N/mm^2$) | | | *IS 4031 Part 6* |
| 3 Days | 30.40 | 27 | |
| 7 Days | 41.35 | 37 | |
| 28 Days | 55.20 | 53 | |

3.2.2. SILICA FUME

Silica fume was obtained from Haryana ceramics Pvt. Ltd., Ambala city. The physical and chemical properties of silica fume as provided by the supplier are given in Table 3.2 and Table 3.3 respectively.

Table 3. 2: Physical properties of Silica fume provided by the supplier.

| Characteristics | Value |
|---|---|
| Color | White |
| Specific gravity | 2.25 |

| | |
|---|---|
| $D_v$ (50) | 16.209 µm |

Table 3. 3: Chemical Composition of silica fume provided by the supplier.

| $SiO_2$ | MgO | $SO_3$ | $H_2O$ | $K_2O$ | $Na_2O$ | CaO | Si | Cl | $Fe_2O_3$ |
|---|---|---|---|---|---|---|---|---|---|
| 92.25% | <1.5% | <1.1% | <0.4% | <2.25% | <1.4% | <0.35% | <0.5% | <0.06% | <2% |

3.2.3. AGGREGATES

The largest fractions of the aggregate have been discarded by most of the researchers since long to have a more homogenous UHPFRC mix. In this study two types of fine sand were used as given below:

*3.2.3.1. Indian standard sand*

As per *IS 650 (1991)* the Indian standard sand shall be procured from Ennore, Tamil Nadu.

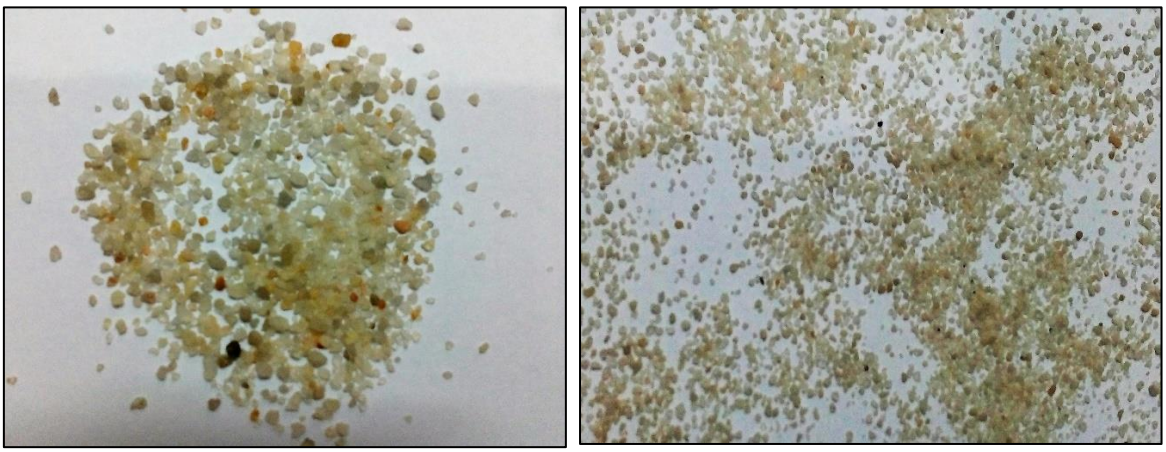

(A) (B)

Figure 3. 2: Indian standard sand (A) Grade II (B) Grade III.

The Indian standard sand is divided into following three types based on particle size distribution:

- Grade I (particle fraction lies between 2 to 1 mm)
- Grade II (particle fraction lies between 1 to 0.5 mm)
- Grade III (particle fraction lies between 0.5 to 0.09 mm)

In the previous studies, generally, sand of size less than 1 mm had been used in the development of UHPFRC. Therefore in this study, Grade II and Grade III standard sand from TAMIN (Tamil

Nadu Minerals Ltd.) are used in mix design of HPFRC. The calculated value of the Fineness modulus (FM) obtained was 2.109 (see Table 3.4) which lies in the range of 2.2 to 2.6 and hence, signifies fine sand.

Table 3. 4: Sieve analysis of Indian standard sand (Grade II and III).

| IS-Sieve size in microns | Weight retained(g) | % wt. retained | Cumulative % wt. retained | Cumulative % wt. passing |
|---|---|---|---|---|
| 1180 | 0 | 0 | 0 | 100 |
| 600 | 260 | 26 | 26 | 74 |
| 300 | 599 | 59.9 | 85.9 | 14.1 |
| 150 | 131 | 13.1 | 99 | 1 |
| 90 | 6 | 0.6 | 99.6 | 0.4 |
| Pan | 4 | 0.4 | - | - |
| Total | 1000 | | $\sum F = 210.9$ | |
| | | | FM = 210.9 / 100 = 2.109 | |

*3.2.3.2. Natural sand*

This sand was a river sand obtained from Pathankot, Punjab and has conformed to Grading Zone II as per *IS 383 (1970).* Fine aggregates are divided into four Grading Zones (I to IV) and fineness of aggregates progressively increases from Zone I to IV. Sieve analysis of graded natural sand is given in Table 3.5. In this study, sand particles only in the range between 1180 μm and 90 μm were used in the formation of HPHFRC. To have a comparative study between Indian standard sand (Grade II and III) and normal river sand, Natural sand in the particles size range 90 to 600 μm and 600 to 1180 μm are mixed in equal proportion in the mix design of HPFRC. The physical properties of Standard sand and Natural sand are given in Table 3.6. The calculated value of FM of Natural sand obtained was 2.076 (see Table 3.5) which is lower than 2.2 hence, signifies very fine sand.

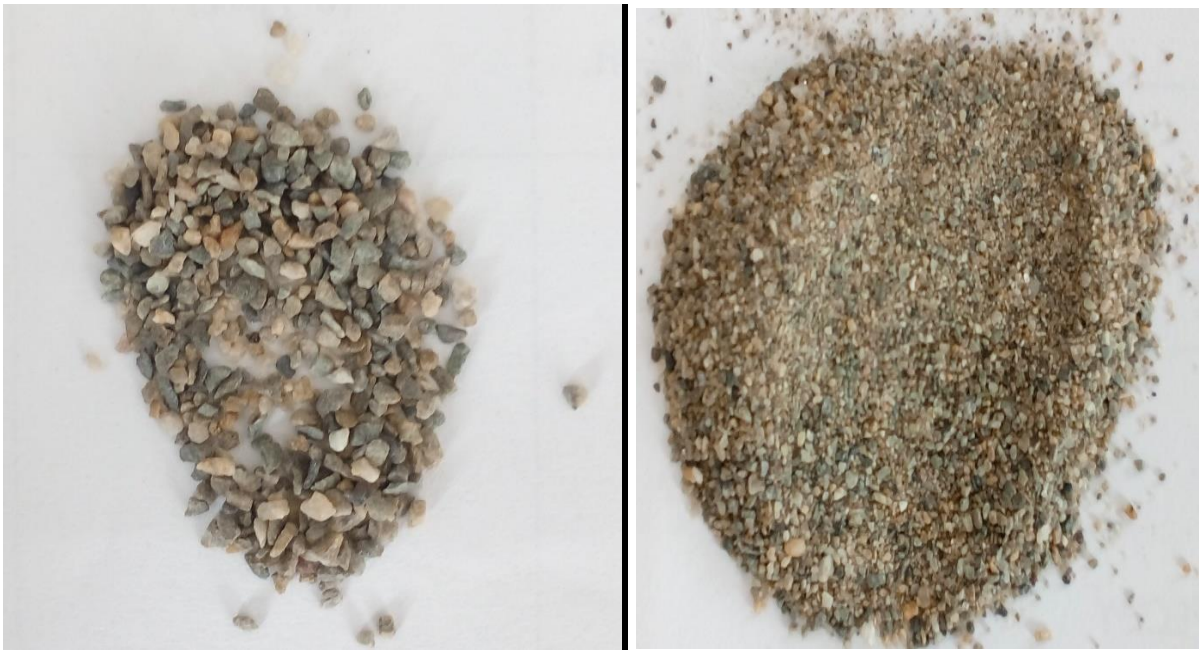

Figure 3. 3: Natural sand graded as Indian standard sand (A) Grade II (B) Grade III.

Table 3. 5: Sieve analysis of Natural sand

| IS-Sieve size in microns | Weight retained(g) | % wt. retained | Cumulative % wt. retained | Cumulative % wt. passing |
|---|---|---|---|---|
| 1180 | 0 | 0 | 0 | 100 |
| 600 | 382 | 38.2 | 38.2 | 61.8 |
| 300 | 374 | 37.4 | 75.6 | 24.4 |
| 150 | 182 | 18.2 | 93.8 | 6.2 |
| 90 | 62 | 6.2 | 100 | 0 |
| Pan | 0 | 0 | - | - |
| Total | 1000 | | ∑F = 207.6 | |
| | | | FM = 207.6 / 100 = 2.076 | |

Table 3. 6: Physical properties of Standard sand and Natural sand.

| Characteristics | Indian Standard sand | Natural sand(graded) |
|---|---|---|
| Specific gravity | 2.64 | 2.55 |
| Water Absorption | 0.80 % | 0.97 % |
| Fineness Modulus | 2.109 | 2.076 |
| Average silicon content | 35.01 | 27.35 |

3.2.4. GGBS (GROUND GRANULATED BLAST FURNACE SLAG)

Alccofine-1203 or GGBS had been taken from Ambuja Cement Ltd., Mumbai (ALCCOFINE MICRO MATERIALS RANGE). The physical and chemical properties of GGBS as provided by the supplier are listed in Table 3.7 and Table 3.8 respectively.

Table 3. 7: Physical properties of Alccofine-1203.

| Characteristics | Value |
|---|---|
| Colour | Grey |
| Specific gravity | 3.1 |
| Bulk density | 680 kg/$m^3$ |
| Specific Surface Area | 3709 $m^2$/kg |
| Dv (10) | 0.612 μm |
| Dv (50) | 3.458 μm |
| Dv (90) | 8.271 μm |

Table 3. 8: Chemical composition of Alccofine -1203.

| Chemical compound | CaO | $SiO_2$ | $Al_2O_3$ | $Fe_2O_3$ | MgO |
|---|---|---|---|---|---|
| Percentage | 33.8 | 34.2 | 22.7 | 1.8 | 6.6 |


Figure 3. 4: Alccofine-1203

3.2.5. STEEL FIBERS

The two types of steel fibers are used in this study that had been provided by Stewols India (P) Ltd, Nagpur, India.

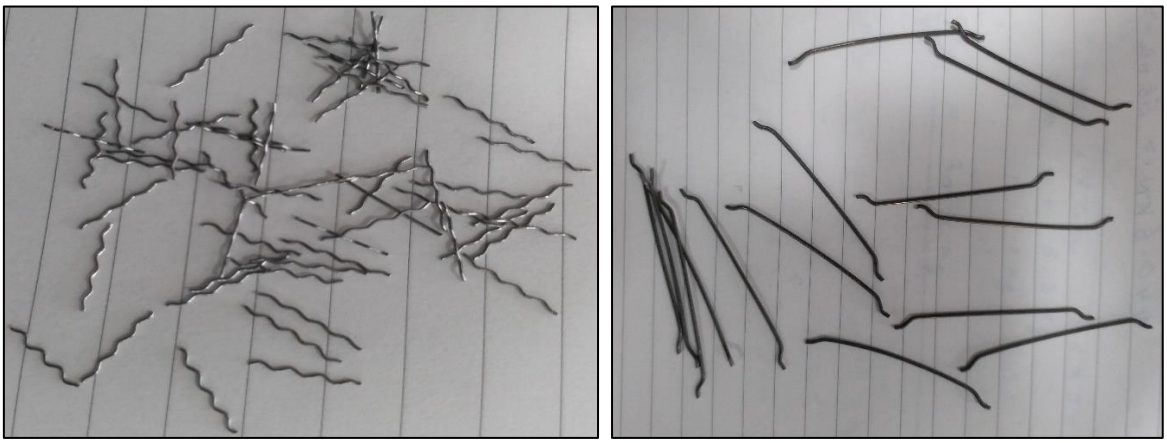

(A) (B)

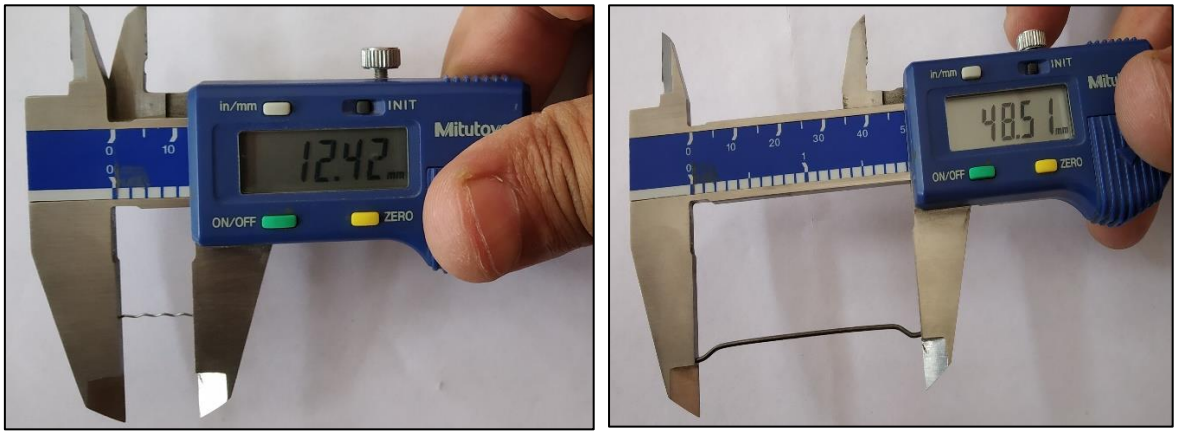


(C) (D)

Figure 3. 5: (A) Short crimped fibers (SCF) (B) Long hooked fibers (LHF) (C) SCF length measurement (D) LHF length measurement.

Table 3. 9: Properties of hybrid steel fibers as provided by the supplier.

| Properties | Type I | Type II |
|---|---|---|
| Shape | Crimped | Hooked |
| Length | 12.44 | 48.48 |
| Diameter | 0.44 | 0.94 |
| Tensile strength (MPa) | >1100 | >1100 |
| Aspect ratio | 28.27 | 51.57 |

3.2.6. SUPERPLASTICIZER (HIGH RANGE WATER REDUCING ADMIXTURE)

MasterGlenium SKY 8233 is the superplasticizer used throughout the course of this study was provided by BASF Construction Chemical Pvt Ltd, Nalagarh, Himachal Pradesh. It is a new generation of admixture based on polycarboxylic ether (PCE). It makes rheoplastic concrete workable more than 45 minutes at 25°C. Workability loss depends on cement type, temperature, transportation method, and initial workability. PCE can reduce water requirement by up to 40 %.

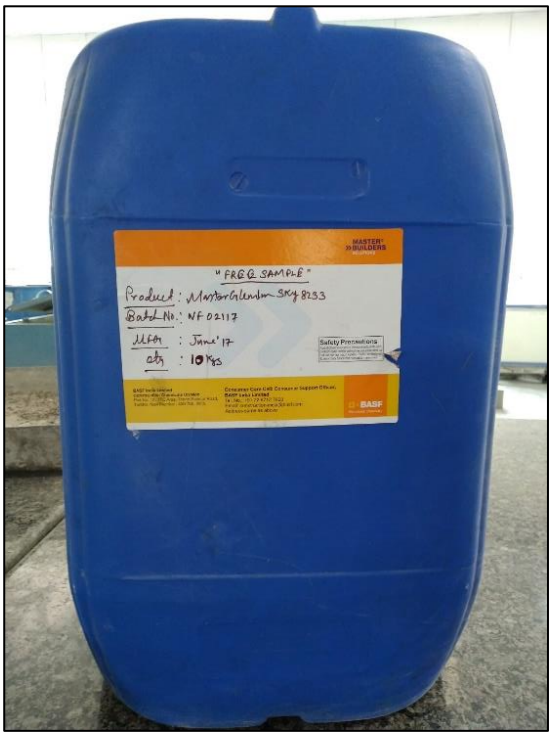


Figure 3. 6: MasterGlenium SKY 8233 (superplasticizer) used in this study.

Table 3. 10: Properties of superplasticizer as provided by the supplier.

| Characteristics | Value |
|---|---|
| Specific Gravity | 1.08 |
| Relative Density | 1.08± 0.01 at 25ºC |
| Colour | Reddish Brown Liquid |
| Chloride ion content | < 0.2% |
| pH | ≥ 6 |

3.2.7. WATER

Water is an essential and cheapest ingredient in concrete. Since potable water is considered satisfactory to be used in mixing and curing of concrete, so the potable tap water in the laboratory was used in both mixing and curing of concrete.

## 3.3. PREPARATION OF SAMPLE

The constituent materials for HPHFRC were weighted as per mix design and placed in the separate container. Digi mortar mixer of 5 liter nominal capacity was used for mixing the ingredients for the preparation of samples. At first, cement and silica fume were added to the mixer and mixed for 5 minutes. Then with the addition of sand mixing was continued for another 5 minutes at low speed till uniform colour was seen. Water and superplasticizer were mixed separately in a beaker and nearly 70 % of the solution was added in the mixer slowly through the opening provided at its top right corner. The Digi mortar mixer was programmed to rotate firstly at low speed (140 rpm) for 1 minute and then automatically rotate at high speed (285 rpm) for ½ minute. After 5 cycles of this rotation, the remaining solution of water and superplasticizer was added in the mixer and again 5 cycles were completed. Then, the mix was poured into a tray and both the types of steel fibers are uniformly sprayed and the whole mix was mixed with the trowel so that fibers are uniformly mixed.

The long length of the hooked steel fibers was the reason for the manual mixing as fibers got struck in the mixing paddle of the small capacity Digi mortar mixer. After proper mixing, fresh concrete was filled in the properly oiled molds of cube size 70.6 * 70.6* 70.6 mm for compression test, prism size 40* 40* 160 mm for flexure test, cylinder size 100 mm (diameter) * 200 mm (height) for split tensile, Rapid Chloride Permeability and water sorptivity test.


Figure 3. 7: Digi mortar mixer

After casting some vibration was provided to ensure uniform distribution of fibers. Due to the high flowability of this concrete, not much finishing of the surface was required. In the end, moist jute bags were placed over the specimens for 24 hours. After 24 hours, specimens were removed from the moulds and were placed in the curing tank filled with potable water at 23 ± 2$^{o}$C. The specimens were kept in the same condition until the day of testing.

## 3.4. TEST METHODS

To study the effect of replacement of Indian standard sand with graded normal sand, various fresh, mechanical and durability tests were performed on the proposed mix designed HPHFRC. Along with that, the microstructure study was also done.

### 3.4.1. FRESH PROPERTIES

There have been numerous properties of fresh concrete but the most influential one is the workability. Production of HPHFRC is totally dependent on the workability of the mix for the uniform distribution of fibers.

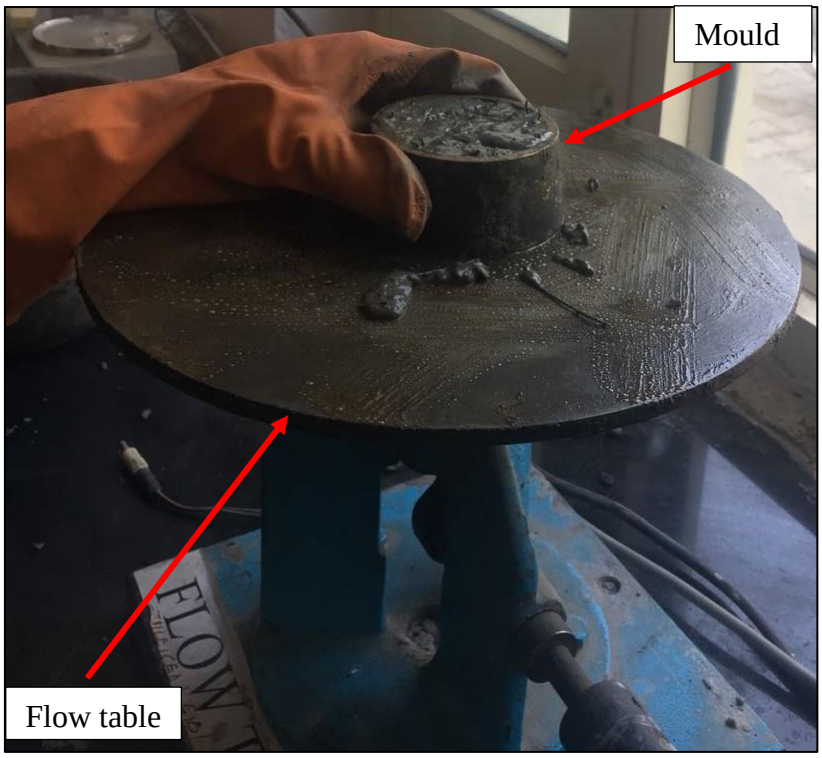


Figure 3. 8: Flow table test.

ASTM C1437 code was referred to study the flowability of HPFRC. The diameter of flow table used was 300 mm. Fresh HPFRC mixture was poured into the mould placed on the flow table. The mould used was a conical frustum having a height of 40 mm with a top diameter of 70 mm and a bottom diameter of 80 mm. After lifting the mould, in a time period of 15 seconds, the table was dropped 25 times. Two diameters are measured of the UHPFRC mixture spread. Flow value of the mix is calculated by:

$$\text{Flow } (\%) = \left(\frac{D_{av} - D_o}{D_o}\right) 100$$

Where $D_{av}$ is the average base diameter of the mix

$D_o$ is the original base diameter.

3.4.2. MECHANICAL TEST

Mechanical test performed in this study are compressive strength, split tensile strength, and flexural strength of UHPFRC.

*3.4.2.1. Compressive strength*

Compressive strength was tested as per *IS: 4031-6 (1988)* at 7 and 28 days using at least three 70.6 mm cube specimens as shown in Figure 3.12 (A). The specimens were tested on CTM

(500 tons capacity) as shown in Figure 3.12 (B). Loading was applied at the rate of 35 N/mm$^2$/min.

(A) (B)

Figure 3. 9: (A) 70.6 mm cubical specimen (B) Testing of cube specimen in CTM.

The peak load shall be recorded and compressive strength was calculated by the formula:

$$f = \frac{M}{A}$$

Where, f = Compressive strength (N/mm$^2$)

M = Maximum load (N)

A = Cross- sectional area of the specimen (mm$^2$)

*3.4.2.2. Split tensile strength*

For the determination of split tensile strength 100 (diameter)* 200 (length) mm cylindrical specimens were tested in CTM as shown in Figure 3.13. The load was applied along the length of the cylindrical specimen until failure. The rate of loading should lie between 1.2 to 2.4 N/mm$^2$/min as per *IS: 5816 (1999).* Two packing strips of hardboard was provided at top and bottom of the specimen so as to lessen the magnitude of compressive stresses in the region of application of load. The split tensile strength was calculated using the formula:

$$f_{sp} = \frac{2\,P}{\pi\, l\, d}$$

Where P is the peak load (N),

l is the length of the specimen, and

d is the cross sectional dimension of the specimen

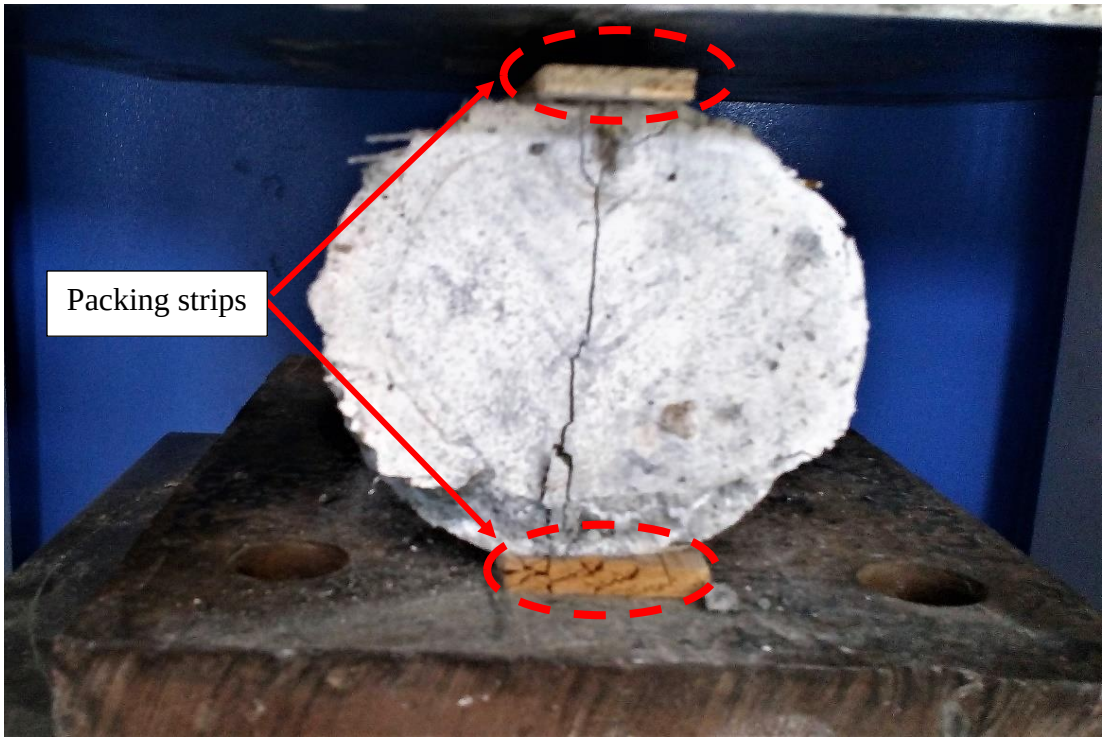


Figure 3. 10: Arrangement and testing of cylindrical specimens in CTM.

*3.4.2.3. Flexural strength*

Flexural strength is also called as Modulus of rupture. To determine the flexural strength of the UHPFRC, prismatic specimens of size 40 * 40 * 160 mm were tested on UTM (Universal Testing Machine) as shown in Figure 3.15.

(A) (B)

Figure 3. 11: (A) Mould for flexure specimen (B) Casted flexure specimens.


Figure 3. 12: Arrangement and testing of the flexural beam.

The rate of loading should be 50 ± 10 N/second as per *EN: 196-1 (1994).* The effective length of the flexural specimen was taken as 120 mm. With the usage of digital dial gauge, mid span deflection is measured at corresponding load values. The arrangement of the dial gauge is shown in Figure 3.15. Under central point loading, the flexural strength was calculated using the formula:

$$f_f = \frac{3\,P\,L}{2\,B\,D^2}$$

Where $f_f$ is the modulus of rupture (MPa)

P is the peak load (N)

L is the span length (mm)

B is the average width of the specimen at fracture (mm)

D is the average depth of the specimen at fracture (mm)

### 3.4.3. DURABILITY TEST

Durability is the resistance of concrete to chemical attack and weathering action so as to remain serviceable for the design life. The durability performance of any concrete depends basically on the easiness of the movement of fluid through it. Concrete in which there is difficulty in the ingression or permeability of fluids results in a durable concrete. Durability test performed in this study are water sorptivity and Rapid Chloride Permeability Test (RCPT).

#### *3.4.3.1. Water sorptivity test*

This test was performed by calculating the increase in the specimen weight with respect to time when only one surface was exposed to water. It is used to calculate the absorption rate of water of both the concrete surface and interior portion.

Table 3. 11: Time and tolerances for the measurements of the mass of the specimen *(ASTM C1585 – 04).*

| Time | Tolerance in time |
|---|---|
| 60 seconds | 2 seconds |
| 5 minutes | 10 seconds |
| 10 minutes | 2 minutes |
| 20 minutes | 2 minutes |
| 30 minutes | 2 minutes |
| 60 minutes | 2 minutes |
| Every hour up to 6 hours | 5 minutes |
| Once a day up to 3 days | 2 hours |
| Day 4 to 7, three measurements 24 hours apart | 2 hours |
| Day 7 to 9, one measurement | 2 hours |

For water sorptivity test, 100 * 200 mm casted cylindrical specimens at the age of 7 and 28 days were cut to the size 100 (diameter) * 50 mm (length) as specified in the *ASTM C1585 – 04* (see Figure 3.16 (A)). The specimens were then placed in an environmental chamber at 50$^{o}$C and relative humidity of 77 % for 3 days. After that, the specimens were stored in a container

for 15 days. After removing the specimen from the container, its mass was recorded and its diameter was measured at four locations. The side surfaces were sealed with epoxy and surface not to be exposed to water were sealed with a plastic sheet as shown in Figure 3.16 (B) and Figure 3.17.

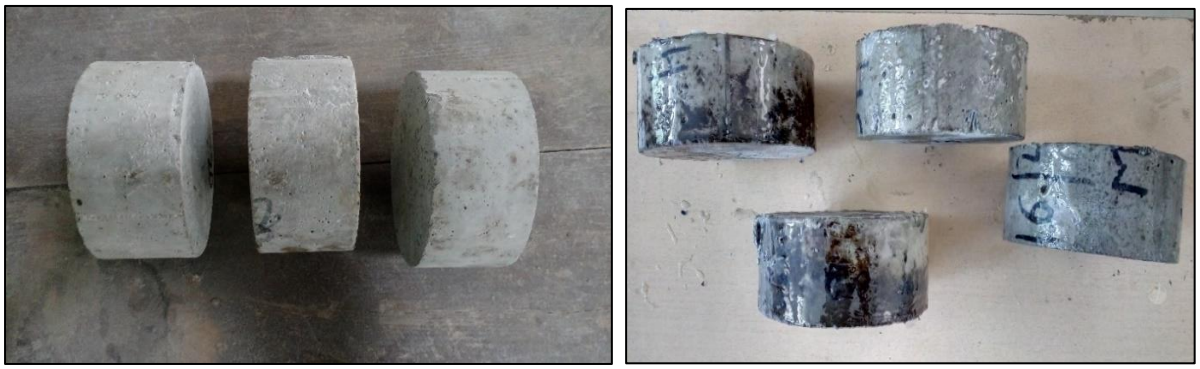

(A) (B)

Figure 3. 13: (A) 50 mm cylindrical slice of 100 mm diameter (B) Epoxy coated specimens.

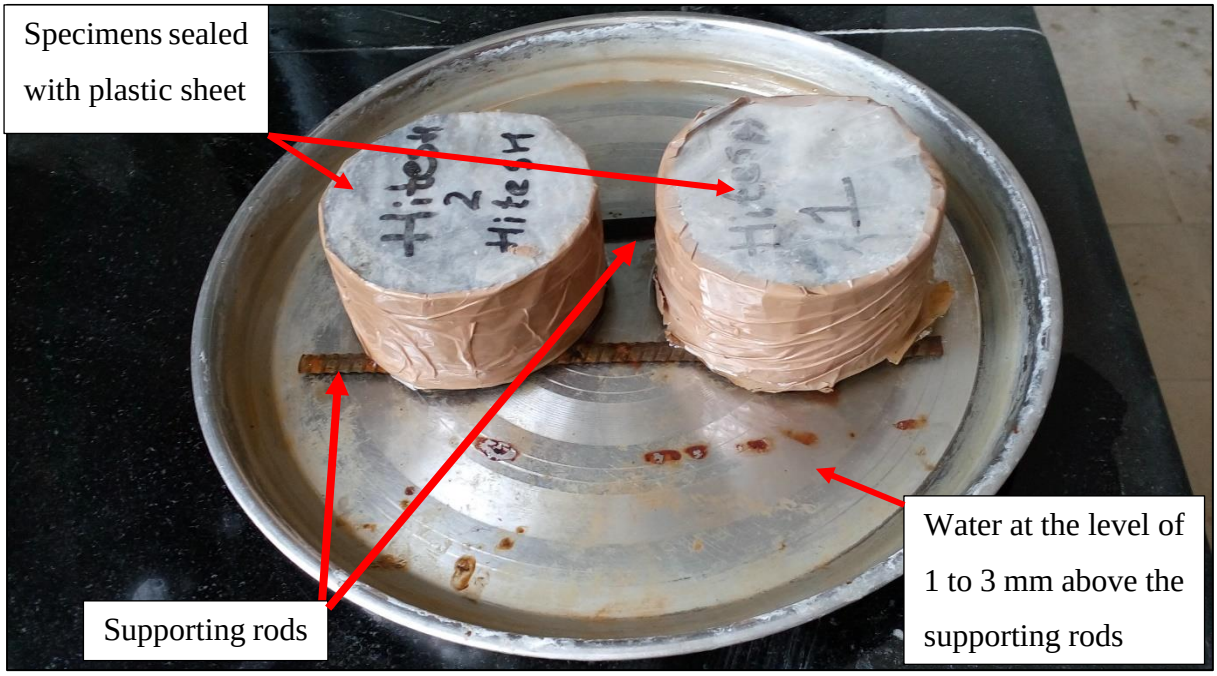


Figure 3. 14: Arrangement for water sorptivity test.

The mass of the sealed specimen was measured and referred to as initial mass of the specimen for this test. Water was maintained at a level 1 to 3 mm above the top of the supporting rods placed in the pan as shown in Figure 3.17. The specimens were placed on the supports along with that stopwatch was started. The mass of the specimen was recorded at the time intervals

as given in Table 3. 14. At each measurement, wiping out any surface water was done with a dampened cloth. After taking a measurement, place back the specimen at the supports.

*3.4.3.2. Rapid Chloride Permeability Test*

*ASTM C1202 – 12* had been referred to perform this test. This test method is used to get a quick manifestation of concrete specimen resistance to penetration of chloride ion by the laboratory assessment of the concrete specimen electrical conductance. The 50 mm length slice was cut from 100 (diameter) * 200 mm (length) cylindrical sample to perform this test as shown in Figure 3.18.


Figure 3. 15: 50 mm length cylindrical slice of 100 mm diameter for RCPT.

Figure 3. 16: Whole arrangement and testing during RCPT.

Epoxy was applied to the sides of specimens and then epoxy was dried, specimens were put in the vacuum chamber for three hours. The specimens were vacuum saturated for one hour and let to soak for eighteen hours. After which the specimens were placed in the test device as shown in Figure 3.19.

On the one side of the test cell 3% NaCl solution was filled and on the other side, 0.3N NaOH solution was filled. Potential of 60-volt was applied for 6 hours after the system was connected. Values (charge passed in coulombs) were noted every 30 minutes. At the end of the test after 6 hours the sample was taken out from the test cell and the total charge passed in coulombs was noted.

Table 3. 12: Permeability based on charge passed *(ASTM C1202 – 12).*

| Charge Passed (in coulombs) | Chloride ion Penetrability | Typical of |
|---|---|---|
| >4000 | High | High W/C ratio (>0.60) conventional PCC |
| 2000-4000 | Moderate | Moderate W/C ratio (0.40–0.50) conventional PCC |
| 1000-2000 | Low | Low W/C ratio (<0.4) conventional PCC |
| 100-1000 | Very Low | Latex-modified concrete or internally-sealed concrete |
| <100 | Negligible | Polymer-impregnated concrete, Polymer concrete |

### 3.4.4. MICROSTRUCTURE TESTS

At some stage, the characteristics of all materials are associated to their microstructure. For a better understanding of the mechanical and durability properties of any concrete, microstructure analysis plays a significant role. The various techniques used in the present study are Scanning Electron Microscopy (SEM), Energy Dispersive Spectroscopy (EDS), X-Ray Diffraction (XRD), Thermo–gravimetric (TG) and Differential Scanning Calorimetry (DSC).

*3.4.4.1. Thermo–gravimetric (TG) and Differential Scanning Calorimetry (DSC)*

TG is a method for determining the change in mass of a sample with a change in temperature under controlled atmosphere. DSC is a method for measuring the heat flow into or from the sample during programmed heating in a controlled environment. A small sample was taken of both HPC (SS) and HPC (NS) which was crushed and sieved through 75 micron sieve. A sample mass of about 50 mg was placed in an alumina crucible. The test had been conducted at the heating rate 5$^{o}$C /minute from 29$^{o}$C to 1000$^{o}$C under nitrogen environment with a flow rate of 50 ml/minute.

*3.4.4.2. Scanning Electron Microscopy and Energy Dispersive Spectroscopy*

SEM is an important aspect of microstructure study. This technique was used to analyze topography, morphology, and composition (CSH gel, calcium hydroxide, ettringite, monosulfate, sand and steel fibers) of HPHFRC samples at very high magnification. Along with that Energy dispersive spectroscopy was used for chemical analysis of the samples. EDS had been performed on the same samples for elemental identification and their relative concentrations.

A polished sample of 8 mm square side with 2 mm thickness had been analyzed for SEM. To enhance the image signal, an electrically conductive coating of gold had been applied to the sample. Secondary electron mode of imaging had been used.

*3.4.4.3. X-Ray Diffraction*

XRD analysis is used for identification of minerals, compounds, and crystalline phases. Powder method of XRD was adopted in this study. Every diffraction phase has its own diffraction image but weak peaks are observed for amorphous phases. A small sample (excluding steel fiber) was taken of both HPC (SS) and HPC (NS) which was crushed and sieved through 90 micron sieve. The range of diffraction angle (2 $\theta$) for analysis was 10$^{o}$ to 80$^{o}$ using Fe filtered Co K$\alpha$ radiation.

# CHAPTER 4

# MIX DESIGN OF HPHFRC

In this chapter, the design mix methodology adopted for mix design of HPFRC is discussed. For the mix design of HPHFRC, Modified Andreasen and Andersen particle packing model was adopted. Also, the experimental work was done to validate the designed mix.

## 4.1. MODIFIED ANDREASEN AND ANDERSEN PARTICLE PACKING MODEL

Modified A & A particle packing model is based on the principle of attainment of optimum particle packing by a continuous grading of all the solid ingredients in the mix. Since very fine materials were used in the mix design of HPHFRC in the present study so, Mastersizer 3000 model using laser diffraction technique had been used to determine the particle size distributions of the constituent materials.

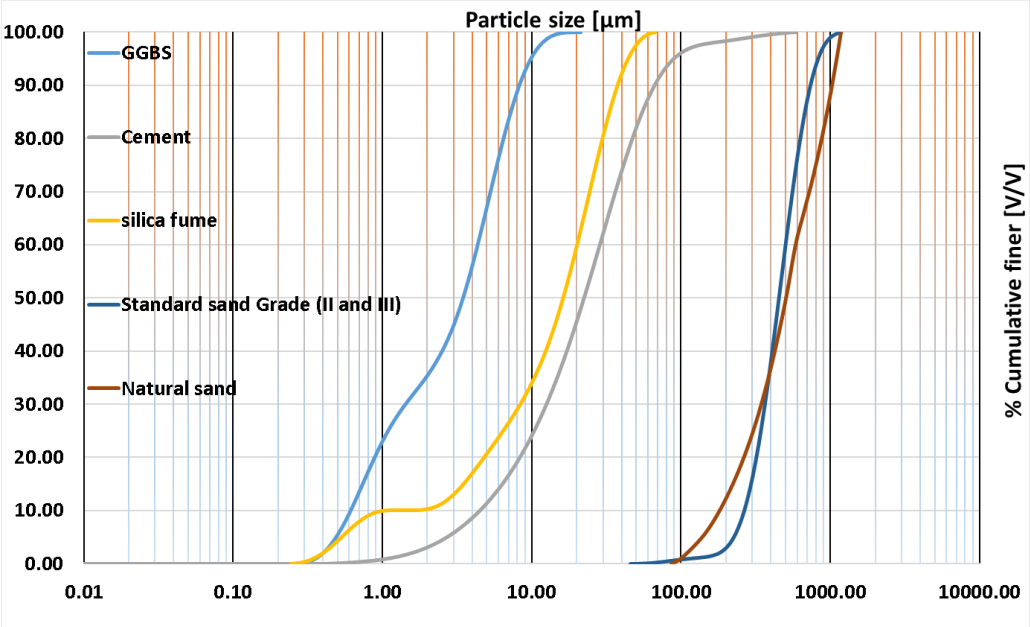


Figure 4. 1: Particle size distribution of the granular materials of HPHFRC.

Particle size distribution curves of the individual materials are shown in Figure 4.1. The target curve is generated using Equation 4.1. The grading curve (computed sieve residue) of the composed mix is produced by using Equation 4.2 and from which cumulative finer curve ($Q_{mix}$) of the composed mix is then generated as shown in Figure 4.2.

$$P\left(D_i^{i+1}\right) = \frac{\left(D_i^{i+1}\right)^{q} - D_{min}^{q}}{D_{max}^{q} - D_{min}^{q}} \qquad (4.1)$$

Where D is the particle size (μm)

P(D) is a fraction of the total particles smaller than the size D

$D_{max}$ is the maximum solid particle size (μm)

$D_{min}$ is the minimum particle size (μm)

i is the discrete particle sizes considered. In this study, a total of 68 discrete particle sizes are considered.

q is the distribution modulus. Generally, q value lower than 0.25 results in mix rich in fine particles hence, in this study q value is taken as 0.23, considering the high proportion of fine particles used in this study.

$$R_{mix}(D_i^{i+1}) = \frac{\sum_{k=1}^{m-2} \frac{v_{sol,k}}{\rho_{sol,k}} Q_{sol,k}(D_i^{i+1})}{\sum_{i=1}^{n} \sum_{k=1}^{m-2} \frac{v_{sol,k}}{\rho_{sol,k}} Q_{sol,k}(D_i^{i+1})} \quad (4.2)$$

Where $v_{sol,k}$ is the volumetric proportion of each solid material

$Q_{sol,k}(D_i^{i+1})$ is the sieve residual of material k on sieve i

$R_{mix}(D_i^{i+1})$ is the computed sieve residue of the composed mix

$\rho_{sol,k}$ is the specific density of material k.

Table 4. 1: Materials test data required for mix design

| Characteristic | Value |
|---|---|
| Specific Gravity of Cement | 3.12 |
| Specific gravity of Natural sand | 2.55 |
| Specific gravity of Indian standard sand | 2.64 |
| Specific gravity of GGBS | 3.10 |
| Specific gravity of Silica fume | 2.25 |
| Specific gravity of Superplasticizer | 1.08 |

The cement content in the model had been decreased from 945 kg/m$^3$ to 800 kg/m$^3$ (from Mix 1 to Mix 16), which causes an increase in the sand content in the mix. The coefficient of determination ($R^2$) for all these mix trials is 0.99(approx.) which signifies a good correlation between the target curve and the resulting grading curve of a mix. After theoretically

optimizing the particle packing by varying the proportions of ingredients, various mix trials had been done to validate the model.

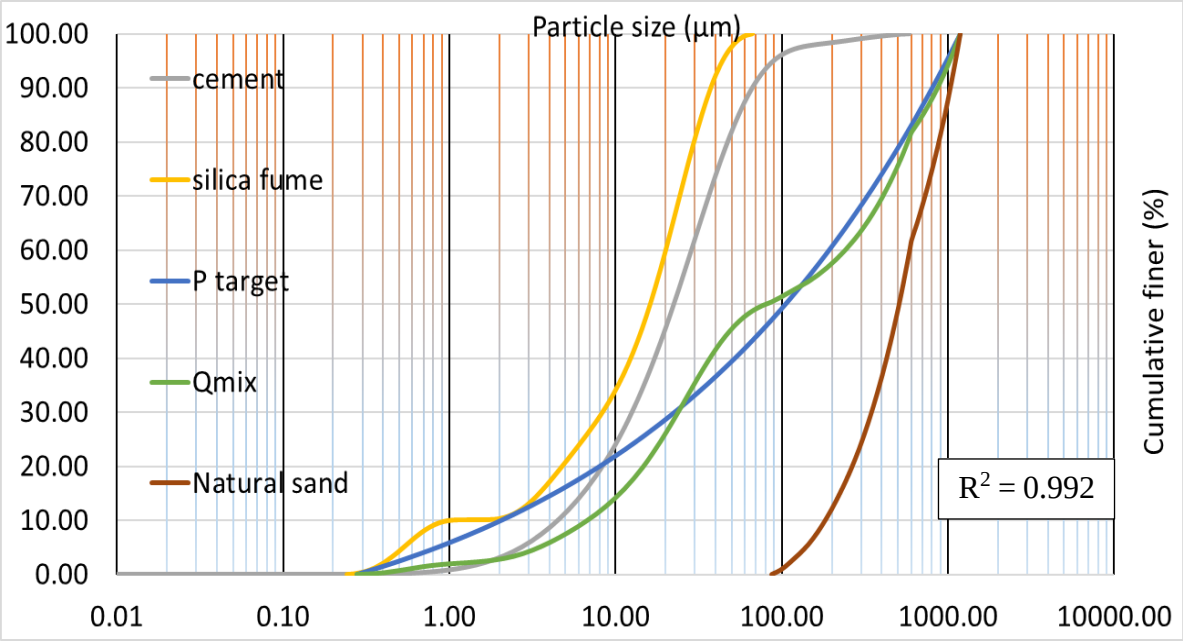


Figure 4. 2: PSDs of the materials, the target curve and the resulting grading curve of the trial Mix 1.

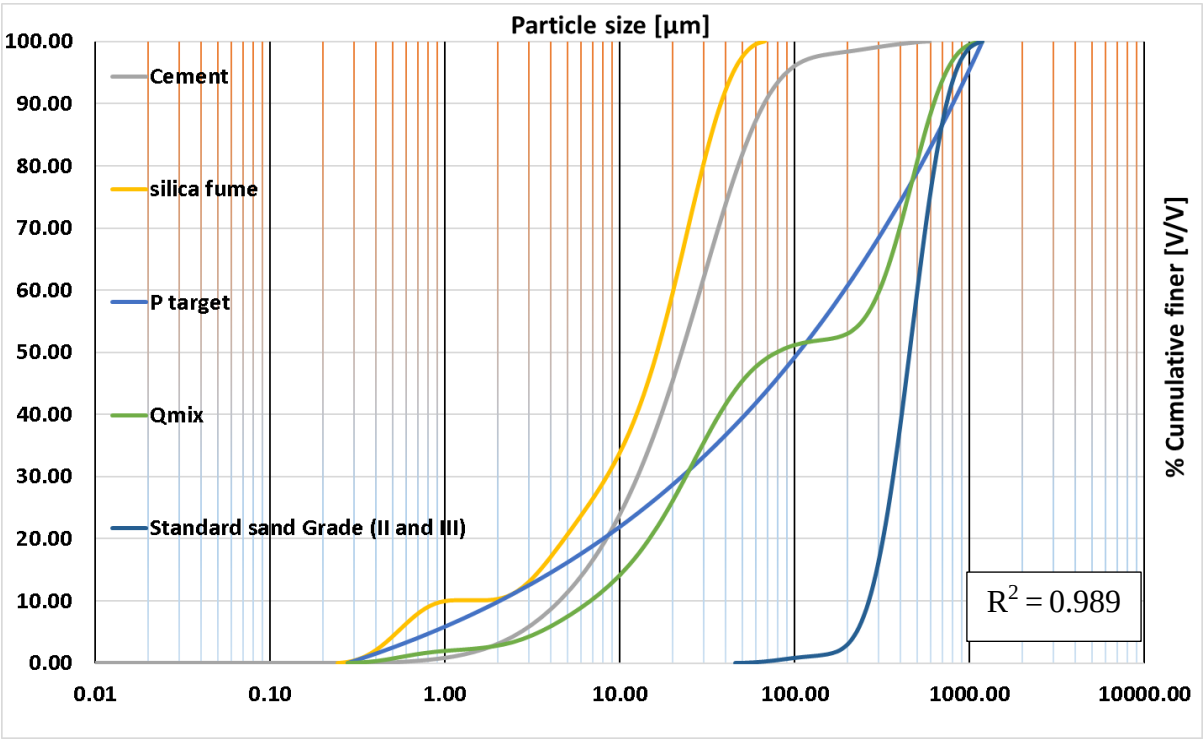


Figure 4. 3: PSDs of the materials, the target curve and the resulting grading curve of the trial Mix 2.

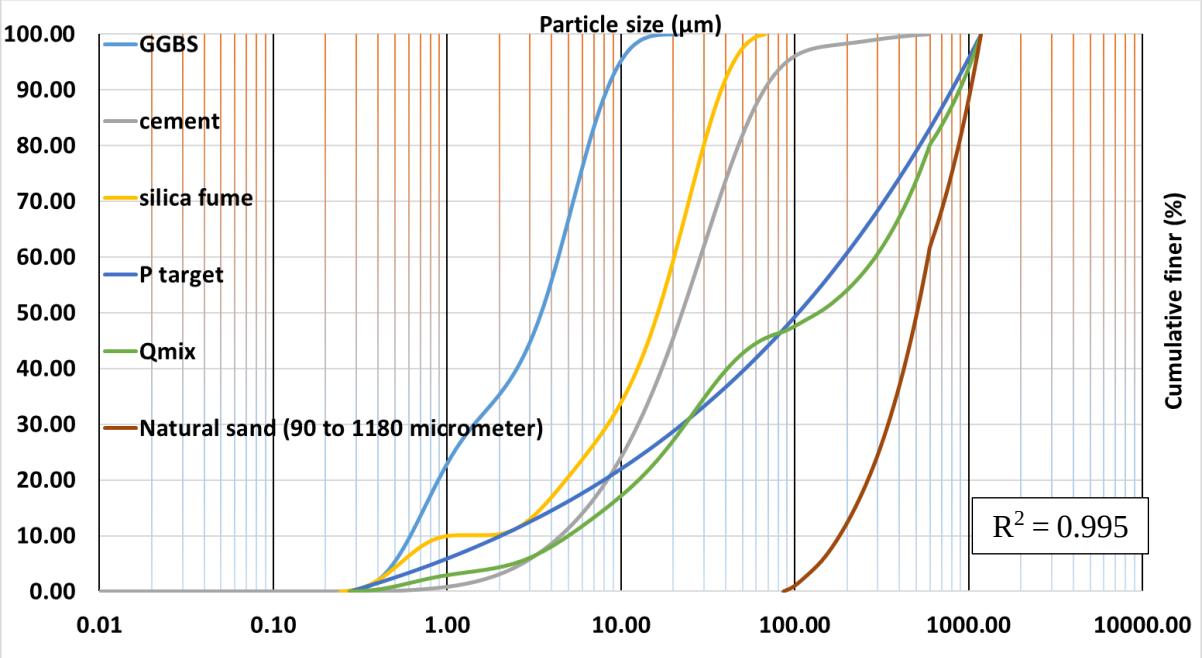


Figure 4. 4: PSDs of the materials, the target curve and the resulting grading curve of the trial Mix 15.

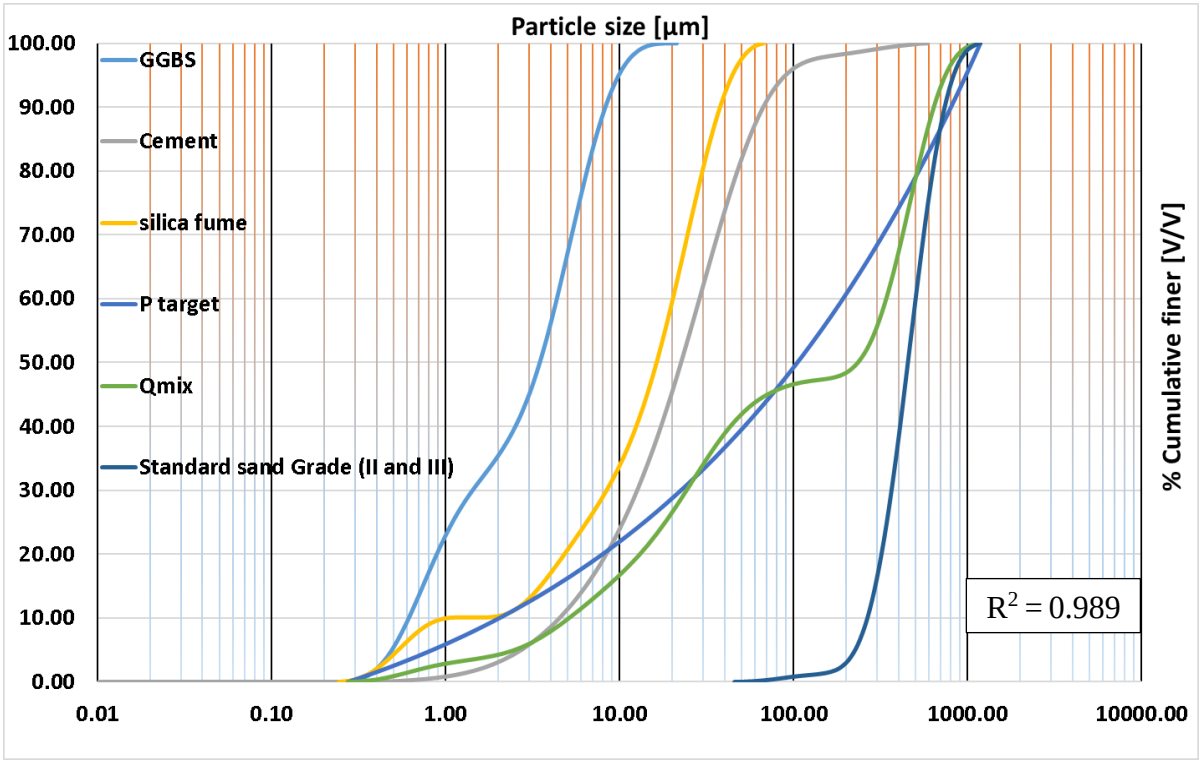


Figure 4. 5: PSDs of the materials, the target curve and the resulting grading curve of the trial Mix 16.

## 4.2. TRIAL MIXES

Using the Modified A & A model and optimizing the particle packing (as discussed in the previous section), HPHFRC mixes using different proportions of materials have been designed. During this course, 16 mix trials (i.e. M 1, M 2, to M 16) were made to have a comparative study of flowability and compressive strength between HPHFRC consisting of Indian standard sand and Natural sand. Silica fume and GGBS contents were fixed at 25 % and 20 % to the weight of cement respectively.

The PSDs of the materials, the target curve and the resulting grading curve of the trial Mix 1, Mix 2, Mix 15, Mix 16 are shown in Figure 4.2 to Figure 4.5. The 7 and 28 days compressive strength of HPHFRC (Natural sand) and HPHFRC (Standard sand) are given in Table 4.2 and illustrated graphically in Figure 4. 7 and Figure 4.8 respectively.

Key factors from trial Mix 1 to Mix 10 are:

- Cement (945kg/$m^3$) and silica fume (25% weight of cement) are used as binder materials.
- The total fiber content had been fixed as 1.5 % of the volume of concrete (0.5 % short crimped and 1.0 % long hooked fibers).
- From trial Mix 1 to Mix 10, water binder ratio had been decreased from 0.2 to 0.18 and superplasticizer content increased from 2.0 to 2.5 % of the binder content. As it was expected, the flowability decreases and compressive strength increases with a decrease in w/b ratio (*Mueller and Haist 2009)* (as given in Table 4.2 and graphically illustrated in Figure 4.6 - 4.8).

Key factors from trial Mix 11 to Mix 16 are:

- Cement content had been reduced from 900 to 800 kg/$m^3$ which causes an increase in sand proportion in the mix (Absolute volume method).
- GGBS (20 % weight of cement) along with cement and silica fume were used as binder materials.
- The w/b ratio had been reduced to 0.16 which decreases the flowability of the mix (as given in Table 4.2 and graphically illustrated in Figure 4.6). But with the addition of glassy textured GGBS *(Khan et al. 2014)* and increase in the sand content reduces the decrement of flowability.
- With the decrease in the w/b ratio and the inclusion of GGBS, the compressive strength of the mixes increases and reached a maximum value of 104.2 MPa. GGBS due to its

pozzolanic reaction and the filler effect due to its very fine particle size contributed in achieving higher compressive strength.

In all the trials mixes, an important observation was the less flowability of mixes containing the Natural sand than mixes containing the Standard sand. This could be the result of the more sharp cornered Natural sand particles as compared to the Standard sand particles (elaborate discussion is made in Chapter 5).

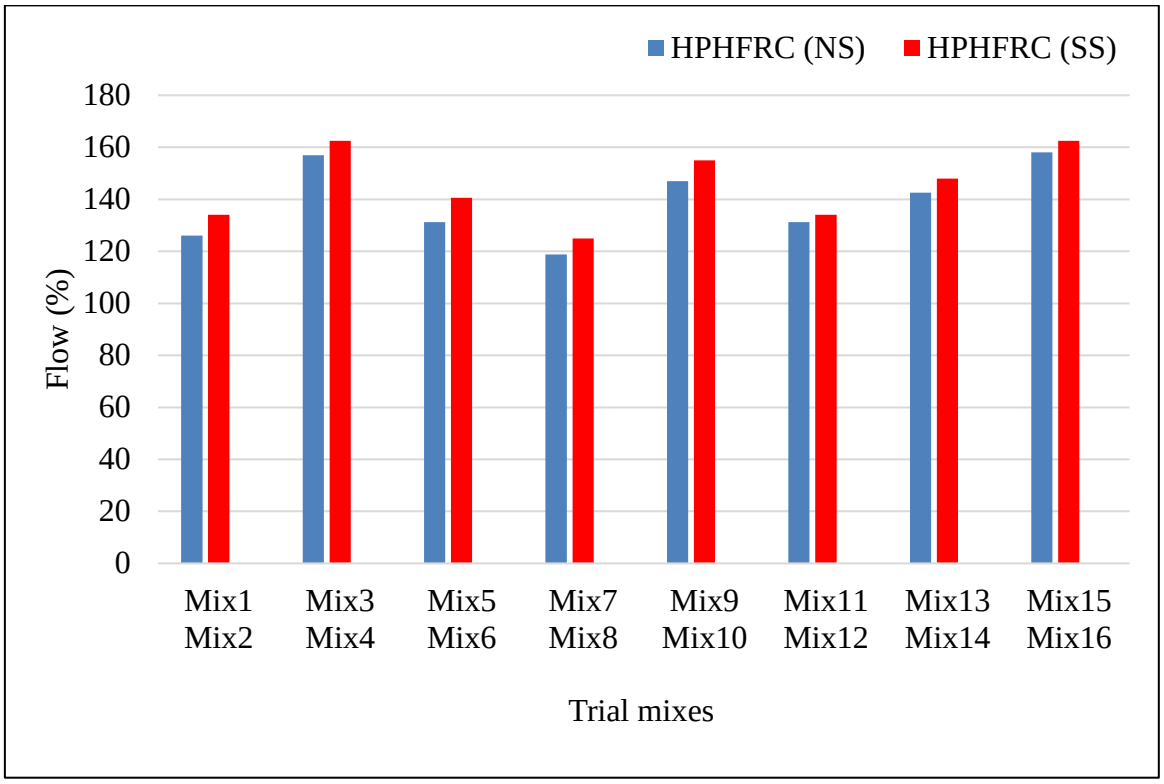


Figure 4. 6: Percentage flow of trial mixes of HPHFRC (NS) and of HPHFRC (SS).

During the mix trials study, workability (flow % > 150) and compressive strength (> 80 MPa) are the two parameters considered to fix the mix proportion of HPHFRC for further mechanical, durability and microstructural study.

Mix 15 and Mix 16 gives the best results in perspective of both workability and compressive strength. The percentage flow values of Mix 16 and Mix 15 were 162.5 and 158 respectively. These values are considered satisfactory to have a highly workable mix *(Graybeal 2006)*. The compressive strength at 28 days of Mix 15 and Mix 16 were 104.2 MPa and 97 MPa respectively. Since both of these trial mixes were workable and along with that had compressive strength around 100 MPa so could be called as High Performance Concrete. Hence, for the further comparative study between the Indian standard sand and the Natural sand, these two mix proportions would be used.

Table 4. 2: Mix proportions of trials

| Mix | C (kg) | Silica fume | | GGBS | | Sand | | | St F (% Vco.) | | w/b | SP/b (%) | Flow (%) | Compressive strength (MPa) | |
|---|---|---|---|---|---|---|---|---|---|---|---|---|---|---|---|
| | | (%)C | (Kg) | (%)C | (Kg) | NS (Kg) | SS(Kg) | | Cr. | H | | | | 7 Day | 28 Day |
| | | | | | | | Grade II | Grade III | | | | | | | |
| Mix 1 | 945 | 25 | 236.25 | - | - | 852 | - | - | 0.5 | 1 | 0.2 | 2.0 | 126 | 44 | 60 |
| Mix 2 | | | | | | - | 441 | 441 | | | | | 134 | 48 | 70 |
| Mix 3 | | | | | | 844 | - | - | | | | 2.3 | 157 | 46 | 62 |
| Mix 4 | | | | | | - | 441 | 441 | | | | | 162.5 | 52 | 76 |
| Mix 5 | | | | | | 873.63 | - | - | | | 0.19 | 2.3 | 131.25 | 54 | 79 |
| Mix 6 | | | | | | - | 453 | 453 | | | | | 140.6 | 55 | 81 |
| Mix 7 | | | | | | 904 | - | - | | | 0.18 | 2.3 | 118.75 | 57 | 83 |
| Mix 8 | | | | | | - | 468 | 468 | | | | | 125 | 59 | 84 |
| Mix 9 | | | | | | 899 | - | - | | | | 2.5 | 147 | 60 | 86 |
| Mix 10 | | | | | | - | 465 | 465 | | | | | 155 | 62 | 86 |

| | | | | | | | | | | | | | | |
|---|---|---|---|---|---|---|---|---|---|---|---|---|---|---|
| Mix 11 | 900 | 25.00 | 225 | 20 | 180 | 804 | - | - | 0.5 | 1.5 | 0.16 | 2.5 | 131.25 | 67 | 89 |
| Mix 12 | | | | | | - | 416 | 416 | | | | | 134 | 70 | 90 |
| Mix 13 | 850 | 25 | 212.5 | 20.00 | 170 | 900 | 0 | 0 | 0.5 | 1.5 | 0.16 | 2.5 | 142.5 | 72 | 93 |
| Mix 14 | | | | | | 0 | 466 | 466 | | | | | 148 | 73 | 94 |
| **Mix 15** | **800** | **25.00** | **200** | **20.00** | **160** | **997** | **0** | **0** | | | **0.16** | **2.5** | **158** | **89** | **97** |
| **Mix 16** | | | | | | **0** | **516** | **516** | | | | | **162.5** | **82** | **104** |

Table 4. 3: Summary of mix trials.

| Mix | Cement (kg/m$^3$) | Silica fume (%C) | GGBS (%C) | Sand (%C) | w/b | SP/b (%) | Total fiber content (% V co.) |
|---|---|---|---|---|---|---|---|
| Mix 1 to Mix 10 | 945 | 25 | 0 | 0.89 to 0.957 | 0.2 to 0.18 | 2.0 to 2.5 | 1.5 |
| Mix 11 to Mix 16 | 900 to 800 | 25 | 20 | 0.89 and 1.29 | 0.16 | 2.5 | 2 |

Table 4. 4: Flow characteristics of HPHFRC mixes.

| Mix | Spread (Image) | Spread (Value in mm) | Flow % |
|---|---|---|---|
| Mix 1 |  | 180.8 | 126 |
| Mix 2 |  | 187.2 | 134 |
| Mix 3 | * | 205.6 | 157 |
| Mix 4 | * | 210 | 162.5 |
| Mix 5 |  | 185 | 131.25 |
| Mix 6 |  | 192.48 | 140.6 |
| Mix 7 |  | 175 | 118.75 |
| Mix 8 |  | 180 | 125 |

| | | | |
|---|---|---|---|
| Mix 9 |  | 197.6 | 147 |
| Mix 10 |  | 203.2 | 154 |
| Mix 11 |  | 185 | 131.25 |
| Mix 12 |  | 187.2 | 134 |
| Mix 13 | * | 194 | 142.5 |
| Mix 14 |  | 198.4 | 148 |
| Mix 15 |  | 206.4 | 158 |

| | | | |
|---|---|---|---|
| Mix 16 |  | 210 | 162.5 |

Note: * indicates that the photograph of spread not available.

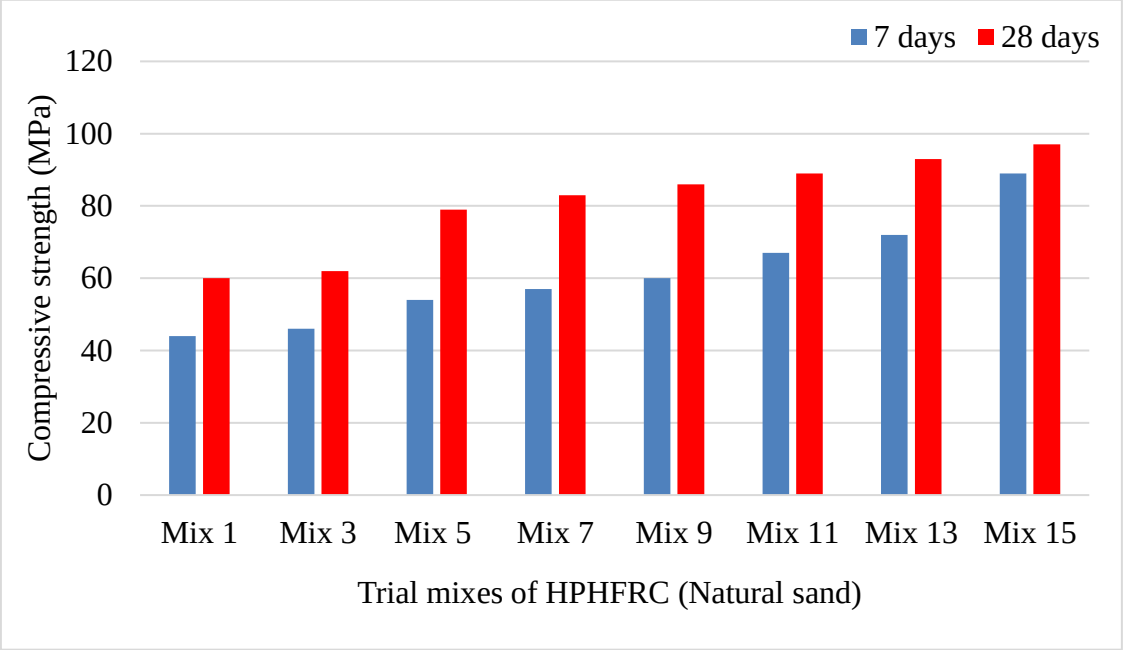


Figure 4. 7: Compressive strength of trial mixes of HPHFRC (NS).

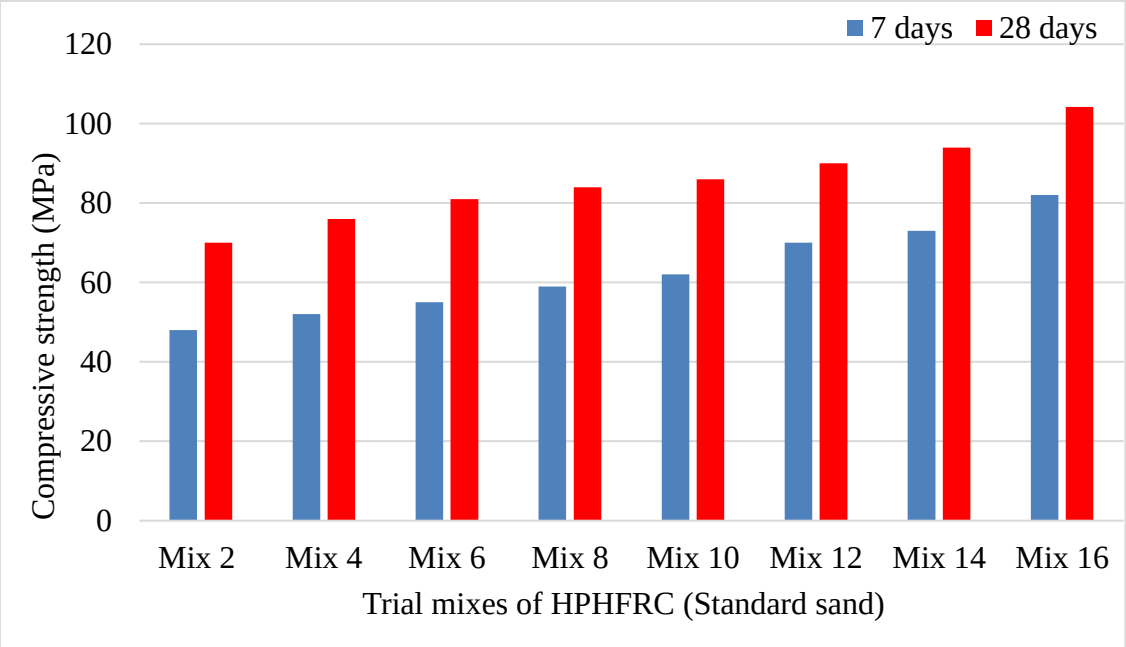


Figure 4. 8: Compressive strength of trial mixes of HPHFRC (SS).

# CHAPTER 5

# RESULTS AND DISCUSSION

## 5.1. GENERAL

This chapter deals with the results obtained from the various fresh, hardened and durability tests performed on the proposed design mix of HPHFRC. Based on workability and compressive strength criteria, trial Mix 15 and Mix 16 are finalized for the further comparative study of replacement of the Indian standard sand with the Natural sand in the production of HPHFRC. For the better understanding of the above mentioned structural properties, the microstructural analysis was also carried out. Analysis of a sample of both HPHFRC (SS) and HPHFRC (NS) was performed by SEM (Scanning electron microscope), EDS (Energy dispersive spectroscopy) and XRD (X-ray diffraction). EDS of the Standard sand and the Natural sand particles were also analyzed.

The mix designs considered for the comparative study of HPHFRC (SS) and HPHFRC (NS) are given in Table 5.1.

Table 5. 1: Mix design (kg/m$^3$) considered for HPHFRC.

| Materials | | HPHFRC (SS) kg/m$^3$ | HPHFRC (NS) kg/m$^3$ |
|---|---|---|---|
| Cement | | 800 | 800 |
| Silica fume | | 200 | 200 |
| GGBS | | 160 | 160 |
| Sand | Grade II | 519.1 | 1038.2 |
| | Grade III | 519.1 | |
| Water/ binder ratio | | 0.16 | 0.16 |
| Superplasticizer/ binder ratio | | 0.025 | 0.025 |

| | | | |
|---|---|---|---|
| Crimped steel fibers | | 39 | 39 |
| Hooked steel fibers | | 117 | 117 |

Table 5. 2: Mix proportion of HPHFRC.

| Ingredient | Cement | Silica fume | GGBS | Sand | water | Superplasticizer | Steel fibers | |
|---|---|---|---|---|---|---|---|---|
| | | | | | | | Cr. | H |
| Proportion | 1 | 0.25 | 0.2 | 1.29 | 0.232 | 0.036 | 0.04875 | 0.146 |

## 5.2. WORKABILITY

The average spread flow on the flow table observed in case of HPHFRC (SS) [Mix 16] was 210 mm and in the case of HPHFRC (NS) [Mix 15] was 206.4 mm. Similarly, there was a slight decrease of 2.7 % in the percentage flow value from 162.5 % to 158 % on the replacement of the Standard sand with the Natural sand as shown in Figure 5.1.

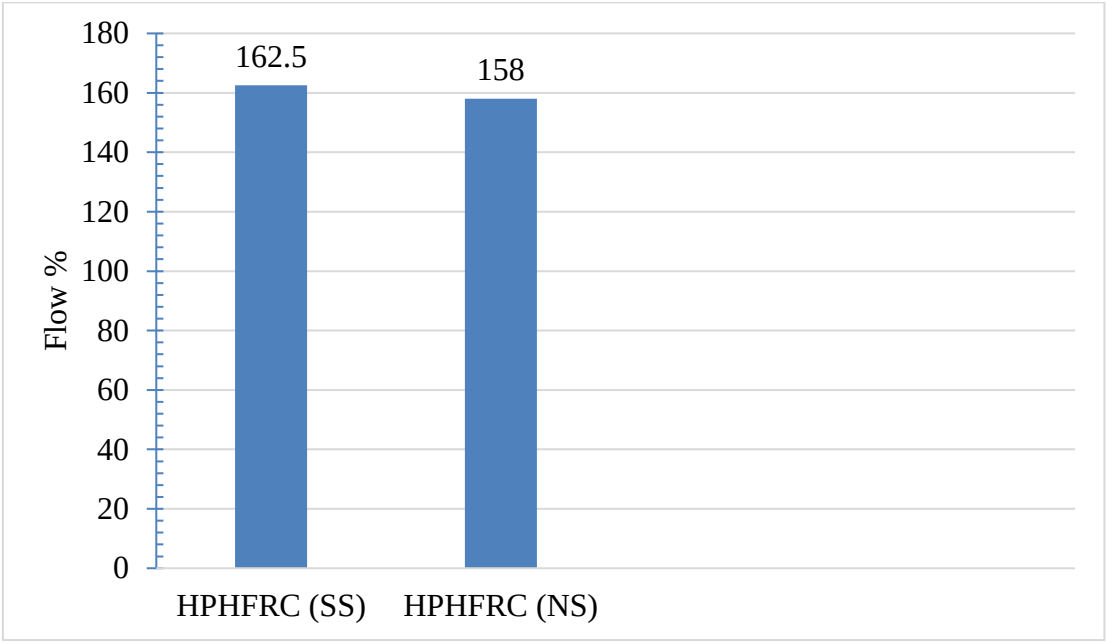


Figure 5. 1: Flow percentage of HPHFRC (Natural sand) and HPHFRC (Standard sand) mixes during Flow Table test.

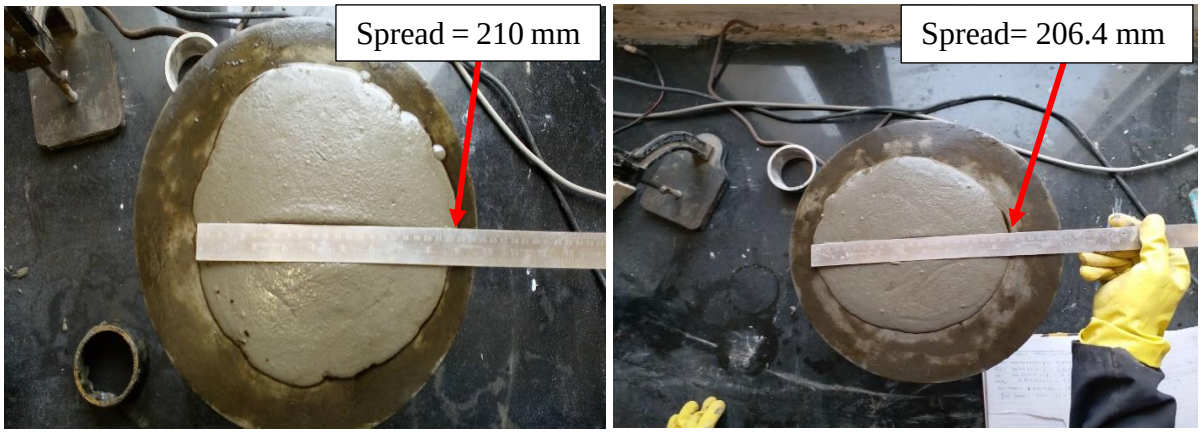


(A) (B)

Figure 5. 2: Spread of (A) HPHFRC (SS) (B) HPHFRC (NS) during Flow table test.

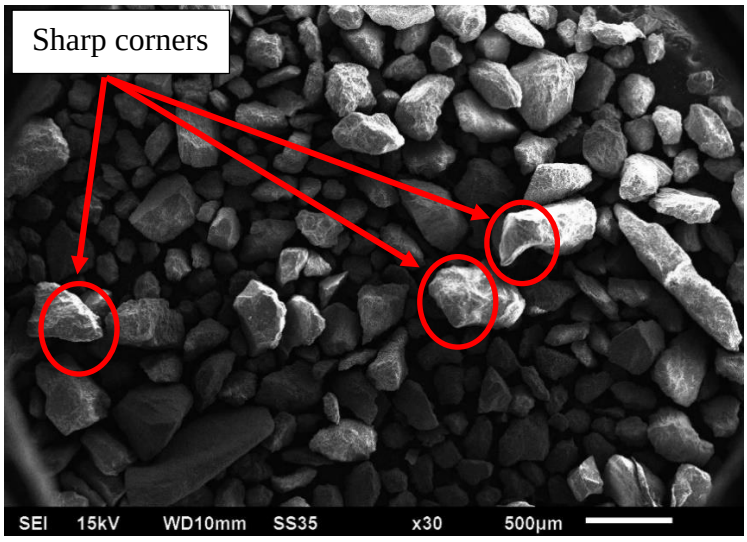


Figure 5. 3: SEM micrograph showing the Natural sand particles.

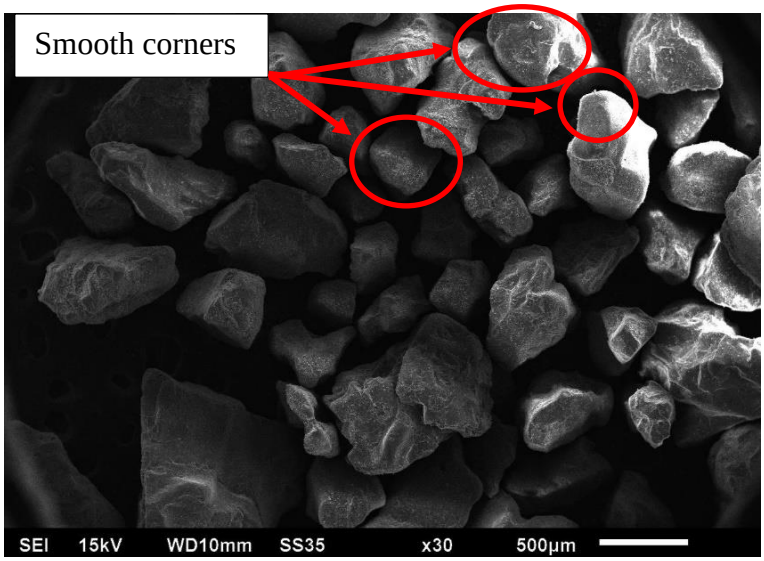


Figure 5. 4: SEM micrograph showing the Standard sand particles.

This could be attributed to the more sharp cornered Natural sand particles which tend to interfere with each other and decrease the flowability of the mix *(source: Infrastructure Technology Institute).* More quantity of flaky and elongated particles of the Natural sand could also be the reason for the decrease in workability of the mix as shown in Figure 5.3. Another reason could be the more water absorption capacity of Natural sand which might result in less free water available for flowability of the mix *(Soliman and Tagnit-Hamou 2017).*

## 5.3 COMPRESSIVE STRENGTH

The average compressive strength of the 3 cubical specimens each of HPFRC (SS) and HPFRC (NS) at 7 and 28 days are given in Table 5.3. From the test results, it is clear that there is not much decrease in compressive strength of HPFRC on replacement of the Standard sand with the Natural sand if the Natural sand is graded in the same sieve sizes as that of the Standard sand. Although 7 days compressive strength of HPFRC (NS) was more than HPFRC (SS) but 28 days strength of latter became a little more. This could be attributed to the epitactic growth of cementitious hydration products on the high silica content contained Standard sand *(Struble et al. 1980).*

Table 5. 3: Results of compression test of UHPFRC 70.6 mm cubical specimens.

| | HPFRC (SS) | | HPFRC (NS) | |
|---|---|---|---|---|
| | 7 days | 28 days | 7 days | 28 days |
| Average Maximum Load (kN) | 408.72 | 519.4 | 443.6 | 483.5 |
| Compressive strength (MPa) | 82 | 104 | 89 | 97 |

A relative more compressive strength of HPHFRC (SS) specimen than HPHFRC (NS) can also be attributed to comparative more elongated particles of the Natural sand than the Standard sand. Elongated particles have a higher surface to volume ratio that might have resulted in more requirement of binder paste for the proper bond between fine aggregate and paste. Another reason could be the more water absorption capacity of the Natural sand which might have resulted in comparative less free water available for hydration of cement in the later stage (i.e. 28 days) than the Standard sand.

Another important observation during the compression test was the failure pattern. The main disadvantage of Ultra High Strength concrete (UHSC) was the sudden explosive brittle failure at the peak load. This behaviour had been transformed into a multiple full lengths (macro) cracks with very little spalling due to the presence of hybrid steel fibers which delayed the crack initiation and restrained the crack propagation as a result of the bond between fibers and the concrete matrix as shown in Figure 5.5. Thus improves the post cracking behaviour and subsequently the energy absorption capacity.

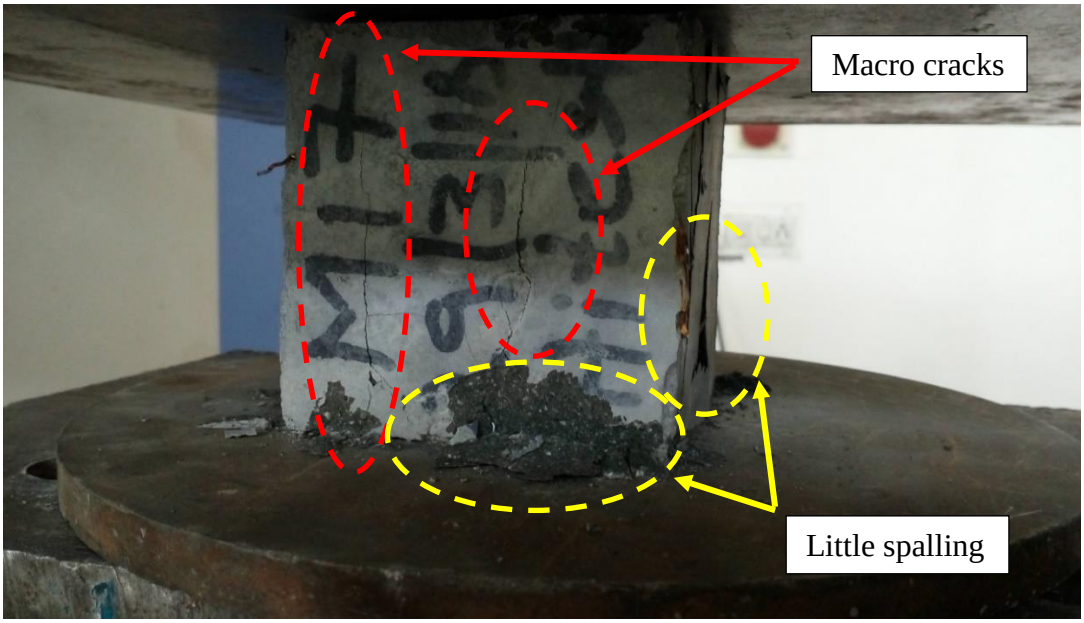


Figure 5. 5: Failure of HPFRC 70.6 mm cubical specimen.


Figure 5. 6: Bundling of long hooked fibers at the corner of the cubical specimen.

Hybrid steel fibers were mixed manually after the mixing of the HPC paste in the Digi mortar mixer due to clogging of long fibers in the mixer. As a result of hand mixing of fibers, the uniform distribution might have not be obtained. Also due to comparative length of long hooked fibers (50 mm) and 70.6 mm mould size, this had resulted in the bundling of long steel fibers at the corners of the mould and resulted in the creation of weak spot as illustrated in Figure 5.6 *(Abbas S. et al. 2015)*. As a consequence of these factors the compressive strength of the mixtures had not reached the 120 MPa value to be called as UHPHFRC.

### 5.4. SPLIT TENSILE STRENGTH

To study the tensile behaviour, 3 cylinders each of HPFRC (SS) and HPFRC (NS), were tested at 7 and 28 days as per *IS: 5816 (1999).* There had not been any significant change observed in the split tensile strength of HPFRC on the replacement of the Standard sand with the Natural sand. The average test results of the three specimens at 7 and 28 days are given in Table 5.4 and graphically in Figure 5.8.

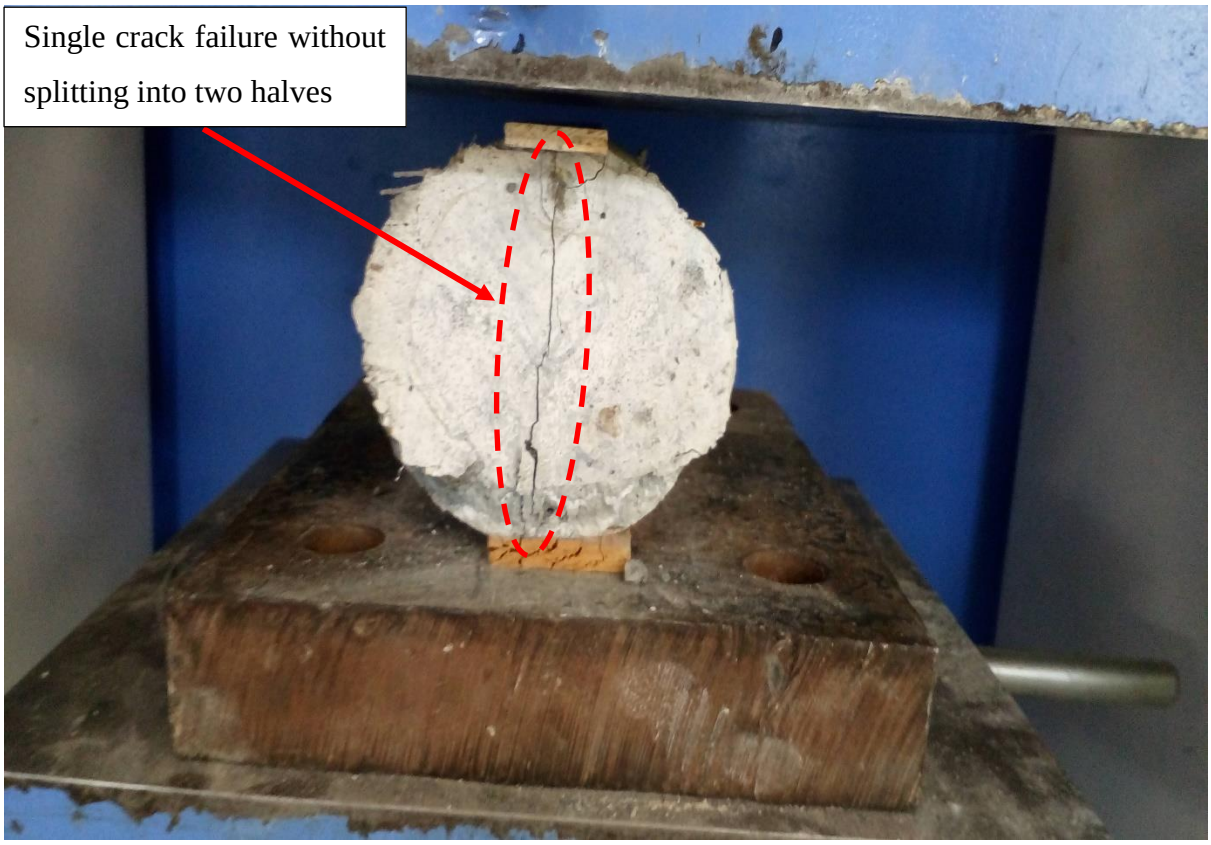


Figure 5. 7: Failure behaviour of HPFRC specimen.

The common phenomenon of normal strength concrete or high strength concrete of splitting of the cylinder into two halves at the time of failure was not observed due to the multi

characteristics steel fibers used in this study in making of HPFRC as shown in Figure 5.7. The hybrid steel fibers hold the concrete intact and did not let it split thus, changing the brittle failure of concrete to ductile. From the test results, it is found that 7 days HPFRC specimens reached around 70 % of the 28 days split tensile strength.

Table 5. 4: Results of the split tensile test of HPFRC cylindrical specimens.

| | HPFRC (SS) | | HPFRC (NS) | |
|---|---|---|---|---|
| | 7 days | 28 days | 7 days | 28 days |
| Average Peak Load (kN) | 291 | 423.33 | 294 | 420.93 |
| Split tensile strength (MPa) | 9.26 | 13.48 | 9.35 | 13.39 |

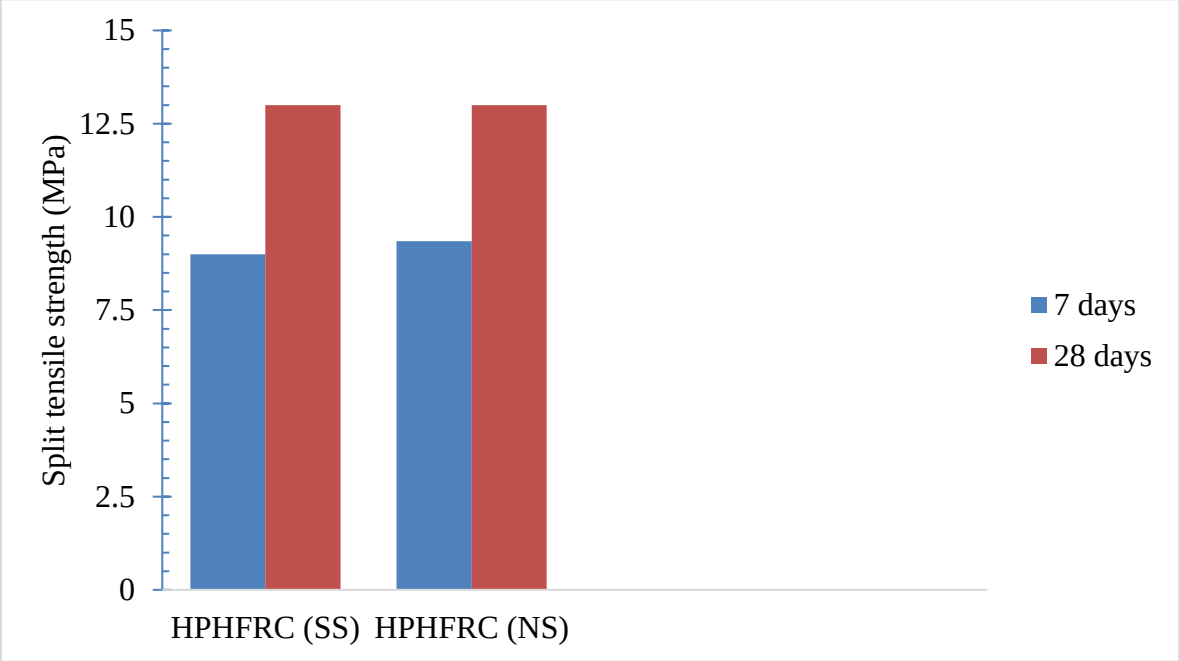


Figure 5. 8: Graphical representation of the split tensile strength of HPHFRC cylindrical specimens.

## 5.5. FLEXURAL STRENGTH

The average flexure test results of 3 beams of size 40 * 40 * 160 mm each of HPHFRC (SS) and HPHFRC (NS) are given in Table 5.5. There had been marginal change observed in the flexural strength of HPHFRC beams on replacement of the Standard sand with the Natural

sand. From the test results, it is found that that the 7 days flexural strength was around 53 % of the 28 days flexural strength.

Load mid-deflection curve of HPHFRC (NS) beam subjected to center-point loading is presented in Figure 5.9. Load deflection curve is basically divided into three parts as, the elastic portion, the strain hardening portion and the strain softening portion. From the onset of the test, until the first crack appears, the elastic (linear) part was observed. Very small deflections were observed in this linear portion as HPHFRC specimens are initially very stiff.

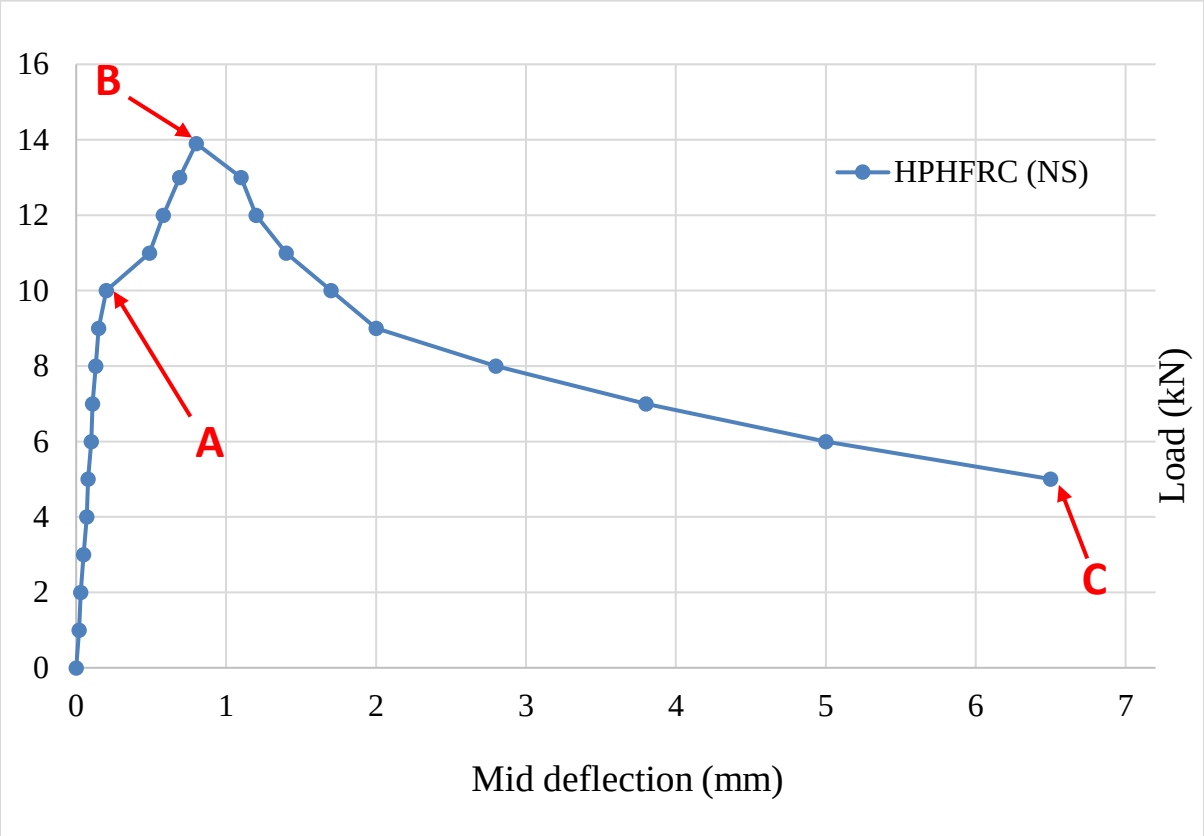


Figure 5. 9: Load deflection curve of HPHFRC (NS) beam under center point loading.

Table 5. 5: Results of flexure test of HPHFRC beams.

| | HPHFRC (SS) | | HPHFRC (NS) | |
|---|---|---|---|---|
| | 7 days | 28 days | 7 days | 28 days |
| Average Peak Load (kN) | 7.3 | 13.86 | 7.03 | 13.7 |
| Flexural strength (MPa) | 21 | 39 | 20 | 39 |


Figure 5. 10: Crack initiation (Point A) in the HPHFRC (NS) beam.


Figure 5. 11: Strain softening starting (Point B) in the HPHFRC (NS) beam.

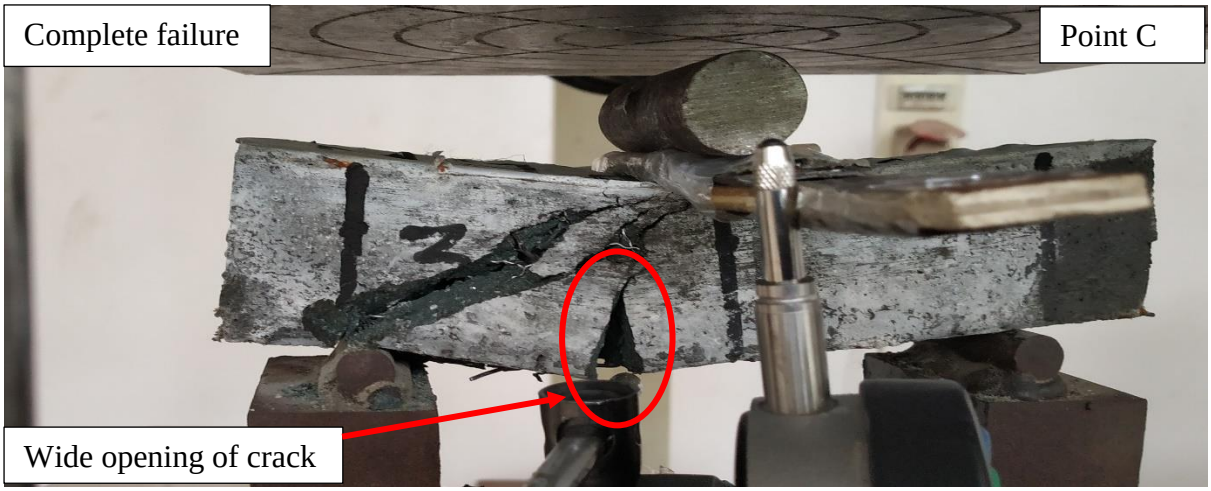


Figure 5. 12: Complete failure (Point C) of the HPHFRC (NS) beam.

The Point A shown in Figure 5.9 represents the crack initiation of the HPHFRC beam. After this elastic phase, the strain hardening phase starts, and a few small cracks originate at different locations in the beam. During this phase, the role of short crimped and long hooked fibers came into view as these fibers would resist the crack growth at the micro and macro level respectively by enduring most of the load.

The point B shown in Figure 5.9 represents beginning of the strain softening phase as pull out of the fibers results in a decrease in the endurance strength of the beam. Due to the hybrid fiber system even after the pull out of the most of the short fibers and few long fibers, the remaining long fibers keep on holding the specimen till the hook ends of the steel fibers were straightened thus, did not result in the sudden failure of the beam. In Figure 5.9 the complete failure is represented as Point C. It could be observed in the Figure 5.13 that even at large deflection in the beam the specimen had not broken apart due to the hybrid fibers holding the concrete.

There has not been much difference in the load deflection curve of HPHFRC (SS) and HPHFRC (NS) specimens as shown in Figure 5.15. So, it could be concluded that on replacement of the Standard sand with the Natural sand there is not much change in the flexural behaviour of HPHFRC beams.

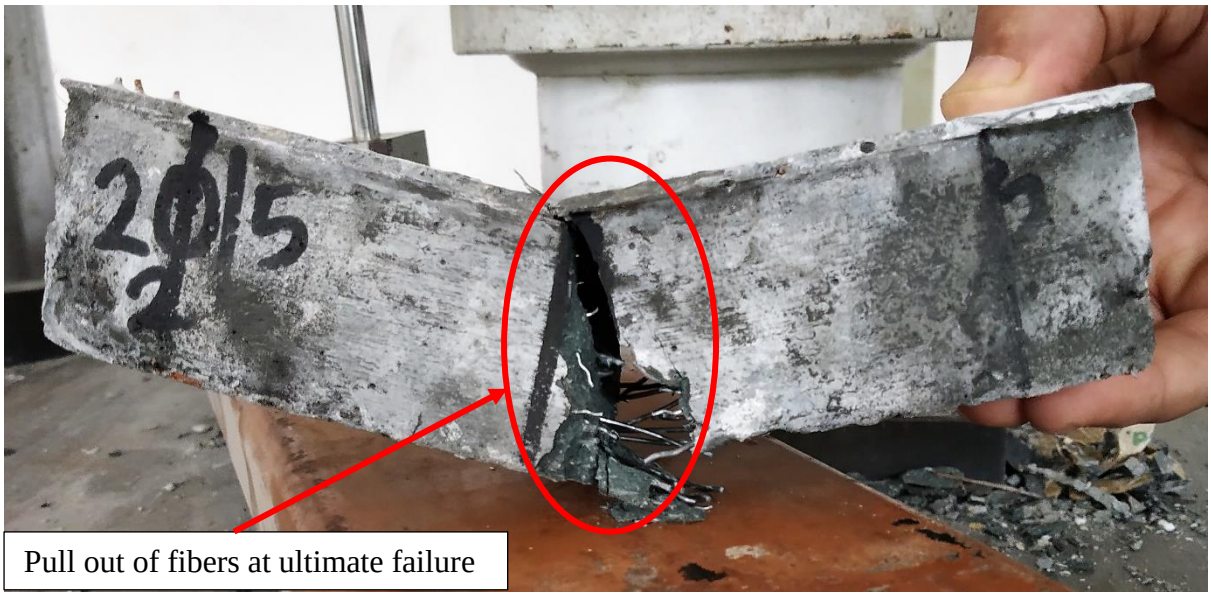


Figure 5. 13: Pull out of the fibers at very large deflection.

The damage of important structures could be reduced during the earthquake of magnitude greater than considered in design because of concrete matrix holding a capacity of steel fibers. Due to this behaviour of steel fibers, failure of HPHFRC structure would be ductile rather than brittle.

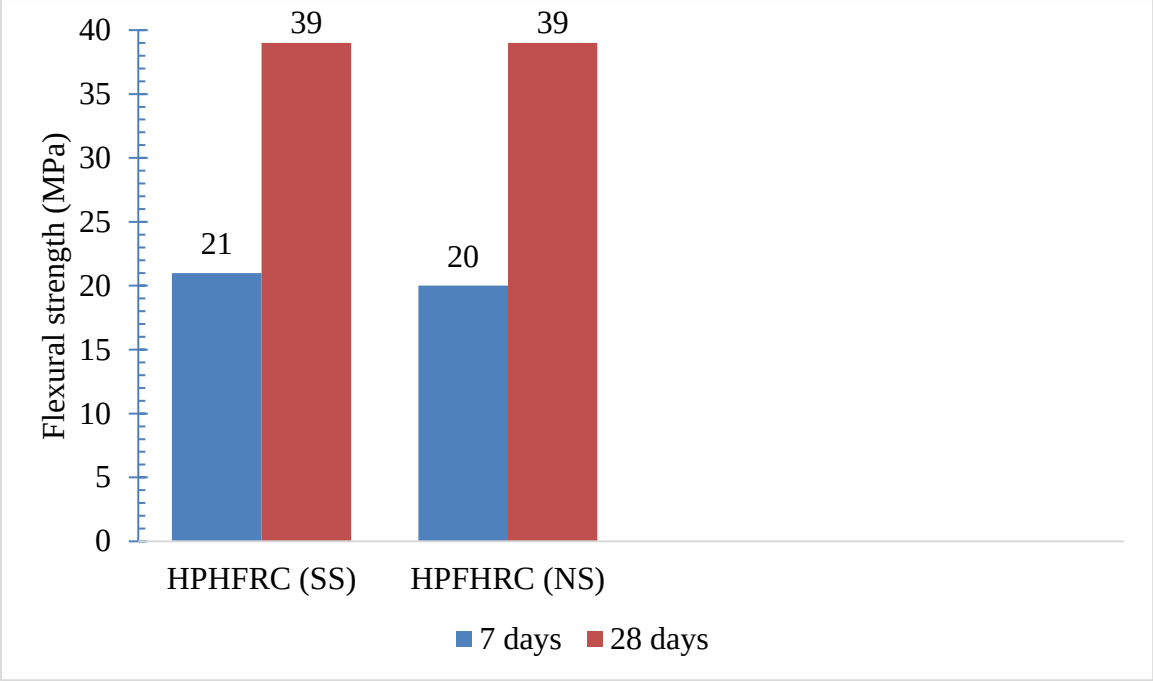


Figure 5. 14: Graphical representation of the flexural strength of HPHFRC (SS) and HPHFRC (NS) beam.

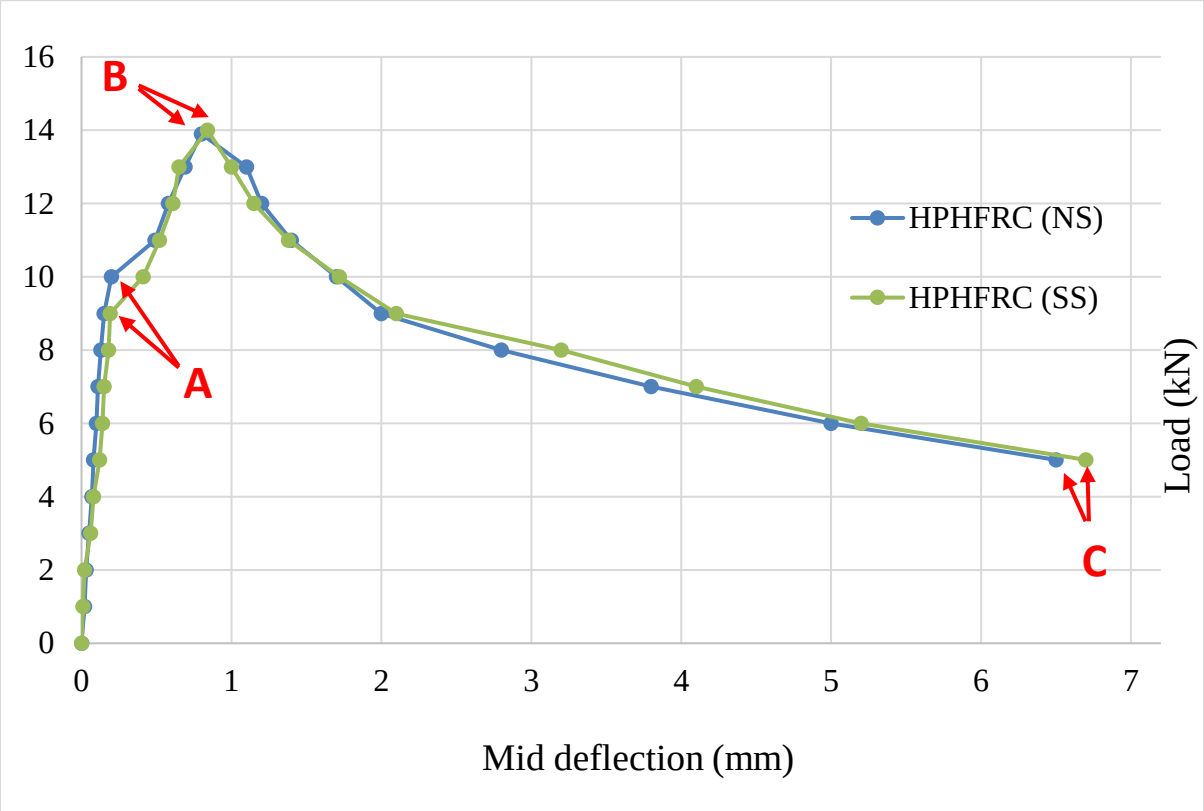


Figure 5. 15: Load deflection curve of HPHFRC (SS) and HPHFRC (NS) beam under center point loading.

## 5.6. RAPID CHLORIDE PERMEABILITY TEST

For the determination of chloride permeability, 50 mm (thick slice) * 100 mm (diameter) specimens were tested as per *ASTM C1202-15*. Since, due to the same length of hooked steel fibers and the specimen, this resulted in the overflow of charge passed through the specimen on the initiation of the experiment. So, this test was performed without the usage of long hooked fibers. The average test results of the 3 specimens each of HPFRC (SS) and HPFRC (NS) at 7 and 28 days are given in Table 5. 6 and the graphical representation is given in Figure 5. 16.

Table 5. 6: RCPT results of HPFRC specimens.

| | HPFRC (SS) | HPFRC (NS) |
|---|---|---|
| | 28 days | 28 days |
| Total charge passed (Coulombs) | 358 | 364 |
| Chloride ion permeability | Very low | Very low |

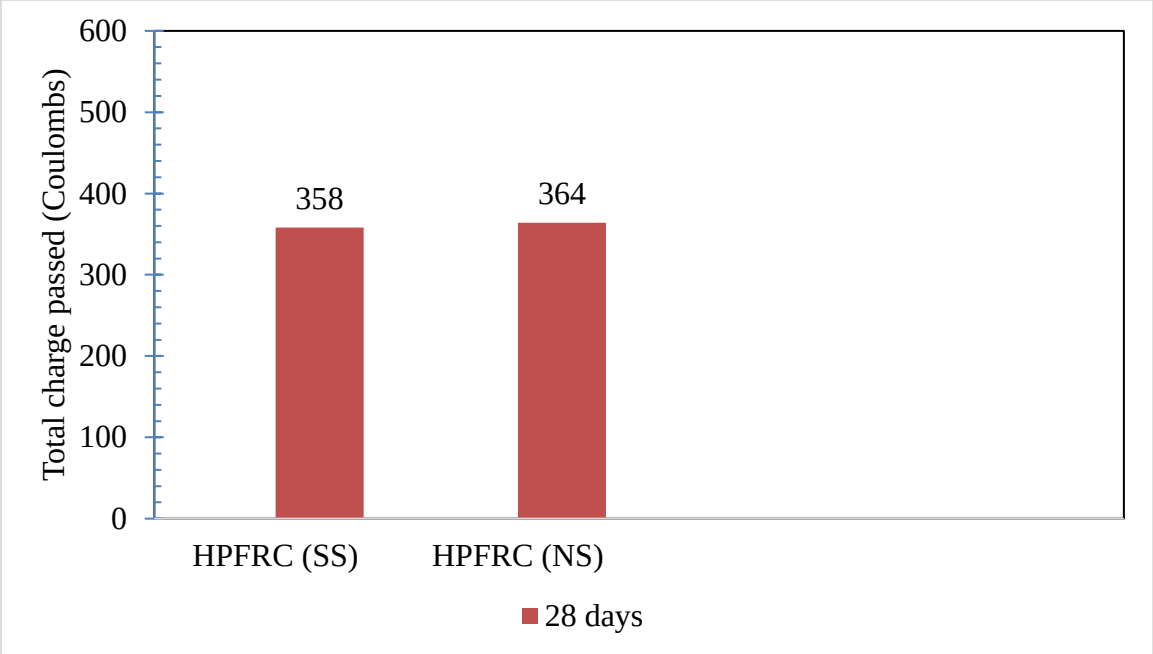


Figure 5. 16: RCPT results of HPFRC specimens.

From the test results, it was observed that all the specimens exhibited excellent resistance against chloride ion transfer as the average charge passed through HPFRC (SS) and HPFRC (NS) specimens were 358 and 364 coulombs which according to the *ASTM C1202 -15* indicates

very low chloride ion penetrability. The reason for very low chloride ion permeability would be the dense concrete matrix with very low porosity due to the pozzolanic and filler effect of silica fume and GGBS and also due the optimum particle packing of the ingredients. There had not been any significant change observed in the chloride ion penetration due to the replacement of the Standard sand with the Natural sand. A little increase in the chloride penetration may be due to comparative more porous nature of HPFRC (NS) specimen due to a little more availability of calcium hydroxide in the concrete mix as shown in XRD analysis.

### 5.7. WATER SORPTIVITY

The average test results of three specimens of HPHFRC with the Standard sand cured for 7 and 28 days are given in Table 5.7 and Table 5.8 respectively. Similarly, the average test results of three specimens of HPHFRC with the Natural sand cured for 7 and 28 days are given in Table 5.9 and Table 5.10 respectively. The absorption (I) for HPHFRC (SS) specimen cured for 7 days (SS 7) was 0.74mm whereas for HPHFRC (NS) cured for 7 days (NS 7) was 0.806 mm. The more water absorption of HPHFRC (NS 7) than HPHFRC (SS 7) may be attributed to the comparative more porous nature of the Natural sand particles than the Standard sand particles. The absorption (I) for HPHFRC (SS 28) was 0.424 mm whereas for HPHFRC (NS 28) was 0.425 mm, which signifies that there might not be a significant change in the resistance against water sorptivity in HPHFRC on replacement of the Indian standard sand with the Natural sand graded as per Table 3.5.

Table 5. 7: Water sorptivity results of HPHFRC (Standard sand) specimens cured for 7 days.

| Test Time | | √Time ($s^{1/2}$) | Mass of specimen (g) | Increment in mass (g) | Increment in Mass/ area/ density of water = I (mm) |
|---|---|---|---|---|---|
| Days | seconds | | | | |
| | 0 | 0 | 993.33 | 0 | 0 |
| | 60 | 8 | 993.83 | 0.50 | 0.06 |
| | 300 | 17 | 994.33 | 1.00 | 0.13 |
| | 600 | 24 | 995.00 | 1.67 | 0.21 |
| | 1200 | 35 | 995.50 | 2.17 | 0.28 |
| | 1800 | 42 | 995.83 | 2.50 | 0.32 |

| | | | | | |
|---|---|---|---|---|---|
| | 3600 | 60 | 996.33 | 3.00 | 0.38 |
| | 7200 | 85 | 996.50 | 3.17 | 0.40 |
| | 10800 | 104 | 997.00 | 3.67 | 0.47 |
| | 14400 | 120 | 997.33 | 4.00 | 0.51 |
| | 18000 | 134 | 997.67 | 4.34 | 0.55 |
| | **21600** | **147** | **997.67** | **4.34** | **0.55** |
| 1 | 92220 | 304 | 998.17 | 4.84 | 0.62 |
| 2 | 193200 | 440 | 998.17 | 4.84 | 0.62 |
| 3 | 268500 | 518 | 998.67 | 5.34 | 0.68 |
| 5 | 432000 | 657 | 998.83 | 5.50 | 0.70 |
| 6 | 527580 | 726 | 999.00 | 5.67 | 0.72 |
| 7 | 622200 | 789 | 999.17 | 5.84 | 0.74 |
| 8 | 691200 | 831 | 999.17 | 5.84 | 0.74 |

Table 5. 8: Water sorptivity results of HPHFRC (Standard sand) specimens cured for 28 days.

| Test Time | | √Time ($s^{1/2}$) | Mass of specimen (g) | Increment in mass (g) | Increment in Mass/ area/ density of water = I (mm) |
|---|---|---|---|---|---|
| Days | seconds | | | | |
| | 0 | 0 | 982 | 0 | 0 |
| | 60 | 8 | 982.50 | 0.50 | 0.06 |
| | 300 | 17 | 983.00 | 1.00 | 0.13 |
| | 600 | 24 | 983.33 | 1.33 | 0.17 |
| | 1200 | 35 | 983.50 | 1.50 | 0.19 |
| | 1800 | 42 | 983.67 | 1.67 | 0.21 |
| | 3600 | 60 | 983.67 | 1.67 | 0.21 |

| | | | | | |
|---|---|---|---|---|---|
| | 7200 | 85 | 983.67 | 1.67 | 0.21 |
| | 10800 | 104 | 983.67 | 1.67 | 0.21 |
| | 14400 | 120 | 983.67 | 1.67 | 0.21 |
| | 18000 | 134 | 983.67 | 1.67 | 0.21 |
| | **21600** | **147** | **983.67** | **1.67** | **0.21** |
| 1 | 92220 | 304 | 984.50 | 2.50 | 0.32 |
| 2 | 193200 | 440 | 984.67 | 2.67 | 0.34 |
| 3 | 268500 | 518 | 985.00 | 3.00 | 0.38 |
| 5 | 432000 | 657 | 985.33 | 3.33 | 0.42 |
| 6 | 527580 | 726 | 985.33 | 3.33 | 0.42 |
| 7 | 622200 | 789 | 985.33 | 3.33 | 0.42 |
| 8 | 691200 | 831 | 985.33 | 3.33 | 0.42 |

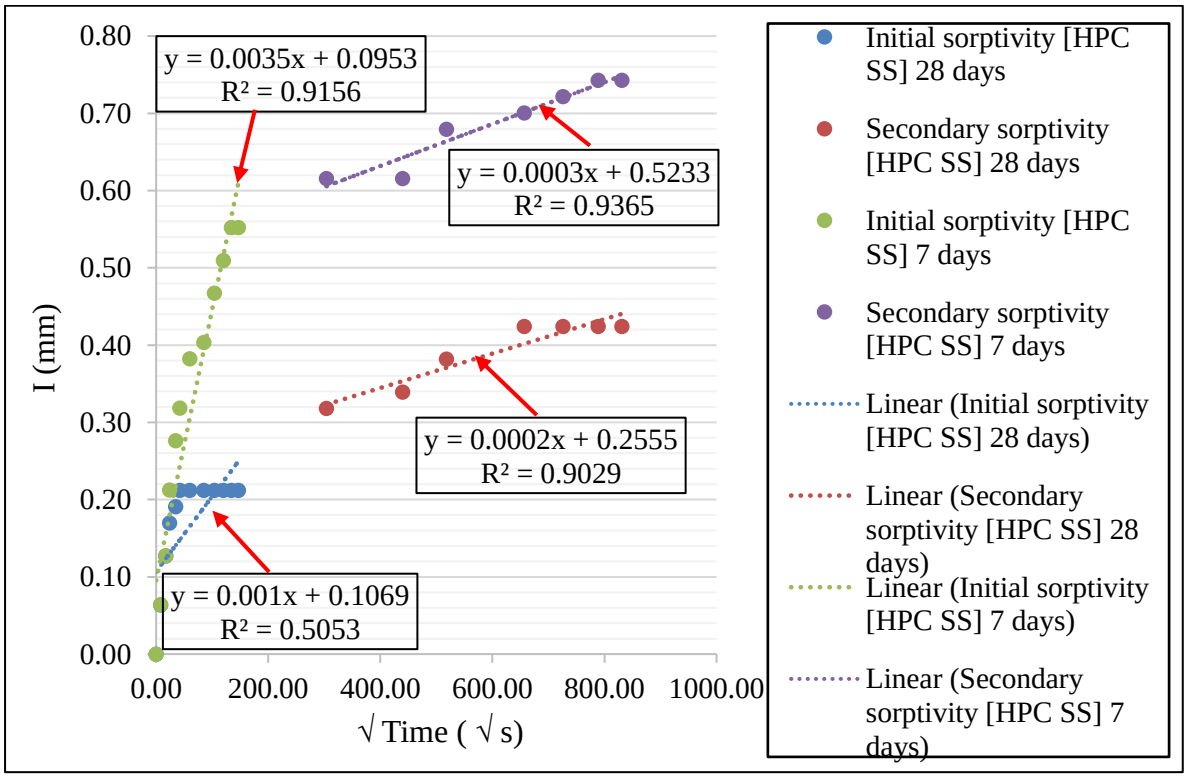


Figure 5. 17: Water sorptivity results of HPFRC (Standard sand) specimens cured for 7 and 28 days along with respective tread lines.

As per *ASTM C 1585 – 04*, the initial and secondary rate of water absorption can only be find out if the values of I from 1 minute to 6 hours and 2nd to 9th day follows a linear relationship (a correlation coefficient ($R^2$) of greater than 0.98) respectively. But as shown in Figure 5.17 to Figure 5.20 in all cases the value of $R^2$ was less than 0.98, so the exact rate of initial and secondary absorption could not be calculated. The approximate values for initial rate of absorption of 1.3 µm / $s^{1/2}$ for HPHFRC (NS 28) and 1.0 µm / $s^{1/2}$ for HPHFRC (SS 28) are much less than Normal strength concrete which generally comes more than 5 µm / $s^{1/2}$. This could be attributed due to pozzolanic and filler effect of silica fume and GGBS and also due the optimum packing density of the ingredients.

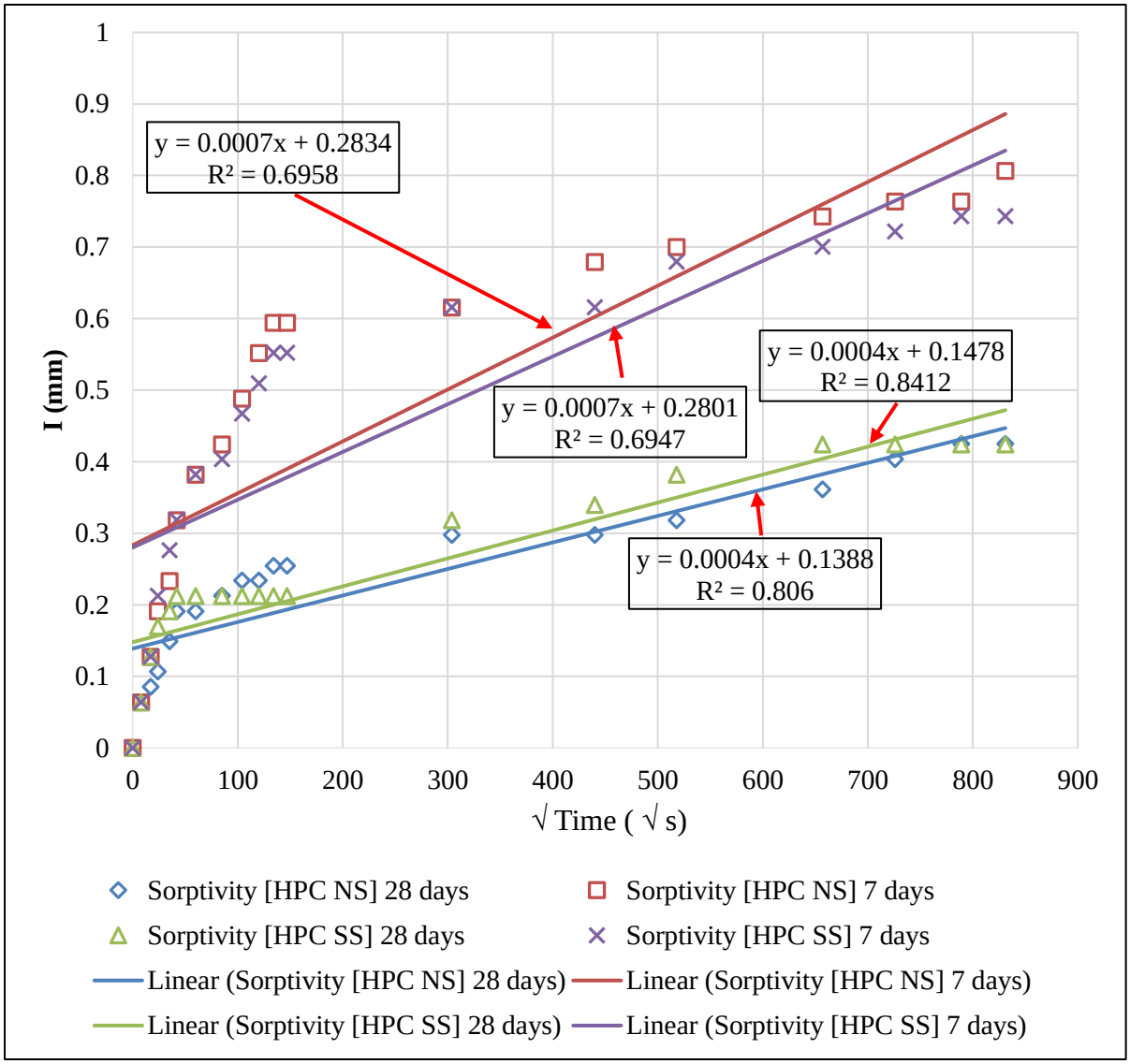


Figure 5. 18: Water sorptivity results of HPHFRC (Standard sand) and HPHFRC (Natural sand) specimens cured for 7 and 28 days along with respective tread lines.

Table 5. 9: Water sorptivity results of HPFRC (Natural sand) specimens cured for 7 days.

| Test Time | | √Time ($s^{1/2}$) | Mass of specimen (g) | Increment in mass (g) | Increment in Mass/ area/ density of water = I (mm) |
|---|---|---|---|---|---|
| Days | seconds | | | | |
| | 0 | 0 | 984 | 0 | 0 |
| | 60 | 8 | 984.5 | 0.5 | 0.063662 |
| | 300 | 17 | 985 | 1 | 0.127324 |
| | 600 | 24 | 985.5 | 1.5 | 0.190985 |
| | 1200 | 35 | 985.8333 | 1.833333 | 0.233427 |
| | 1800 | 42 | 986.5 | 2.5 | 0.318309 |
| | 3600 | 60 | 987 | 3 | 0.381971 |
| | 7200 | 85 | 987.3333 | 3.333333 | 0.424412 |
| | 10800 | 104 | 987.8333 | 3.833333 | 0.488074 |
| | 14400 | 120 | 988.3333 | 4.333333 | 0.551736 |
| | 18000 | 134 | 988.6667 | 4.666667 | 0.594177 |
| | **21600** | **147** | **988.6667** | **4.666667** | **0.594177** |
| 1 | 92220 | 304 | 988.8333 | 4.833333 | 0.615398 |
| 2 | 193200 | 440 | 989.3333 | 5.333333 | 0.67906 |
| 3 | 268500 | 518 | 989.5 | 5.5 | 0.70028 |
| 5 | 432000 | 657 | 989.8333 | 5.833333 | 0.742721 |
| 6 | 527580 | 726 | 990 | 6 | 0.763942 |
| 7 | 622200 | 789 | 990 | 6 | 0.763942 |
| 8 | 691200 | 831 | 990.3333 | 6.333333 | 0.806383 |

Table 5. 10: Water sorptivity results of HPFRC (Natural sand) specimens cured for 28 days.

| Test Time | | √Time ($s^{1/2}$) | Mass of specimen (g) | Increment in mass (g) | Increment in Mass/ area/ density of water = I (mm) |
|---|---|---|---|---|---|
| Days | seconds | | | | |
| | 0 | 0 | 989.16 | 0 | 0 |
| | 60 | 8 | 989.66 | 0.5 | 0.063662 |
| | 300 | 17 | 989.83 | 0.67 | 0.085307 |
| | 600 | 24 | 990 | 0.84 | 0.106952 |
| | 1200 | 35 | 990.33 | 1.17 | 0.148969 |
| | 1800 | 42 | 990.66 | 1.5 | 0.190985 |
| | 3600 | 60 | 990.66 | 1.5 | 0.190985 |
| | 7200 | 85 | 990.83 | 1.67 | 0.212631 |
| | 10800 | 104 | 991 | 1.84 | 0.234276 |
| | 14400 | 120 | 991 | 1.84 | 0.234276 |
| | 18000 | 134 | 991.16 | 2 | 0.254647 |
| | **21600** | **147** | **991.16** | **2** | **0.254647** |
| 1 | 92220 | 304 | 991.5 | 2.34 | 0.297937 |
| 2 | 193200 | 440 | 991.5 | 2.34 | 0.297937 |
| 3 | 268500 | 518 | 991.66 | 2.5 | 0.318309 |
| 5 | 432000 | 657 | 992 | 2.84 | 0.361599 |
| 6 | 527580 | 726 | 992.33 | 3.17 | 0.403616 |
| 7 | 622200 | 789 | 992.5 | 3.34 | 0.425261 |
| 8 | 691200 | 831 | 992.5 | 3.34 | 0.425261 |

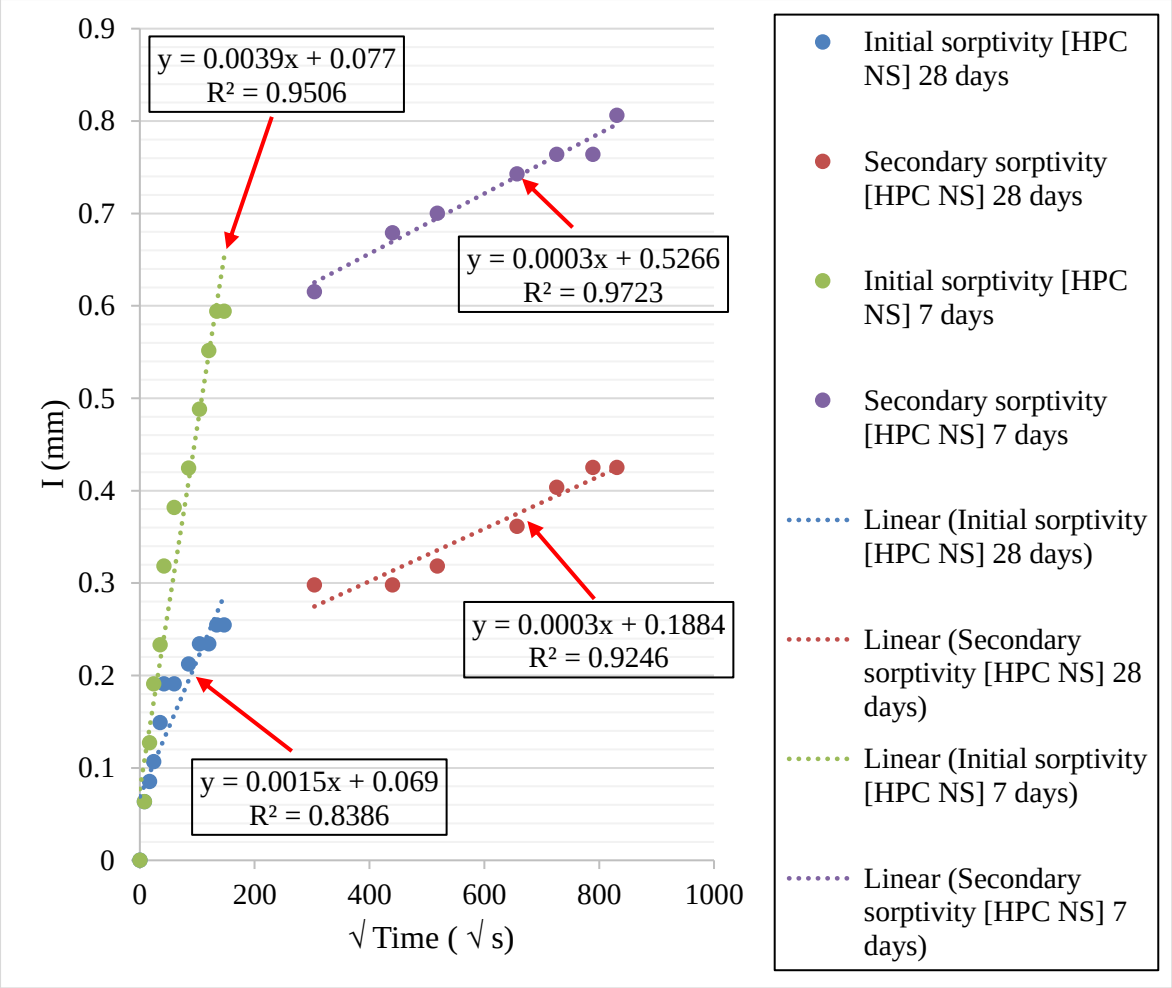


Figure 5. 19: Water sorptivity results of HPFRC (Natural sand) specimens cured for 7 and 28 days along with respective tread lines.

## 5.8. THERMO–GRAVIMETRIC (TG) AND DIFFERENTIAL SCANNING CALORIMETRY (DSC)

From the DSC curves shown in Figure 5.20, it is clear that for both the samples, the major peaks occur around 85°C, 420°C, 575°C, and 680°C. Peak (1) appeared in the temperature range between 30°C to 200°C, which is attributed to a combination of the escape of free water from pores and a part of the bound water from calcium silicate hydrate (CSH gel) *(Shui et al. 2008).* Peak (2) appeared around 420°C which is attributed to the decomposition of calcium hydroxide [$Ca(OH)_2$] *(Shui et al. 2008; Yu et al. 2014).* Peak (3) occurred only in HPC (Standard sand) sample at around 578°C which is attributed to the transformation of quartz present in the Standard sand from α to β modification *(Trník 2016; Scheinherrová et al. 2017).* HPC (Natural sand) sample has not shown any such peak. Peak (4) appeared around 680°C which is attributed

to the decomposition of CSH gel and calcite from carbonated hydrated products *(Scheinherrová et al. 2017).*

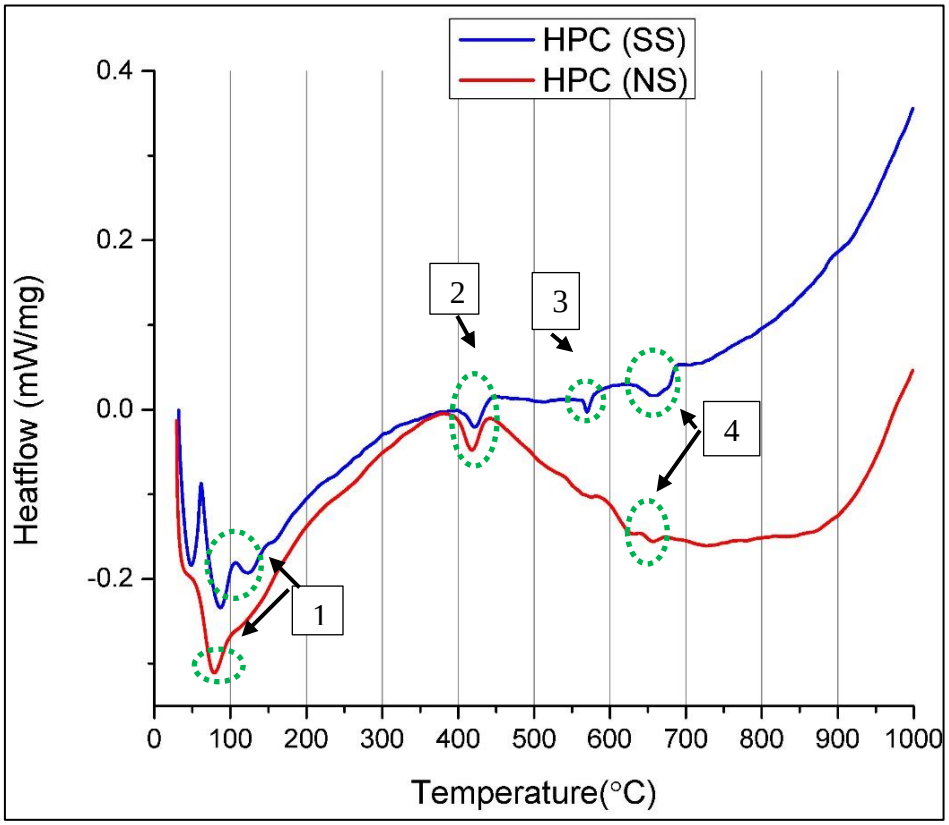


Figure 5. 20: DSC curves of HPC (SS) and HPC (NS) samples.

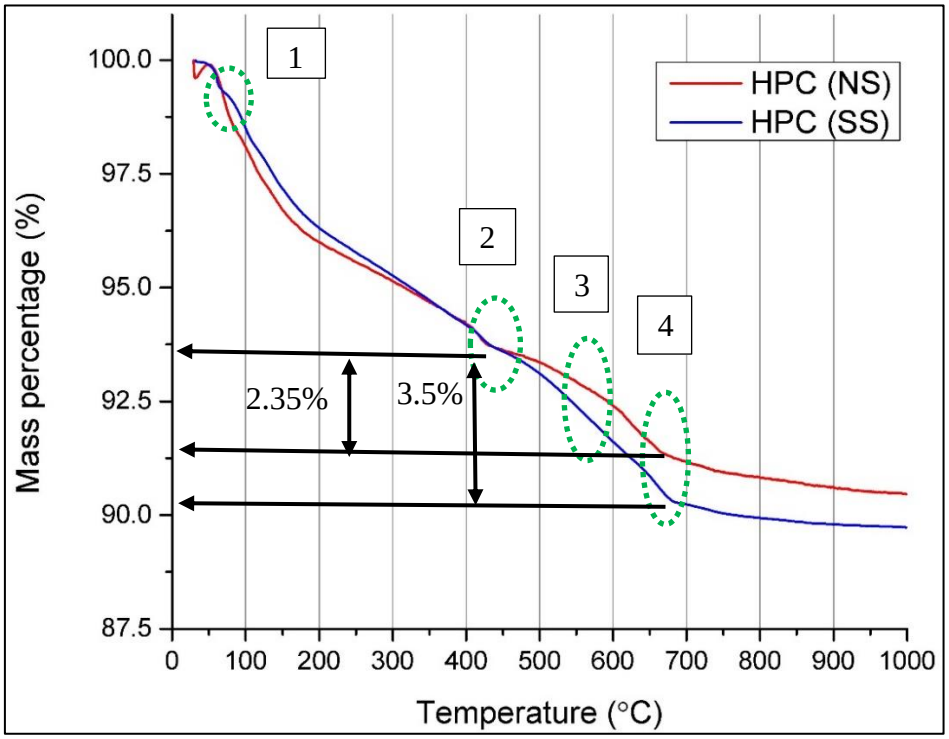


Figure 5. 21: TG curves of HPC (SS) and HPC (NS) samples.

A similar trend of mass loss has been observed for both the samples during TG analysis. From the TG curve shown in Figure 5.21, it is observed that the in HPC (NS) sample, the mass loss of free water and bound water in CSH gel is more than that in HPC (SS) sample (shown as Point (1) in Figure 5.21). This is attributed to the more water absorption capacity of the Natural sand particles as already mentioned in the previous chapter. However, same mass loss of calcium hydroxide in the HPC (SS) sample and HPC (NS) sample takes place (shown as Point (2) in Figure 5.21). Nevertheless, the mass loss of the calcite in HPC (SS) sample and HPC (NS) sample are 3.5 % and 2.35 % respectively. Less mass loss in HPC (NS) sample could be attributed to less formation of hydration products and consequently, less strength.

## 5.9. SCANNING ELECTRON MICROSCOPY AND ENERGY DISPERSIVE SPECTROSCOPY

### 5.9.1 HPHFRC (SS) AND HPHFRC (NS) SAMPLE

A very dense microstructure is observed in both the HPHFRC (SS) and HPHFRC (NS) as shown in Figure 5.22 (A and B). No prominent ITZ could be seen due to the elimination of coarse aggregate in the mixtures. The calcium hydroxide crystals were not observed in both the samples due to the high pozzolanic activity of the silica fume and GGBS. Also, it could be attributed to the low w/b ratio that results in low porosity which limits the growth of calcium hydroxide crystals.

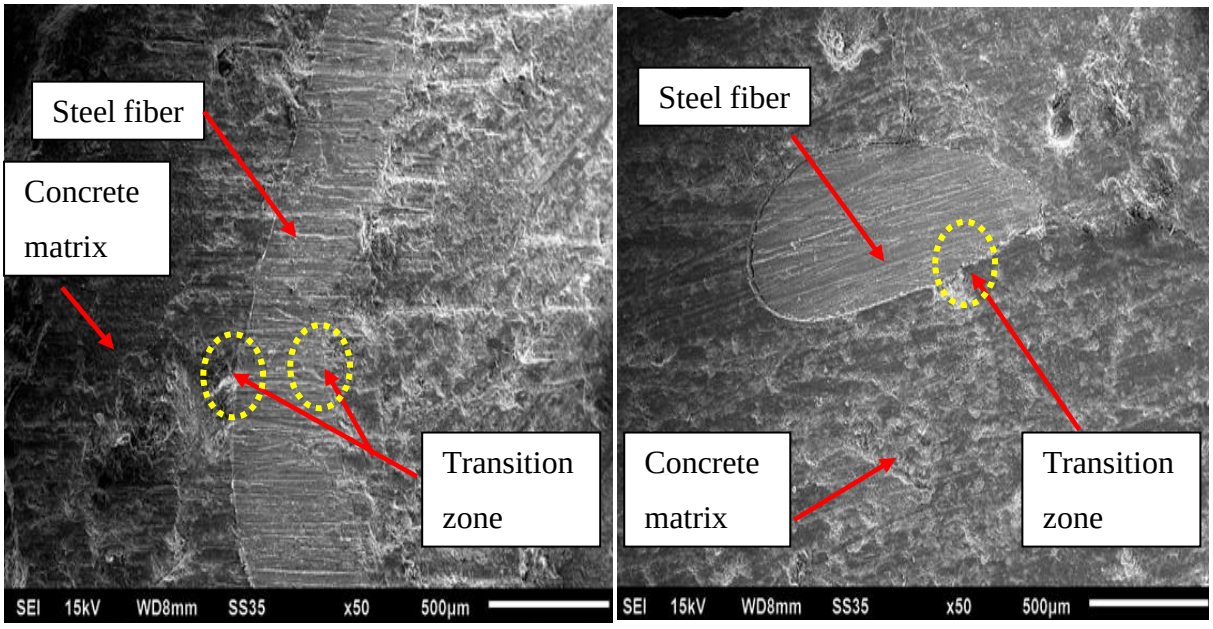


(A) (B)

Figure 5. 22: SEM micrograph showing steel fiber surrounded by the dense concrete matrix: (A) HPHFRC (SS) sample (B) HPHFRC (NS) sample [x50].

A rough interface between the concrete matrix and steel fiber has been observed as shown in Figure 5.23 which would result in a better bond. Along with that, it has a broad interface (gap) which would result in a weak bond between the concrete matrix and fiber so, would result in lower mechanical performance.

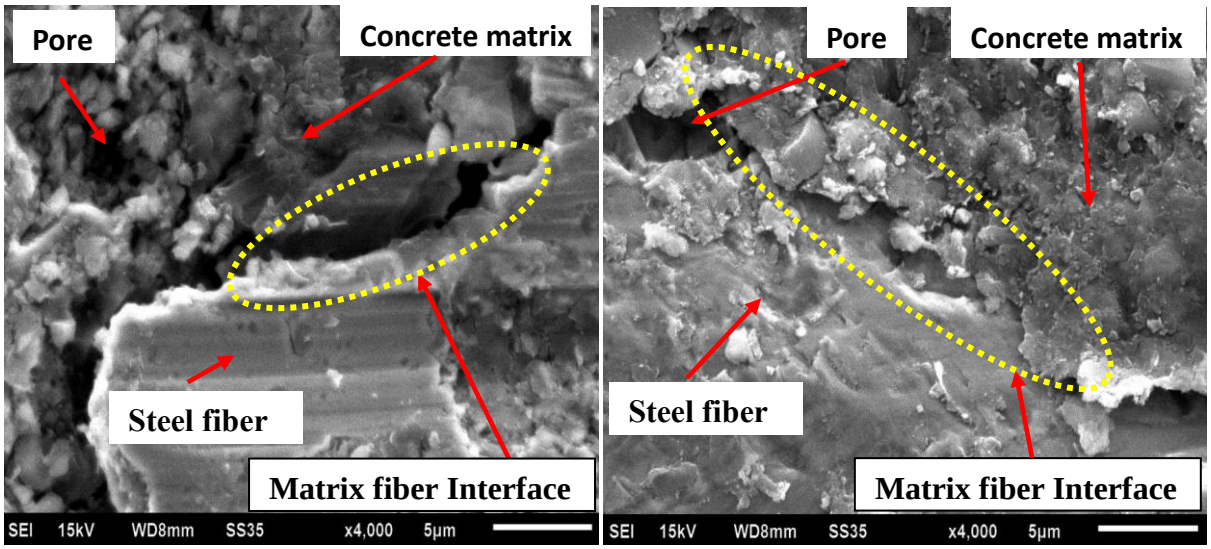


(A) (B)

Figure 5. 23: SEM micrograph showing transition zone between steel fiber and concrete matrix: (A) HPHFRC (SS) sample (B) HPHFRC (NS) sample [x4000].

EDS of HPHFRC (SS) and HPHFRC (NS) sample are shown in Figure 5.24 and Figure 5.25 respectively. There have been a minor change in the elemental composition of both these samples as given in Table 5.11.

Table 5. 11: Elemental composition of HPHFRC (SS) and HPHFRC (NS) sample under EDS spectra.

| Sample | | Weight (%) | | | | | | | |
|---|---|---|---|---|---|---|---|---|---|
| | Element | O | Mg | Al | Si | Ca | Fe | Na | S |
| HPHFRC (SS) | | 40.25 | 1.23 | 5.31 | 9.08 | 36.99 | 6.46 | 0.43 | 0.26 |
| HPHFRC (NS) | | 46.34 | 1.20 | 0.95 | 10.71 | 40.80 | - | - | - |

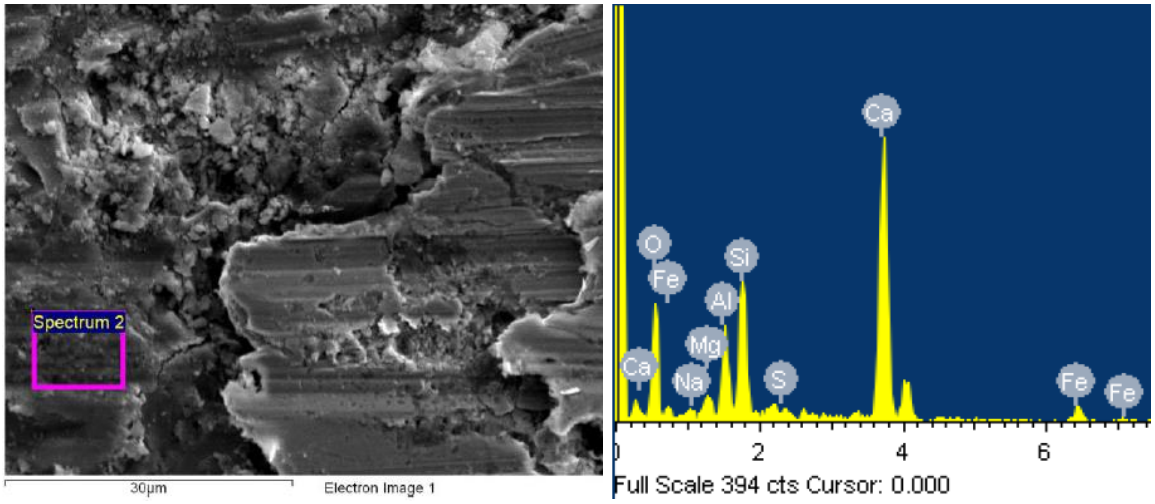


Figure 5. 24: HPHFRC (SS) sample SEM image and EDS spectra of spectrum 2.

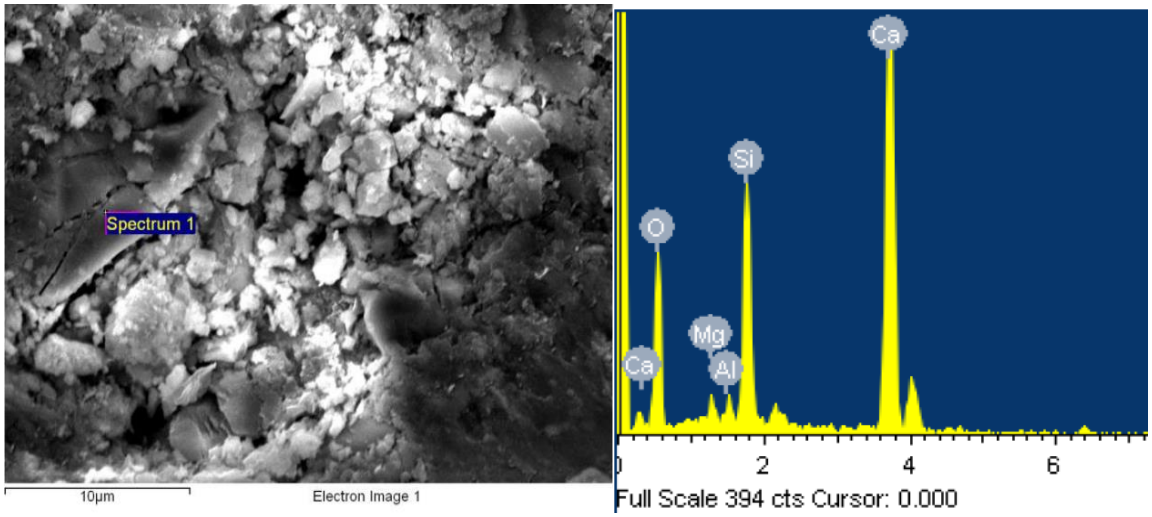


Figure 5. 25: HPHFRC (NS) sample SEM image and EDS spectra of spectrum 1.

5.9.2. STANDARD SAND AND NATURAL SAND

The elemental composition of the Standard and the Natural sand particles are given in Table 5.12. The average silicon content as determined from EDS analysis is more in the Standard sand than the Natural sand. The more silicon content in the Standard sand might have resulted in the epitactic growth of cementitious hydration products on the high silica content Standard sand and could be the reason of high mechanical and durability properties of silica sand HPHFRC *(Struble et al. 1980).*

From the Figure 5.26 (B) and Figure 5.27 (B) the presence of higher intensity of cations is observed which indicates more chances of alkali silica reaction in the Natural sand HPHFRC *(Pedersen, B. M. 2004).*

Table 5. 12: Element percentage weight in both the sands.

| | Weight% | | | | | | | | |
|---|---|---|---|---|---|---|---|---|---|
| Element | Si | O | Al | Fe | K | Na | Mg | Ca | C |
| Standard sand | 35.01 | 60.47 | 1.83 | 0.326 | 0.183 | 0.073 | 0.133 | 0.076 | 1.9 |
| Natural sand | 27.35 | 57.05 | 3.79 | 0.89 | 3.25 | 0.57 | 0.52 | 2.04 | 4.54 |

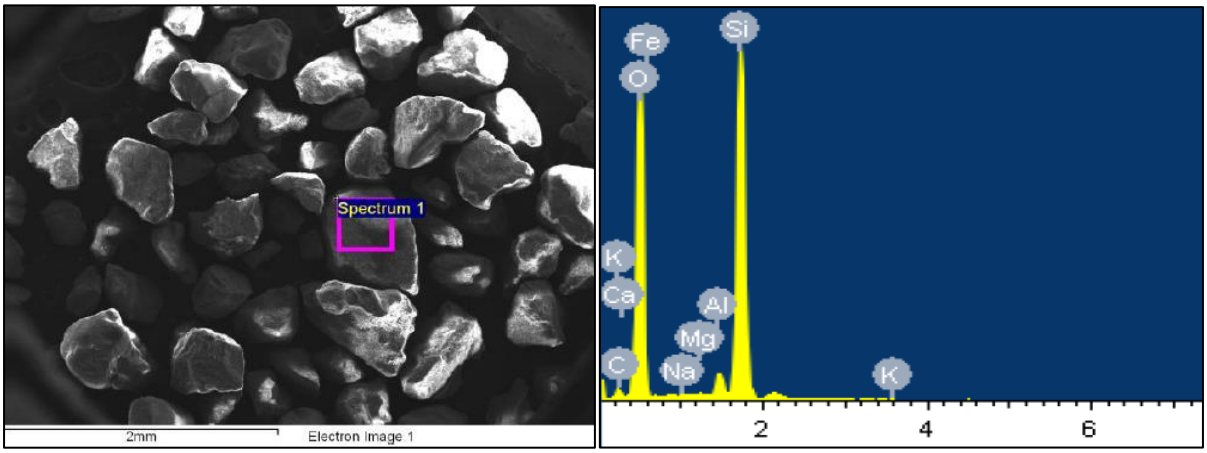


(A) (B)

Figure 5. 26: Standard sand (A) SEM image (B) EDS spectra.

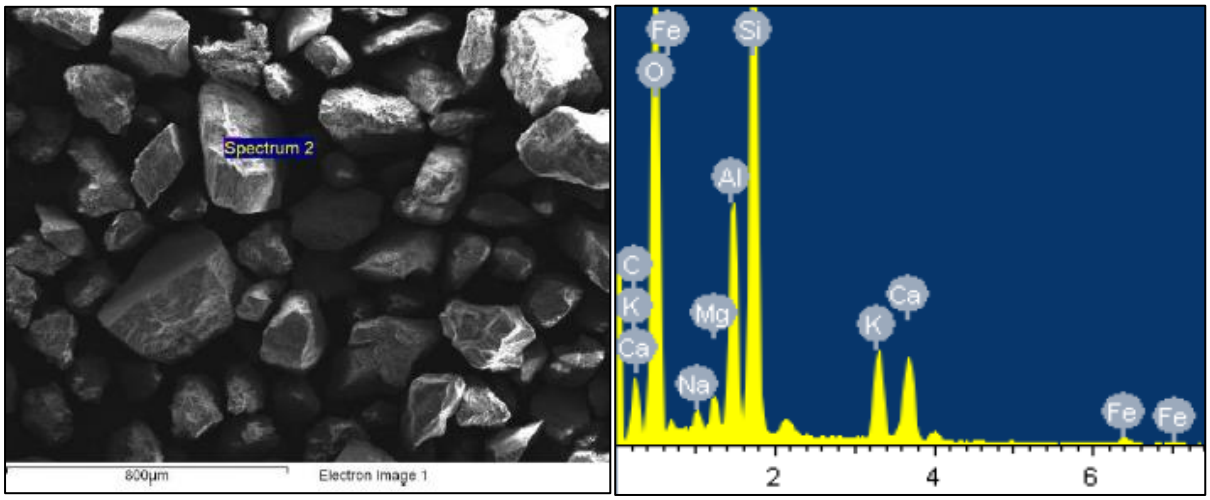


(A) (B)

Figure 5. 27: Natural sand (A) SEM image (B) EDS spectra.

## 5.10. XRD ANALYSIS

To examine the difference in the mineralogical characteristics of HPC (SS) and HPC (NS) XRD analysis was performed

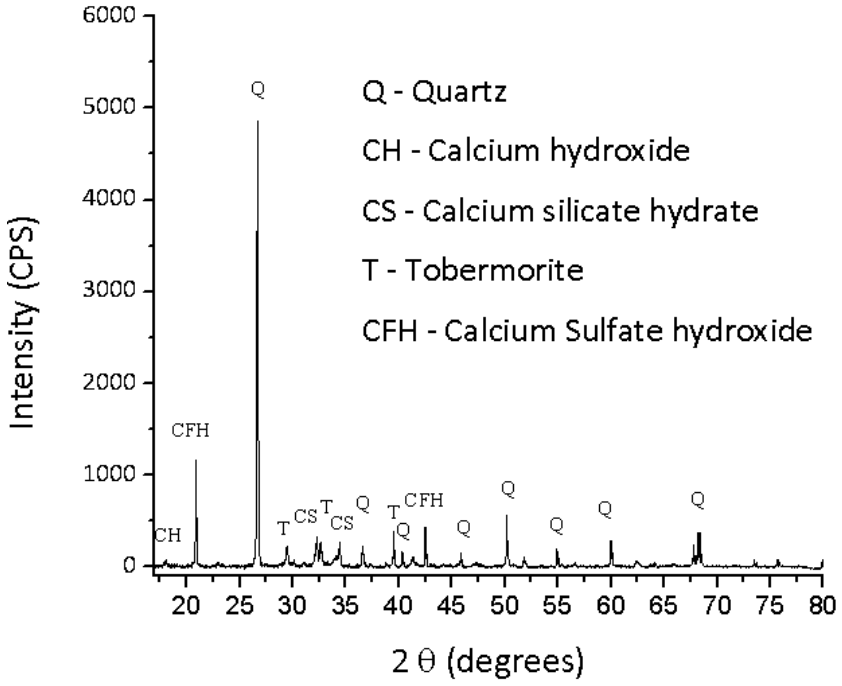


Figure 5. 28: XRD pattern of HPC (SS).

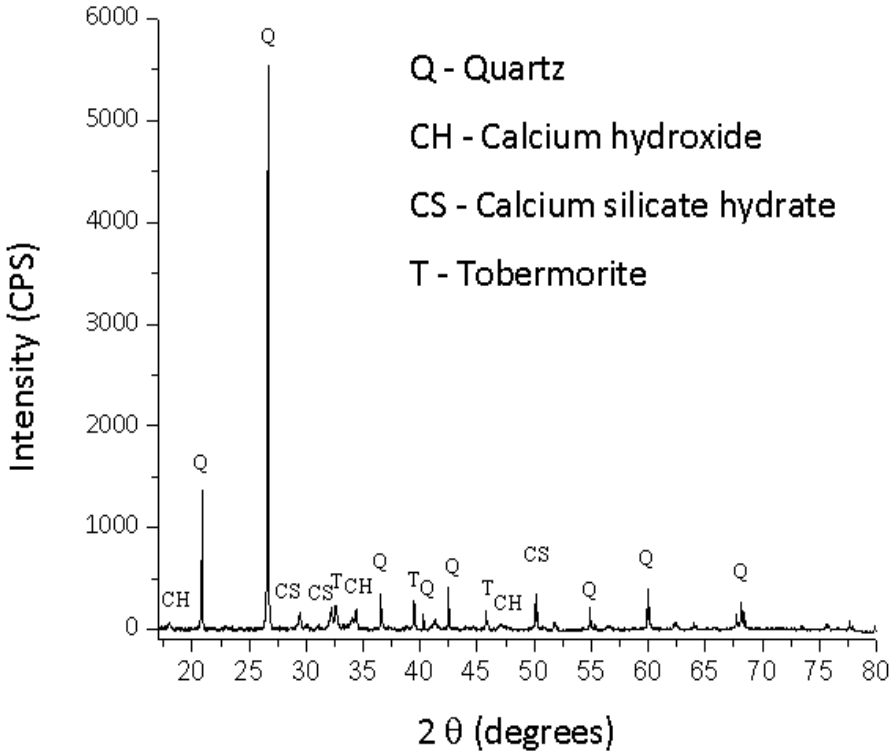


Figure 5. 29: XRD pattern of HPC (NS).

During the XRD analysis, there has not been much difference in peaks observed in diffractograms of HPC (SS) and HPC (NS) as shown in Figure 5.28 and Figure 5.29.

Distinct high intensity quartz peaks were seen which indicates that the sand particles have a crystalline nature of quartz. Calcium Silicate hydrate (CSH) peaks have been observed which are due to the water reaction with calcium silicate minerals ($C_3S$ and $C_2S$) and calcium aluminate/ferrite minerals ($C_3A$ and $C_4AF$) present in Portland cement. Additional CSH formation occurs due to the pozzolanic reaction of silica fume and the calcium hydroxide released during the hydration of cement. Hydration of silicates present in GGBS also results in CSH gel formation. The reaction of tricalcium aluminate and gypsum (present in cement) results in the formation of Ettringite.

But in the XRD analysis, Ettringite peaks were not observed which concludes that it had been converted to monosulfoaluminate due to less availability of gypsum (calcium sulfate dehydrate). Though there were calcium sulfate hydroxide peaks observed in UHPC (SS) sample which are the result of the reaction between hydroxylellestadite (HE: $Ca_{10}(SiO_4)_3(SO_4)_3(OH)_2$) with the dissolved quartz. Hydroxylellestadite is produced with sulfur released from monosulfate-14. Tobermorite, another CSH gel product is formed along with anhydrite ($CaSO_4$) as observed on the diffractograms of both the samples *(Kikuma et al. 2009; Limantono et al. 2016).* A little higher presence of calcium hydroxide peaks in HPC (NS) signifies more porosity and hence less strength and durability properties.

# CHAPTER 6

# OBSERVATIONS

## 6.1 GENERAL

The present study was undertaken firstly to mix design HPHFRC using Modified A & A particle packing model based on workability and compressive strength criteria. Secondly, to see the effect of replacement of the Standard sand with the Natural sand in HPHFRC.

## 6.2 CONCLUSIONS

After analyzing the test results, the following conclusions can be drawn:

- The Modified A & A particle packing model is used to develop the HPHFRC through the optimum particle packing of the concrete mix. From the experimental study, it has been found that using this model a dense cementitious matrix is obtained with a compressive strength above 100 MPa.
- Total 16 mix trials are prepared, the addition of GGBS improves the workability of the mix as compared to silica fume contained sample even with the low amount of water/binder ratio i.e. 0.16. The GGBS improved the flow behaviour because of its smooth glassy texture. The trial Mix 15 and 16 fulfills both the preset workability (percentage flow greater than 150) and compressive strength (greater than 80 MPa) criteria.
- The highest compressive strength, split tensile strength and flexural strength obtained were 104 MPa, 13 MPa, and 39 MPa respectively, which signifies the excellent mechanical strength of mix designed HPHFRC. It is attributed to the formation of a dense matrix with the inclusion of SCMs and their optimum packing using the Modified A & A model.
- Due to the same length of hooked steel fibers and the specimen cut, RCPT could not be performed because of the overflow of charge passed through the specimen on the initiation of the experiment. Without the usage of long hooked fibers, the average charge passed through HPFRC (SS) and HPFRC (NS) specimens were 358 and 364 coulombs respectively. These values according to the ASTM C1202 -15 represents very low chloride ion penetrability.

- In the water sorptivity test, the absorption (I) for HPHFRC (SS) specimens was 0.74 mm whereas for HPHFRC (NS) specimens it was 0.806 mm at 7 days curing, which are much less than normal strength concrete. Hence, signifies a dense microstructure of mix designed HPHFRC.
- From the SEM analysis, a very dense microstructure is observed in both the HPHFRC (SS) and HPHFRC (NS) samples. The higher presence of CH compound found in XRD analysis might be one of the reasons for the lower strength of HPHFRC (NS) than HPHFRC (SS). In TG analysis, lesser mass loss of HPC (NS) sample justifies the lesser formation of hydration products than HPC (SS).
- The addition of hybrid fibers significantly increases the tensile and flexural strength which are laying in the range of UHP-HFRC even without heat curing. However, the compressive strength is not in the range of UHPHFRC. It implies that the synergistic effect of hybrid fiber more pronounced to improve the tensile and flexural properties as compared to compressive strength.
- With the usage of Natural sand in HPHFRC, a marginal reduction in fresh and hardened properties are observed as compared to the Indian standard sand contained HPHFRC. Therefore, the Natural sand can be used to develop the HPHFRC for strength more than 100 MPa using the Modified A & A model.
- Considering the higher mechanical and durability properties even with traditional mixing, casting and at ambient curing (at $27\ ^{0}$ C) shows the practical applicability of the mix designed HPHFRC. The prepared HPHFRC by Modified A & A model can be improved further, with the application of heat or steam curing and achieve the strength criteria of Ultra High Performance Concrete (UHPC).

## 6.3 SCOPE FOR FUTURE WORK

- Since the total content of steel fibers after the mix trials in this study was fixed as 2 % of the volume of concrete with 0.5 % short crimped and 1.5 % long hooked fibers. Further research could be done by varying the relative proportions of steel fibers or the total content of steel fibers for better mechanical properties of HPHFRC.
- Usage of other supplementary cementitious materials like fly ash, rice husk ash along with silica fume and GGBS could be done in mix design of HPHFRC.
- Impact and blast resistance of the design mix could be investigated.

- More durability tests like sulphate attack, water absorption, and freeze thawing resistance could be examined.

# REFERENCES


- Abbas, S., Soliman, A. M., & Nehdi, M. L. (2015). Exploring mechanical and durability properties of ultra-high performance concrete incorporating various steel fiber lengths and dosages. Construction and Building Materials, 75, 429-441.
- Afroughsabet, V., & Ozbakkaloglu, T. (2015). Mechanical and durability properties of high-strength concrete containing steel and polypropylene fibers. Construction and building materials, 94, 73-82.
- Ahlborn, T. M., Peuse, E. J., & Misson, D. L. (2008). Ultra-high-performance-concrete for michigan bridges material performance–phase I (No. MDOT RC-1525).
- Alkaysi, M., El-Tawil, S., Liu, Z., & Hansen, W. (2016). Effects of silica powder and cement type on durability of ultra high performance concrete (UHPC). Cement and Concrete Composites, 66, 47-56.
- ASTM, C1202- 12. Standard Test Method for Electrical Indication of Concrete's Ability to Resist Chloride Ion Penetration," American Society for Testing and Materials.
- ASTM C1585- 04 Standard Test Method for Measurement of Rate of Absorption of Water by Hydraulic-Cement Concretes.
- Benson, S. D. P., & Karihaloo, B. L. (2005). CARDIFRC®-Development and mechanical properties. Part III: Uniaxial tensile response and other mechanical properties. Magazine of Concrete Research, 57(8), 433-443.
- Bindiganavile, V., Banthia, N., & Aarup, B. (2002). Impact response of ultra-high-strength fiber-reinforced cement composite. Materials Journal, 99(6), 543-548.
- Blunt, J., Jen, G., & Ostertag, C. P. (2015). Enhancing corrosion resistance of reinforced concrete structures with hybrid fiber reinforced concrete. Corrosion Science, 92, 182-191.
- Bonneau, O., Lachemi, M., Dallaire, E., Dugat, J., & Aitcin, P. C. (1997). Mechanical properties and durability of two industrial reactive powder concretes. Materials Journal, 94(4), 286-290.
- BS EN 196-1: (1995). Methods of testing cement. Determination of strength.
- Deeb, R., Ghanbari, A., & Karihaloo, B. L. (2012). Development of self-compacting high and ultra high performance concretes with and without steel fibres. Cement and concrete composites, 34(2), 185-190.

- De Larrard, F., & Sedran, T. (1994). Optimization of ultra-high-performance concrete by the use of a packing model. Cement and Concrete Research, 24(6), 997-1009.
- De Larrard, F., & Sedran, T. (2002). Mixture-proportioning of high-performance concrete. Cement and concrete research, 32(11), 1699-1704.
- Fuller, W. B., & Thompson, S. E. (1907). The laws of proportioning concrete.
- Funk, J. E., & Dinger, D. R. (2013). Predictive process control of crowded particulate suspensions: applied to ceramic manufacturing. Springer Science & Business Media.
- Goldman, A., & Bentur, A. (1994). Properties of cementitious systems containing silica fume or nonreactive microfillers. Advanced Cement Based Materials, 1(5), 209-215.
- Graybeal, B. A. (2006). Material property characterization of ultra-high performance concrete (No. FHWA-HRT-06-103).
- Graybeal, B. A. (2007). Compressive behavior of ultra-high-performance fiber-reinforced concrete. ACI materials journal, 104(2), 146.
- Habel, K. (2004). Structural behaviour of elements combining ultra-high performance fibre reinforced concretes (UHPFRC) and reinforced concrete.
- Habel, K., Charron, J. P., Braike, S., Hooton, R. D., Gauvreau, P., & Massicotte, B. (2008). Ultra-high performance fibre reinforced concrete mix design in central Canada. Canadian Journal of Civil Engineering, 35(2), 217-224.
- Habel, K., & Gauvreau, P. (2008). Response of ultra-high performance fiber reinforced concrete (UHPFRC) to impact and static loading. Cement and Concrete Composites, 30(10), 938-946.
- Heinz, D., & Ludwig, H. M. (2004, September). Heat treatment and the risk of DEF delayed ettringite formation in UHPC. In Proceedings of the International Symposium on Ultra-High Performance Concrete, Kassel, Germany, Sept. 13 (Vol. 15, pp. 717-730).
- Heinz, D., Urbonas, L., & Dehn, F. (2004, September). Fire resistance of ultra high performance concrete (UHPC)-Testing of laboratory samples and columns under load. In International Symposium on Ultra High Performance Concrete (pp. 703-715).
- Herold, G., & Müller, H. S. (2004, September). Measurement of porosity of ultra high strength fibre reinforced concrete. In Proceedings of the International Symposium on Ultra-High Performance Concrete, Kassel, Germany (pp. 685-694).
- Ho, D. W. S., Chua, C. W., & Tam, C. T. (2003). Steam-cured concrete incorporating mineral admixtures. Cement and concrete research, 33(4), 595-601.

- http://www.iti.northwestern.edu/cement/monograph/Monograph13_1_2.html.
- Hughes, B. P., & Fattuhi, N. I. (1976). The workability of steel-fibre-reinforced concrete. Magazine of concrete research, 28(96), 157-161.
- IS 456: (2000). PLAIN AND REINFORCED CONCRETE – CODE OF PRACTICE.
- IS 12269: (2013). ORDINARY PORTLAND CEMENT, 53 GRADE — SPECIFICATION.
- IS 4031-11: (1988). Methods of physical tests for hydraulic cement, Part 11: Determination of density.
- IS 4031-6: (1988). Methods of physical tests for hydraulic cement, Part 6: Determination of compressive strength of hydraulic cement (other than masonry cement).
- IS 5816: (1999). Method of Test Splitting Tensile Strength of Concrete.
- IS 4031-4: (1988). Methods of physical tests for hydraulic cement, Part 4: Determination of consistency of standard cement paste.
- IS 4031-5: (1988). Methods of physical tests for hydraulic cement, Part 5: Determination of initial and final setting times.
- IS 4031-6: (1988). Methods of physical tests for hydraulic cement, Part 6: Determination of compressive strength of hydraulic cement (other than masonry cement).
- IS 650: (1991). Specification for Standard Sand for Testing of Cement.
- IS 383: (1970). Specification for Coarse and Fine Aggregates From Natural Sources For Concrete.
- Jacobsen, S., Sellevold, E. J., Maage, M., Smeplass, S., Kjellsen, K. O., Lindgård, J., ... & Bjøntegaard, Ø. (2009). TKT 4215 Concrete Technology 1.
- Khaloo, A. R., Karimi, H., Asadollahi, S., & Dehestani, M. (2017). A New Mixture Design Method for Ultra-High-Strength Concrete. ACI Materials Journal, 114(2).
- Khan, S. U., Nuruddin, M. F., Ayub, T., & Shafiq, N. (2014). Effects of different mineral admixtures on the properties of fresh concrete. The Scientific World Journal, 2014.
- Khater, H., & Ahmed, S. (2016). Effect of Steel Fibers on Behavior of Ultra High Performance Concrete, First International Interactive Symposium on UHPC-2016.

- Kikuma, J., Tsunashima, M., Ishikawa, T., Matsuno, S., Ogawa, A., Matsui, K., & Sato, M. (2009). Formation of Autoclaved Aerated Concrete Studied by In Situ X-ray Diffraction under Hydrothermal Condition. Research Frontiers 2009, 142-143.
- Köksal, F., Altun, F., Yiğit, İ., & Şahin, Y. (2008). Combined effect of silica fume and steel fiber on the mechanical properties of high strength concretes. Construction and building materials, 22(8), 1874-1880.
- Kou, S. C., Poon, C. S., & Agrela, F. (2011). Comparisons of natural and recycled aggregate concretes prepared with the addition of different mineral admixtures. Cement and Concrete Composites, 33(8), 788-795.
- Lei, V. Y., Nematollahi, B., Said, A. B. M., Gopal, B. A., & Yee, T. S. (2012). Application of ultra high performance fiber reinforced concrete–the malaysia perspective. International Journal of Sustainable Construction Engineering and Technology, 3(1), 26-44.
- Limantono, H., Ekaputri, J. J., & Susanto, T. E. (2016). EFFECT OF SILICA FUME AND GLASS POWDER ON HIGH-STRENGTH PASTE. Key Engineering Materials, 673.
- Malagavelli, V., & Rao, P. N. (2010). High performance concrete with GGBS and ROBO sand. International journal of engineering science and technology, 2(10), 5107-5113.
- Mazloom, M., Ramezanianpour, A. A., & Brooks, J. J. (2004). Effect of silica fume on mechanical properties of high-strength concrete. Cement and Concrete Composites, 26(4), 347-357.
- Mohammadi, Y., Singh, S. P., & Kaushik, S. K. (2008). Properties of steel fibrous concrete containing mixed fibres in fresh and hardened state. Construction and Building Materials, 22(5), 956-965.
- Mueller, H. S., & Haist, M. (2009). FIB, structural concrete. textbook on behaviour, design and performance—updated knowledge of the CEB/FIP Model Code 1990. *fib Bulletin*, *1*, 35-95.
- Okuma, H. A. (2006). The first highway bridge applying ultra high strength fiber reinforced concrete in Japan. In Proceedings of the 7th International Conference on Short and Medium Span Bridges, Montreal, 2006.
- Pedersen, B. M. (2004). Alkali-reactive and inert fillers in concrete. Rheology of fresh mixtures and expansive reactions.

- Prem, P.R., Bharatkumar, B.H., and Iyer, N.R. (2012). Mechanical properties of Ultra High Performance Concrete, International Journal of Civil, Environmental, Structural, Construction and Architectural Engineering, 6(8), 676-685.
- Qian, C. X., & Stroeven, P. (2000). Development of hybrid polypropylene-steel fibre-reinforced concrete. Cement and concrete research, 30(1), 63-69.
- Ramezanianpour, A. A., Esmaeili, M., Ghahari, S. A., & Najafi, M. H. (2013). Laboratory study on the effect of polypropylene fiber on durability, and physical and mechanical characteristic of concrete for application in sleepers. Construction and Building Materials, 44, 411-418.
- Reda, M. M., Shrive, N. G., & Gillott, J. E. (1999). Microstructural investigation of innovative UHPC. Cement and Concrete Research, 29(3), 323-329.
- Richard, P., & Cheyrezy, M. H. (1994). Reactive powder concretes with high ductility and 200-800 MPa compressive strength. Special Publication, 144, 507-518.
- Richard, P., & Cheyrezy, M. H. (1994). Reactive powder concretes with high ductility and 200-800 MPa compressive strength. Special Publication, 144, 507-518.
- Richard, P., & Cheyrezy, M. (1995). Composition of reactive powder concretes. Cement and concrete research, 25(7), 1501-1511.
- Rossi, P. (2001). Ultra-High Performance Fiber-Reinforced Concretes. Concrete international, 23(12), 46-52.
- Rossi, P., Arca, A., Parant, E., & Fakhri, P. (2005). Bending and compressive behaviours of a new cement composite. Cement and Concrete Research, 35(1), 27-33.
- Scheinherrová, L., Fořt, J., Pavlík, Z., & Černý, R. (2017, July). Simultaneous thermal analysis and thermodilatometry of hybrid fiber reinforced UHPC. In AIP Conference Proceedings (Vol. 1866, No. 1, p. 040033). AIP Publishing.
- Schmidt, M., & Fehling, E. (2005). Ultra-high-performance concrete: research, development and application in Europe. ACI Special publication, 228, 51-78.
- Schydt, J., Herold, G., & Müller, H. S. (2008, March). Long term behavior of ultra high performance concrete under the attack of chlorides and aggressive waters. In Proceedings of the 2nd international symposium on ultra high performance concrete (pp. 231-238).
- Shui, Z., Xuan, D., Wan, H., & Cao, B. (2008). Rehydration reactivity of recycled mortar from concrete waste experienced to thermal treatment. Construction and Building materials, 22(8), 1723-1729.

- Soliman, N. A., & Tagnit-Hamou, A. (2017). Using glass sand as an alternative for quartz sand in UHPC. Construction and Building Materials, 145, 243-252.
- Stiel, T., Karihaloo, B., & Fehling, E. (2004, September). Effect of casting direction on the mechanical properties of CARDIFRC. In Proceedings of the International Symposium on Ultra-High Performance Concrete, Kassel, Germany (pp. 481-493).
- Struble, L., Skalny, J., & Mindess, S. (1980). A review of the cement-aggregate bond. Cement and concrete research, 10(2), 277-286.
- Suresh, D., & Nagaraju, K. (2015). Ground Granulated Blast Slag (GGBS) In Concrete–A Review. IOSR Journal of Mechanical and Civil Engineering (IOSR-JMCE), 12(4), 76-82.
- Tasdemir, C. (2003). Combined effects of mineral admixtures and curing conditions on the sorptivity coefficient of concrete. cement and concrete research, 33(10), 1637-1642.
- Thomas, M., Green, B., O'Neal, E., Perry, V., Hayman, S., & Hossack, A. (2012, March). Marine performance of UHPC at Treat Island. In Proceedings of the 3rd International Symposium on UHPC and Nanotechnology for High Performance Construction Materials, Kassel, Germany (pp. 365-370).
- Toutlemonde, F., & Resplendino, J. (Eds.). (2011). Designing and Building with UHPFRC: State of the Art and Development. ISTE.
- Trník, A., Fořt, J., Pavlíková, M., Čáchová, M., Čítek, D., Kolísko, J., ... & Pavlík, Z. (2016, July). UHPFRC at high temperatures–Simultaneous thermal analysis and thermodilatometry. In AIP Conference proceedings (Vol. 1752, No. 1, p. 040028). AIP Publishing.
- Tue, N. V., Ma, J., & Orgass, M. (2008). Influence of addition method of superplasticizer on the properties of fresh UHPC. In Proceedings of Second International Symposium on Ultra High Performance Concrete, University of Kassel, Germany (pp. 93-100).
- Uysal, M., Yilmaz, K., & Ipek, M. (2012). The effect of mineral admixtures on mechanical properties, chloride ion permeability and impermeability of self-compacting concrete. Construction and Building Materials, 27(1), 263-270.
- Vogt, C. (2010). Ultrafine particles in concrete: Influence of ultrafine particles on concrete properties and application to concrete mix design (Doctoral dissertation, KTH).

- Wille, K., Naaman, A. E., & Parra-Montesinos, G. J. (2011). Ultra-High Performance Concrete with Compressive Strength Exceeding 150 MPa (22 ksi): A Simpler Way. ACI Materials Journal, 108(1).
- www.wikipedia.com
- Xing, F., Huang, L. D., Cao, Z. L., & Deng, L. P. (2006). Study on preparation technique for low-cost green reactive powder concrete. In Key Engineering Materials (Vol. 302, pp. 405-410). Trans Tech Publications.
- Yang, S. L., Millard, S. G., Soutsos, M. N., Barnett, S. J., & Le, T. T. (2009). Influence of aggregate and curing regime on the mechanical properties of ultra-high performance fibre reinforced concrete (UHPFRC). Construction and Building Materials, 23(6), 2291-2298.
- Yardımcı, M. Y., Aydın, S., & Karabulut, A. Ş. (2009). Mechanical properties of reactive powder concrete containing mineral admixtures under different curing regimes. Construction and building materials, 23(3), 1223-1231.
- Yeau, K. Y., & Kim, E. K. (2005). An experimental study on corrosion resistance of concrete with ground granulate blast-furnace slag. Cement and Concrete Research, 35(7), 1391-1399.
- Yu, R., Spiesz, P., & Brouwers, H. J. H. (2014). Mix design and properties assessment of ultra-high performance fibre reinforced concrete (UHPFRC). Cement and concrete research, 56, 29-39.
- Yu, R., Spiesz, P., & Brouwers, H. J. H. (2015). Development of Ultra-High Performance Fibre Reinforced Concrete (UHPFRC): Towards an efficient utilization of binders and fibres. Construction and Building Materials, 79, 273-282.

# APPENDIX

## MIX DESIGN DATASHEET

Table A. 1: Mix design of trial Mix 1.

| Particle size (μm) | Residue volume (%) | | | Target function | Volume fraction | | | Composed mix | |
|---|---|---|---|---|---|---|---|---|---|
| | | | | | $V_{ss}$ | $V_c$ | $V_{sf}$ | Cumulative residue (%) | Cumulative passing (%) |
| | SS | C | SF | P (D) | SS | C | SF | $R_{mix}(D)$ | $Q_{mix}(D)$ |
| 0.24 | | | 0.17 | 0.00 | | | 0.11 | 100.00 | 0.00 |
| 0.28 | | | 0.38 | 0.00 | | | 0.11 | 99.97 | 0.03 |
| 0.31 | | | 0.65 | 0.52 | | | 0.11 | 99.90 | 0.10 |
| 0.36 | | 0.00 | 0.95 | 1.04 | | 0.30 | 0.11 | 99.76 | 0.24 |
| 0.41 | | 0.06 | 1.23 | 1.58 | | 0.30 | 0.11 | 99.54 | 0.46 |
| 0.46 | | 0.07 | 1.42 | 2.13 | | 0.30 | 0.11 | 99.22 | 0.78 |
| 0.52 | | 0.09 | 1.47 | 2.71 | | 0.30 | 0.11 | 98.83 | 1.17 |
| 0.59 | | 0.11 | 1.37 | 3.30 | | 0.30 | 0.11 | 98.40 | 1.60 |
| 0.68 | | 0.13 | 1.12 | 3.91 | | 0.30 | 0.11 | 97.96 | 2.04 |
| 0.77 | | 0.16 | 0.78 | 4.54 | | 0.30 | 0.11 | 97.53 | 2.47 |
| 0.87 | | 0.20 | 0.42 | 5.19 | | 0.30 | 0.11 | 97.16 | 2.84 |
| 0.99 | | 0.25 | 0.14 | 5.85 | | 0.30 | 0.11 | 96.84 | 3.16 |
| 1.13 | | 0.31 | 0.00 | 6.53 | | 0.30 | 0.11 | 96.58 | 3.42 |
| 1.28 | | 0.38 | 0.00 | 7.24 | | 0.30 | 0.11 | 96.33 | 3.67 |
| 1.45 | | 0.46 | 0.00 | 7.97 | | 0.30 | 0.11 | 96.08 | 3.92 |
| 1.65 | | 0.56 | 0.09 | 8.71 | | 0.30 | 0.11 | 95.82 | 4.18 |
| 1.88 | | 0.66 | 0.30 | 9.48 | | 0.30 | 0.11 | 95.50 | 4.50 |
| 2.13 | | 0.78 | 0.62 | 10.27 | | 0.30 | 0.11 | 95.11 | 4.89 |
| 2.42 | | 0.91 | 1.02 | 11.09 | | 0.30 | 0.11 | 94.61 | 5.39 |
| 2.75 | | 1.05 | 1.40 | 11.93 | | 0.30 | 0.11 | 93.96 | 6.04 |

| | | | | | | | | | |
|---|---|---|---|---|---|---|---|---|---|
| 3.13 | | 1.20 | 1.72 | 12.80 | | 0.30 | 0.11 | 93.17 | 6.83 |
| 3.55 | | 1.35 | 1.94 | 13.69 | | 0.30 | 0.11 | 92.23 | 7.77 |
| 4.03 | | 1.52 | 2.07 | 14.61 | | 0.30 | 0.11 | 91.16 | 8.84 |
| 4.58 | | 1.70 | 2.13 | 15.55 | | 0.30 | 0.11 | 89.97 | 10.03 |
| 5.21 | | 1.89 | 2.17 | 16.52 | | 0.30 | 0.11 | 88.70 | 11.30 |
| 5.92 | | 2.10 | 2.24 | 17.53 | | 0.30 | 0.11 | 87.35 | 12.65 |
| 6.72 | | 2.33 | 2.37 | 18.56 | | 0.30 | 0.11 | 85.95 | 14.05 |
| 7.64 | | 2.59 | 2.58 | 19.62 | | 0.30 | 0.11 | 84.50 | 15.50 |
| 8.68 | | 2.87 | 2.90 | 20.72 | | 0.30 | 0.11 | 82.97 | 17.03 |
| 9.86 | | 3.17 | 3.33 | 21.84 | | 0.30 | 0.11 | 81.36 | 18.64 |
| 11.20 | | 3.50 | 3.88 | 23.01 | | 0.30 | 0.11 | 79.65 | 20.35 |
| 12.73 | | 3.84 | 4.51 | 24.20 | | 0.30 | 0.11 | 77.78 | 22.22 |
| 14.46 | | 4.19 | 5.18 | 25.43 | | 0.30 | 0.11 | 75.74 | 24.26 |
| 16.43 | | 4.53 | 5.81 | 26.70 | | 0.30 | 0.11 | 73.50 | 26.50 |
| 18.66 | | 4.84 | 6.32 | 28.01 | | 0.30 | 0.11 | 71.06 | 28.94 |
| 21.21 | | 5.09 | 6.61 | 29.35 | | 0.30 | 0.11 | 68.44 | 31.56 |
| 24.09 | | 5.27 | 6.60 | 30.74 | | 0.30 | 0.11 | 65.69 | 34.31 |
| 27.37 | | 5.35 | 6.25 | 32.16 | | 0.30 | 0.11 | 62.88 | 37.12 |
| 31.10 | | 5.31 | 5.56 | 33.63 | | 0.30 | 0.11 | 60.11 | 39.89 |
| 35.34 | | 5.13 | 4.60 | 35.14 | | 0.30 | 0.11 | 57.45 | 42.55 |
| 40.15 | | 4.81 | 3.48 | 36.70 | | 0.30 | 0.11 | 55.01 | 44.99 |
| 45.61 | 0.04 | 4.37 | 2.35 | 38.30 | 0.33 | 0.30 | 0.11 | 52.86 | 47.14 |
| 51.82 | 0.08 | 3.82 | 1.35 | 39.95 | 0.33 | 0.30 | 0.11 | 51.02 | 48.98 |
| 58.88 | 0.12 | 3.20 | 0.52 | 41.65 | 0.33 | 0.30 | 0.11 | 49.50 | 50.50 |
| 66.90 | 0.17 | 2.54 | | 43.41 | 0.33 | 0.30 | | 48.30 | 51.70 |
| 76.01 | 0.20 | 1.91 | | 45.21 | 0.33 | 0.30 | | 47.38 | 52.62 |
| 86.36 | 0.20 | 1.35 | | 47.07 | 0.33 | 0.30 | | 46.66 | 53.34 |

| | | | | | | | | | |
|---|---|---|---|---|---|---|---|---|---|
| 98.11 | 0.17 | 0.90 | | 48.98 | 0.33 | 0.30 | | 46.12 | 53.88 |
| 111.47 | 0.14 | 0.57 | | 50.95 | 0.33 | 0.30 | | 45.74 | 54.26 |
| 126.65 | 0.17 | 0.36 | | 52.98 | 0.33 | 0.30 | | 45.49 | 54.51 |
| 143.90 | 0.30 | 0.25 | | 55.07 | 0.33 | 0.30 | | 45.30 | 54.70 |
| 163.49 | 0.69 | 0.21 | | 57.22 | 0.33 | 0.30 | | 45.08 | 54.92 |
| 185.75 | 1.50 | 0.21 | | 59.43 | 0.33 | 0.30 | | 44.70 | 55.30 |
| 211.04 | 2.82 | 0.23 | | 61.71 | 0.33 | 0.30 | | 43.95 | 56.05 |
| 239.78 | 4.64 | 0.24 | | 64.06 | 0.33 | 0.30 | | 42.60 | 57.40 |
| 272.43 | 6.82 | 0.24 | | 66.48 | 0.33 | 0.30 | | 40.43 | 59.57 |
| 309.53 | 9.07 | 0.22 | | 68.97 | 0.33 | 0.30 | | 37.27 | 62.73 |
| 351.67 | 11.00 | 0.20 | | 71.54 | 0.33 | 0.30 | | 33.10 | 66.90 |
| 399.56 | 12.23 | 0.17 | | 74.18 | 0.33 | 0.30 | | 28.07 | 71.93 |
| 453.96 | 12.44 | 0.16 | | 76.90 | 0.33 | 0.30 | | 22.49 | 77.51 |
| 515.77 | 11.56 | 0.09 | | 79.70 | 0.33 | 0.30 | | 16.82 | 83.18 |
| 586.00 | 9.72 | | | 82.58 | 0.33 | | | 11.57 | 88.43 |
| 665.79 | 7.30 | | | 85.56 | 0.33 | | | 7.19 | 92.81 |
| 756.45 | 4.76 | | | 88.61 | 0.33 | | | 3.89 | 96.11 |
| 859.45 | 2.58 | | | 91.77 | 0.33 | | | 1.74 | 98.26 |
| 976.48 | 1.04 | | | 95.01 | 0.33 | | | 0.58 | 99.42 |
| 1109.44 | 0.24 | | | 98.35 | 0.33 | | | 0.11 | 99.89 |
| 1180.00 | | | | 100.00 | 0.33 | | | 0.00 | 100.00 |

Table A. 2: Mix design of trial Mix 15.

| Par. size (μm) | Residue volume (%) | | | | T fn. | Volume fraction | | | | Composed mix | |
|---|---|---|---|---|---|---|---|---|---|---|---|
| | | | | | | Vgg | $V_{ss}$ | $V_c$ | $V_{sf}$ | Cumu. residue (%) | Cumu. passing (%) |
| | GGBS | NS | C | SF | P (D) | GGBS | NS | C | SF | $R_{mix}$(D) | $Q_{mix}$(D) |
| 0.24 | | | | 0.17 | | | | | 0.09 | 100.00 | 0.00 |
| 0.28 | 0.28 | | | 0.38 | 0.00 | 0.05 | | | 0.09 | 99.98 | 0.02 |
| 0.31 | 0.64 | | | 0.65 | 0.52 | 0.05 | | | 0.09 | 99.91 | 0.09 |
| 0.36 | 1.16 | | | 0.95 | 1.04 | 0.05 | | | 0.09 | 99.78 | 0.22 |
| 0.41 | 1.76 | | 0.06 | 1.23 | 1.58 | 0.05 | | 0.26 | 0.09 | 99.58 | 0.42 |
| 0.46 | 2.39 | | 0.07 | 1.42 | 2.13 | 0.05 | | 0.26 | 0.09 | 99.29 | 0.71 |
| 0.52 | 2.93 | | 0.09 | 1.47 | 2.71 | 0.05 | | 0.26 | 0.09 | 98.94 | 1.06 |
| 0.59 | 3.34 | | 0.11 | 1.37 | 3.30 | 0.05 | | 0.26 | 0.09 | 98.54 | 1.46 |
| 0.68 | 3.52 | | 0.13 | 1.12 | 3.91 | 0.05 | | 0.26 | 0.09 | 98.12 | 1.88 |
| 0.77 | 3.48 | | 0.16 | 0.78 | 4.54 | 0.05 | | 0.26 | 0.09 | 97.72 | 2.28 |
| 0.87 | 3.24 | | 0.20 | 0.42 | 5.19 | 0.05 | | 0.26 | 0.09 | 97.37 | 2.63 |
| 0.99 | 2.87 | | 0.25 | 0.14 | 5.85 | 0.05 | | 0.26 | 0.09 | 97.06 | 2.94 |
| 1.13 | 2.49 | | 0.31 | 0.00 | 6.53 | 0.05 | | 0.26 | 0.09 | 96.80 | 3.20 |
| 1.28 | 2.17 | | 0.38 | 0.00 | 7.24 | 0.05 | | 0.26 | 0.09 | 96.57 | 3.43 |
| 1.45 | 2.00 | | 0.46 | 0.00 | 7.97 | 0.05 | | 0.26 | 0.09 | 96.33 | 3.67 |
| 1.65 | 2.01 | | 0.56 | 0.09 | 8.71 | 0.05 | | 0.26 | 0.09 | 96.09 | 3.91 |
| 1.88 | 2.23 | | 0.66 | 0.30 | 9.48 | 0.05 | | 0.26 | 0.09 | 95.80 | 4.20 |
| 2.13 | 2.61 | | 0.78 | 0.62 | 10.27 | 0.05 | | 0.26 | 0.09 | 95.44 | 4.56 |
| 2.42 | 3.16 | | 0.91 | 1.02 | 11.09 | 0.05 | | 0.26 | 0.09 | 94.98 | 5.02 |
| 2.75 | 3.89 | | 1.05 | 1.40 | 11.93 | 0.05 | | 0.26 | 0.09 | 94.39 | 5.61 |
| 3.13 | 4.74 | | 1.20 | 1.72 | 12.80 | 0.05 | | 0.26 | 0.09 | 93.67 | 6.33 |

| | | | | | | | | | | | |
|---|---|---|---|---|---|---|---|---|---|---|---|
| 3.55 | 5.54 | | 1.35 | 1.94 | 13.69 | 0.05 | | 0.26 | 0.09 | 92.81 | 7.19 |
| 4.03 | 6.18 | | 1.52 | 2.07 | 14.61 | 0.05 | | 0.26 | 0.09 | 91.84 | 8.16 |
| 4.58 | 6.52 | | 1.70 | 2.13 | 15.55 | 0.05 | | 0.26 | 0.09 | 90.75 | 9.25 |
| 5.21 | 6.50 | | 1.89 | 2.17 | 16.52 | 0.05 | | 0.26 | 0.09 | 89.59 | 10.41 |
| 5.92 | 6.12 | | 2.10 | 2.24 | 17.53 | 0.05 | | 0.26 | 0.09 | 88.38 | 11.62 |
| 6.72 | 5.39 | | 2.33 | 2.37 | 18.56 | 0.05 | | 0.26 | 0.09 | 87.11 | 12.89 |
| 7.64 | 4.43 | | 2.59 | 2.58 | 19.62 | 0.05 | | 0.26 | 0.09 | 85.80 | 14.20 |
| 8.68 | 3.38 | | 2.87 | 2.90 | 20.72 | 0.05 | | 0.26 | 0.09 | 84.45 | 15.55 |
| 9.86 | 2.35 | | 3.17 | 3.33 | 21.84 | 0.05 | | 0.26 | 0.09 | 83.03 | 16.97 |
| 11.20 | 1.45 | | 3.50 | 3.88 | 23.01 | 0.05 | | 0.26 | 0.09 | 81.53 | 18.47 |
| 12.73 | 0.77 | | 3.84 | 4.51 | 24.20 | 0.05 | | 0.26 | 0.09 | 79.91 | 20.09 |
| 14.46 | 0.31 | | 4.19 | 5.18 | 25.43 | 0.05 | | 0.26 | 0.09 | 78.14 | 21.86 |
| 16.43 | 0.08 | | 4.53 | 5.81 | 26.70 | 0.05 | | 0.26 | 0.09 | 76.21 | 23.79 |
| 18.66 | 0.00 | | 4.84 | 6.32 | 28.01 | | | 0.26 | 0.09 | 74.11 | 25.89 |
| 21.21 | | | 5.09 | 6.61 | 29.35 | | | 0.26 | 0.09 | 71.85 | 28.15 |
| 24.09 | | | 5.27 | 6.60 | 30.74 | | | 0.26 | 0.09 | 69.49 | 30.51 |
| 27.37 | | | 5.35 | 6.25 | 32.16 | | | 0.26 | 0.09 | 67.07 | 32.93 |
| 31.10 | | | 5.31 | 5.56 | 33.63 | | | 0.26 | 0.09 | 64.68 | 35.32 |
| 35.34 | | | 5.13 | 4.60 | 35.14 | | | 0.26 | 0.09 | 62.39 | 37.61 |
| 40.15 | | | 4.81 | 3.48 | 36.70 | | | 0.26 | 0.09 | 60.29 | 39.71 |
| 45.61 | | | 4.37 | 2.35 | 38.30 | | | 0.26 | 0.09 | 58.44 | 41.56 |
| 51.82 | | | 3.82 | 1.35 | 39.95 | | | 0.26 | 0.09 | 56.87 | 43.13 |
| 58.88 | | | 3.20 | 0.52 | 41.65 | | | 0.26 | 0.09 | 55.59 | 44.41 |
| 66.90 | | | 2.54 | | 43.41 | | | 0.26 | | 54.60 | 45.40 |
| 76.01 | | | 1.91 | | 45.21 | | | 0.26 | | 53.88 | 46.12 |
| 86.36 | | 0.84 | 1.35 | | 47.07 | | 0.39 | 0.26 | | 53.33 | 46.67 |
| 98.11 | | 1.38 | 0.90 | | 48.98 | | 0.39 | 0.26 | | 52.52 | 47.48 |

| | | | | | | | | | | | |
|---|---|---|---|---|---|---|---|---|---|---|---|
| 111.47 | | 1.57 | 0.57 | | 50.95 | | 0.39 | 0.26 | | 51.54 | 48.46 |
| 126.65 | | 1.78 | 0.36 | | 52.98 | | 0.39 | 0.26 | | 50.57 | 49.43 |
| 143.90 | | 2.27 | 0.25 | | 55.07 | | 0.39 | 0.26 | | 49.54 | 50.46 |
| 163.49 | | 2.70 | 0.21 | | 57.22 | | 0.39 | 0.26 | | 48.30 | 51.70 |
| 185.75 | | 3.07 | 0.21 | | 59.43 | | 0.39 | 0.26 | | 46.84 | 53.16 |
| 211.04 | | 3.48 | 0.23 | | 61.71 | | 0.39 | 0.26 | | 45.19 | 54.81 |
| 239.78 | | 3.96 | 0.24 | | 64.06 | | 0.39 | 0.26 | | 43.32 | 56.68 |
| 272.43 | | 4.53 | 0.24 | | 66.48 | | 0.39 | 0.26 | | 41.20 | 58.80 |
| 309.53 | | 5.25 | 0.22 | | 68.97 | | 0.39 | 0.26 | | 38.78 | 61.22 |
| 351.67 | | 5.97 | 0.20 | | 71.54 | | 0.39 | 0.26 | | 36.00 | 64.00 |
| 399.56 | | 6.78 | 0.17 | | 74.18 | | 0.39 | 0.26 | | 32.85 | 67.15 |
| 453.96 | | 7.71 | 0.16 | | 76.90 | | 0.39 | 0.26 | | 29.29 | 70.71 |
| 515.77 | | 8.76 | 0.09 | | 79.70 | | 0.39 | 0.26 | | 25.25 | 74.75 |
| 586.00 | | 1.75 | 0.0 | | 82.58 | | 0.39 | | | 20.69 | 79.31 |
| 600.00 | | 4.33 | | | 83.13 | | 0.39 | | | 19.79 | 80.21 |
| 665.79 | | 5.97 | | | 85.56 | | 0.39 | | | 17.54 | 82.46 |
| 756.45 | | 6.78 | | | 88.61 | | 0.39 | | | 14.45 | 85.55 |
| 859.45 | | 7.71 | | | 91.77 | | 0.39 | | | 10.93 | 89.07 |
| 976.48 | | 8.76 | | | 95.01 | | 0.39 | | | 6.94 | 93.06 |
| 1109.44 | | 4.65 | | | 98.35 | | 0.39 | | | 2.41 | 97.59 |
| 1180.00 | | 0.00 | | | 100.00 | | 0.39 | | | 0.00 | 100.00 |